SUPPORTING INFORMATION

for

Natural-Product-inspired [3+2] cycloaddition based new spirooxindoles as dual anticancer agents: Synthesis, characterization, biological evaluation by *in vitro* and *in silico* methods

Narayanasamy Nivetha[a], Jevid Don Hamid[a], Akshaya Simha N[b], Devanand Devegowda[c], Ramith Ramu[b] and Sivan Velmathi[a]*

[a] *Organic and Polymer Synthesis Laboratory, Department of Chemistry, National Institute of Technology, Tiruchirappalli - 620015 Tamil Nadu, India.*

[b] *Department of Biotechnology and Bioinformatics, JSS Academy of Higher Education and Research, Mysuru - 570015, Karnataka, India.*

[c] *Center of Excellence in Molecular Biology and Regenerative Medicine, Department of Biochemistry, JSS Medical College, JSS Academy of Higher Education & Research, Mysuru, India.*

*Corresponding author

Email: velmathis@nitt.edu

TABLE OF CONTENTS

Experimental section

General procedure

All the chemicals were purchased from Sigma Aldrich and used as received. Thin Layer Chromatography was performed in Merck silica gel 60 F_{254} plates and visualized under UV light. Melting point were recorded using Veego (VMP-DS) apparatus and were uncorrected. Column chromatography was carried out in 100-200 mesh silica gel using hexane/ ethyl acetate. ^{1}H and ^{13}C NMR spectra were collected using DMSO-d_6 as solvent and TMS as internal standard in Bruker Avance III spectrometer. FT-IR spectra were obtained on Shimadzu IR Tracer-100 spectrometer using KBr pellets. High resolution mass spectral data were recorded using Agilent's QTOF G6545 spectrometer in ESI mode with 50,000 resolutions. MDA-MB-468 and HCT 15 cell lines were procured from the National Center for Cell Science, Pune, Maharashtra, India. Cell culture grade DMSO, 5-fluorouracil, all cell culture plastics were from Techno Plastic Products (TPP) Pvt Ltd. (Bengaluru, Karnataka, India). Dulbecco's modified Eagle medium (DMEM) with high glucose (4.5 g/L), trypsin-EDTA (0.25%), Dulbecco's phosphate-buffered saline (DPBS), ciprofloxacin, acridine orange (AO), and ethidium bromide (EtBr) were purchased from HiMedia.

Synthesis of chalcone derivatives (1a-f)

Substituted (E)-3-(4-ethoxy-3-methoxyphenyl)-1-phenylprop-2-en-1-one was prepared according to the reported procedure[1]. Vanillin (4-hydroxy-3-methoxybenzaldehyde) (1.0 mmol) and anhydrous K_2CO_3 (1.5 mmol) were added to a two neck-round bottom flask containing DMF (3 mL) and heated the reaction mixture at 90 ^{o}C for 30 min followed by iodoethane (1.0 mmol) added dropwise. Upon completion of iodoethane addition, the entire reaction mixture was heated under N_2 for 3 h. After the reaction was completed, the reaction mixture was poured into water and extracted with ethyl acetate. The organic layer was dried over anhydrous $NaSO_4$ and evaporated by using rotary evaporator to get 4-ethoxy-3-methoxybenzaldehyde, which was used without further purification in the next step. The 4-ethoxy-3-methoxybenzaldehyde (1.0 mmol) was dissolved in EtOH (5 mL) and 10% NaOH solution (10 mL) was added dropwise. After stirring the reaction mixture for 30 min at 0 ^{o}C, the acetophenone derivatives (1.0 mmol) were added and stirred for 3-4 h. The precipitate appeared was poured into crushed ice, filtered, and washed several times with water. The obtained solid was finally recrystallized from ethanol to get vanillin-based chalcones **1(a-f)**.

General procedure for the synthesis of pyrrolidine, pyrrolizidine and pyrrolothiazole containing spirooxindole derivatives 4/5/6(a-f)

A mixture of vanillin-based chalcones **1(a-f)** (1.0 mmol), isatin **2** (1.0 mmol) and amino acids **3(a-c)** (1.0 mmol) in ethanol (10 mL) was heated under reflux for the appropriate time of 3 h. After the completion of the reaction, the reaction mixture was poured into water and extracted with ethyl acetate. The extract was then dried over $NaSO_4$ and concentrated under reduced pressure. The crude was subjected to column chromatography using 100-200 mesh silica gel as stationary phase and hexane/ethyl acetate as an eluent to afford pure spirooxindole derivatives.

Spectral characterization data

3'-benzoyl-4'-(4-ethoxy-3-methoxyphenyl)-1'-methylspiro[indoline-3,2'-pyrrolidin]-2-one (**4a**)

White solid. Yield: 83%. M.p. 65-67 ^{o}C. FT-IR (KBr, cm^{-1}) ν_{max}: 3284 (NH), 1712 (C=O), 1610 (C=O). ^{1}H NMR (500 MHz, DMSO-d_6) δ_H: 1.28 (CH_3) (t, 3H, J = 7.0 Hz), 2.06 (N-CH_3) (s, 3H), 3.37 (H-5) (t, 1H, J = 7.8 Hz), 3.43 (H-5) (t, 1H, J = 9.3 Hz), 3.76 (O-CH_3) (s, 3H), 3.95 (O-CH_2) (q, 2H, J = 6.8 Hz), 4.28-4.33 (H-4) (m, 1H), 4.43 (H-3) (d, 1H, J = 9.5 Hz), 6.48 (d, 1H, J = 7.5 Hz, Ar-H), 6.82 (t, 1H, J = 7.3 Hz, Ar-H), 6.87 (d, 1H, J = 8.0 Hz, Ar-H), 6.90 (dd, 1H, J = 1.5 & 8.5 Hz, Ar-H), 6.94 (d, 1H, J = 7.5 Hz, Ar-H), 6.97 (td, 1H, J = 1.2 & 7.7 Hz, Ar-H), 7.04 (d, 1H, J = 2.0 Hz, Ar-H), 7.26 (t, 2H, J = 7.8 Hz, Ar-H), 7.38 (d, 2H, J = 7.5 Hz, Ar-H), 7.42 (t, 1H, J = 7.5 Hz, Ar-H), 10.48 (NH) (s, 1H). ^{13}C NMR (125 MHz, DMSO-d_6) δ_C:15.24 (CH_3), 34.91 (N-CH_3), 44.27 (C-4), 55.92 (O-CH_3), 60.31 (C-5), 62.04 (C-3), 64.21 (O-CH_2), 73.10 (C-2), 109.56, 112.35, 113.72, 119.92, 122.08, 126.55, 127.26, 127.66, 128.83, 129.42, 133.48, 134.29, 137.18, 142.54, 147.35, 149.44, 179.53 (C=O), 197.74 (C=O). HRMS (ESI, m/z): $[M+H]^+$ Calcd. for $C_{28}H_{29}N_2O_4$ 457.2127; Found 457.2130.

4'-(4-ethoxy-3-methoxyphenyl)-3'-(4-fluorobenzoyl)-1'-methylspiro[indoline-3,2'-pyrrolidin]-2-one (**4b**)

White solid. Yield: 91%. M.p. 74-76 ^{o}C. FT-IR (KBr, cm^{-1}) ν_{max}: 3292 (NH), 1712 (C=O), 1597 (C=O). ^{1}H NMR (500 MHz, DMSO-d_6) δ_H: 1.33 (CH_3) (t, 1H, J = 7.0 Hz), 2.10 (N-CH_3) (s, 3H), 3.41 (H-5) (t, 1H, J = 8.0 Hz), 3.46 (H-5) (t, 1H, J = 9.3 Hz), 3.99 (O-CH_2) (q, 2H, J = 6.8 Hz), 3.81 (O-CH_3) (s, 3H), 4.30-4.36 (H-4) (m, 1H), 4.44 (H-3) (d, 1H, J = 9.5 Hz), 6.54 (d, 1H, J = 7.5 Hz, Ar-H), 6.87 (td, 1H, J = 1.0 & 7.5 Hz, Ar-H), 6.90 (d, 1H, J = 8.5 Hz, Ar-

H), 6.93 (d, 1H, J = 2.0 Hz, Ar-H), 6.95-6.97 (m, 1H, Ar-H), 7.03 (td, 1H, J = 1.2 & 7.7 Hz, Ar-H), 7.08 (d, 1H, J = 2.0 Hz, Ar-H), 7.13 (t, 2H, J = 8.8 Hz, Ar-H), 7.47-7.49 (m, 2H, Ar-H), 10.47 (NH) (s, 1H). ^{13}C NMR (125 MHz, DMSO-d_6) δ_C: 15.24 (CH_3), 34.93 (N-CH_3), 44.12 (C-4), 55.92 (O-CH_3), 60.36 (C-5), 62.16 (C-3), 64.22 (O-CH_2), 73.10 (C-2), 109.59, 112.37, 113.71, 115.86 (d, J_{CF} = 21.3 Hz), 119.96, 122.11, 126.45, 127.19, 129.50, 130.62 (d, J_{CF} = 10.0 Hz), 133.97, 134.22, 142.50, 147.36, 149.45, 164.14, 166.14, 179.40 (C=O), 196.36 (C=O). HRMS (ESI, m/z): $[M+H]^+$ Calcd. for $C_{28}H_{28}FN_2O_4$ 475.2033; Found 475.2033.

3'-(4-chlorobenzoyl)-4'-(4-ethoxy-3-methoxyphenyl)-1'-methylspiro[indoline-3,2'-pyrrolidin]-2-one (**4c**)

White solid. Yield: 87%. M.p. 80-82 ^{o}C. FT-IR (KBr, cm^{-1}) ν_{max}: 3284 (NH), 1712 (C=O), 1618 (C=O). ^{1}H NMR (500 MHz, DMSO-d_6) δ_H: 1.28 (CH_3) (t, 3H, J = 7.0 Hz), 2.06 (N-CH_3) (s, 3H), 3.27 (H-5) (t, 1H, J = 8.0 Hz), 3.43 (H-5) (t, 1H, J = 9.0 Hz), 3.77 (O-CH_3) (s, 3H), 3.95 (O-CH_2) (q, 2H, J = 7.0 Hz), 4.27-4.32 (H-4) (m, 1H), 4.40 (H-3) (d, 1H, J = 9.0 Hz), 6.50 (d, 1H, J = 7.5 Hz, Ar-H), 6.82 (dd, 1H, J = 1.0 & 7.5 Hz, Ar-H), 6.85 (d, 1H, J = 1.0 Hz, Ar-H), 6.86 (d, 1H, J = 8.5 Hz, Ar-H), 6.90 (d, 1H, J = 2.0 Hz, Ar-H), 6.93 (d, 1H, J = 7.5 Hz, Ar-H), 7.00 (td, 1H, J = 1.2 & 7.7 Hz, Ar-H), 7.1 (d, 1H, J = 1.5 Hz, Ar-H), 7.30-7.37 (m, 4H, Ar-H), 10.47 (NH) (s, 1H). ^{13}C NMR (125 MHz, DMSO-d_6) δ_C: 15.23 (CH_3), 34.91 (N-CH_3), 44.08 (C-4), 55.93 (O-CH_3), 60.39 (C-5), 62.24 (C-3), 64.21 (O-CH_2), 73.08 (C-2), 109.63, 112.38, 113.72, 119.98, 122.14, 126.47, 127.12, 128.90,129.49, 129.54, 134.20, 135.85, 138.35, 142.51, 147.39, 149.47, 179.34 (C=O), 196.84 (C=O). HRMS (ESI, m/z): $[M+H]^+$ Calcd. for $C_{28}H_{28}ClN_2O_4$ 491.1738; Found 491.1744.

3'-(4-bromobenzoyl)-4'-(4-ethoxy-3-methoxyphenyl)-1'-methylspiro[indoline-3,2'-pyrrolidin]-2-one (**4d**)

White solid. Yield: 85%. M.p. 69-71 ^{o}C. FT-IR (KBr, cm^{-1}) ν_{max}: 3290 (NH), 1710 (C=O), 1617 (C=O). ^{1}H NMR (500 MHz, DMSO-d_6) δ_H: 1.29 (CH_3) (t, 3H, J = 7.0 Hz), 2.06 (N-CH_3) (s, 3H), 3.37 (H-5) (t, 1H, J = 8.0 Hz), 3.42 (H-5) (t, 1H, J = 9.3 Hz), 3.77 (O-CH_3) (s, 3H), 3.96 (O-CH_2) (q, 2H, J = 7.0 Hz), 4.26-4.31 (H-4) (m, 1H), 4.39 (H-3) (d, 1H, J = 9.0 Hz), 6.50 (d, 1H, J = 7.5 Hz, Ar-H), 6.82-6.85 (m, 1H, Ar-H), 6.87 (d, 1H, J = 3.5 Hz, Ar-H), 6.89 (d, 1H, J = 1.5 Hz, Ar-H), 6.92 (d, 1H, J = 7.5 Hz, Ar-H), 7.00 (td, 1H, J = 1.2 & 7.7 Hz, Ar-H), 7.04 (d, 1H, J = 2.0 Hz, Ar-H), 7.28 (d, 2H, J = 9.0 Hz, Ar-H), 7.47 (d, 2H, J = 8.5 Hz, Ar-H), 10.46 (NH) (s, 1H). ^{13}C NMR (125 MHz, DMSO-d_6) δ_C: 15.24 (CH_3), 34.91 (N-CH_3), 44.08 (C-4), 55.96 (O-CH_3), 60.38 (C-5), 62.19 (C-3), 64.25 (O-CH_2), 73.07 (C-2), 109.64, 112.40,

113.77, 119.98, 122.15, 126.48, 127.10, 127.56, 129.59, 131.88, 134.20, 136.17, 142.51, 147.39, 149.48, 179.31 (C=O), 197.07 (C=O). HRMS (ESI, m/z): $[M+H]^+$ Calcd. for $C_{28}H_{28}BrN_2O_4$ 535.1232; Found 535.1231.

4'-(4-ethoxy-3-methoxyphenyl)-1'-methyl-3'-(4-nitrobenzoyl)spiro[indoline-3,2'-pyrrolidin]-2-one (**4e**)

White solid. Yield: 79%. M.p. 96-98 ^oC. FT-IR (KBr, cm^{-1}) ν_{max}: 3292 (NH), 1701 (C=O), 1608 (C=O). ^1H NMR (500 MHz, DMSO-d_6) δ_H: 1.28 (CH_3) (t, 3H, J = 7.0 Hz), 2.06 (N-CH_3) (s, 3H), 3.38 (H-5) (t, 1H, J = 8.0 Hz), 3.43 (H-5) (t, 1H, J = 8.5 Hz), 3.78 (O-CH_3) (s, 3H), 3.95 (O-CH_2) (q, 2H, J = 7.0 Hz), 4.28-4.33 (H-4) (m, 1H), 4.49 (H-3) (d, 1H, J = 9.0 Hz), 6.43 (d, 1H, J = 8.0 Hz, Ar-H), 6.83-6.88 (m, 2H, Ar-H), 6.93-6.95 (m, 2H, Ar-H), 6.98 (td, 1H, J = 1.3 & 7.7 Hz, Ar-H), 7.08 (d, 1H, J = 2.0 Hz, Ar-H), 7.52 (d, 1H, J = 9.0 Hz, Ar-H), 8.05 (d, 1H, J = 7.5 Hz, Ar-H), 10.42 (NH) (s, 1H). ^{13}C NMR (125 MHz, DMSO-d_6) δ_C: 15.21 (CH_3), 34.86 (N-CH_3), 43.92 (C-4), 55.94 (O-CH_3), 60.49 (C-5), 63.06 (C-3), 64.24 (O-CH_2), 72.98 (C-2), 109.73, 112.45, 113.72, 120.06, 122.26, 123.74, 126.39, 126.92, 129.05, 129.71, 134.09, 141.78, 142.54, 147.45, 149.50, 149.86, 179.10 (C=O), 197.37 (C=O). HRMS (ESI, m/z): $[M+H]^+$ Calcd. for $C_{28}H_{28}N_3O_6$ 502.1978; Found 502.1977.

4'-(4-ethoxy-3-methoxyphenyl)-1'-methyl-3'-(4-methylbenzoyl)spiro[indoline-3,2'-pyrrolidin]-2-one (**4f**)

White solid. Yield: 80%. M.p. 71-73 ^oC. FT-IR (KBr, cm^{-1}) ν_{max}: 3294 (NH), 1712 (C=O), 1680 (C=O). ^1H NMR (500 MHz, DMSO-d_6) δ_H: 1.28 (CH_3) (t, 3H, J = 7.0 Hz), 2.06 (N-CH_3) (s, 3H), 3.37 (H-5) (t, 1H, J = 8.0 Hz), 3.42 (H-5) (t, 1H, J = 9.3 Hz), 3.94 (O-CH_2) (q, 2H, J = 7.0 Hz), 3.75 (O-CH_3) (s, 3H), 4.28-4.33 (H-4) (m, 1H), 4.40 (H-3) (d, 1H, J = 9.5 Hz), 6.51 (d, 1H, J = 7.5 Hz, Ar-H), 6.82 (td, 1H, J = 1.0 & 7.5 Hz, Ar-H), 6.87 (d, 2H, J = 4.5 Hz, Ar-H), 6.95 (d, 1H, J = 7.5 Hz, Ar-H), 6.99 (td, 1H, J = 1.2 & 7.7 Hz, Ar-H), 7.02 (d, 1H, J = 1.5 Hz, Ar-H), 7.07 (d, 2H, J = 8.0 Hz, Ar-H), 7.31 (d, 2H, J = 8.5 Hz, Ar-H), 10.48 (NH) (s, 1H). ^{13}C NMR (125 MHz, DMSO-d_6) δ_C: 15.23 (CH_3), 21.45 (CH_3), 34.92 (N-CH_3), 44.38 (C-4), 55.93 (O-CH_3), 60.29 (C-5), 61.78 (C-3), 64.22 (O-CH_2), 73.19 (C-2), 109.56, 112.36, 113.76, 119.88, 122.05, 126.68, 127.31, 127.82, 129.39, 129.42, 134.37, 134.83, 142.53, 143.89, 147.34, 149.45, 179.55 (C=O), 197.12 (C=O). HRMS (ESI, m/z): $[M+H]^+$ Calcd. for $C_{29}H_{31}N_2O_4$ 471.2284; Found 471.2286.

2'-benzoyl-1'-(4-ethoxy-3-methoxyphenyl)-1',2',5',6',7',7a'-hexahydrospiro[indoline-3,3'-pyrrolizin]-2-one (**5a**)

White solid. Yield: 80%. M.p. 107-109 °C. FT-IR (KBr, cm^{-1}) ν_{max}: 3203 (NH), 1718 (C=O), 1680 (C=O). ^1H NMR (500 MHz, DMSO-d_6) δ_H: 1.27 (CH_3) (t, 3H, J = 7.0 Hz), 1.68-1.77 (H-6) (m, 2H), 1.85-1.89 (H-7) (m, 2H), 2.33-2.37 (H-8) (m, 1H), 2.57-2.61 (H-8) (m, 1H), 3.78 (O-CH_3) (s, 3H), 3.83 (H-4) (t, 1H, J = 10.8 Hz), 3.94 (O-CH_2 & H-3) (q, 3H, J = 7.0 Hz), 4.84 (H-5) (d, 1H, J = 11.5 Hz), 6.54 (d, 1H, J = 7.5 Hz, Ar-H), 6.87 (d, 1H, J = 8.0 Hz, Ar-H), 6.91-6.96 (m, 2H, Ar-H), 7.04 (d, 1H, J = 2.0 Hz, Ar-H), 7.07-7.10 (m, 1H, Ar-H), 7.24 (d, 1H, J = 7.5 Hz, Ar-H), 7.29 (t, 2H, J = 7.8 Hz, Ar-H), 7.41 (d, 2H, J = 7.0 Hz, Ar-H), 7.46 (t, 1H, J = 7.3 Hz, Ar-H), 10.22 (NH) (s, 1H). ^{13}C NMR (125 MHz, DMSO-d_6) δ_C: 15.26 (CH_3), 27.11 (C-7), 30.06 (C-6), 48.03 (C-4), 52.55 (C-8), 55.95 (O-CH_3), 63.38 (C-3), 64.17 (O-CH_2), 71.76 (C-5), 72.98 (C-2), 110.01, 112.23, 113.71, 119.90, 121.45, 125.33, 127.85, 127.92, 128.78, 129.62, 132.91, 133.51, 137.29, 142.40, 147.36, 149.42, 179.90 (C=O), 197.37 (C=O). HRMS (ESI, m/z): $[M+H]^+$ Calcd. for $C_{30}H_{31}N_2O_4$ 483.2284; Found 483.2288.

1'-(4-ethoxy-3-methoxyphenyl)-2'-(4-fluorobenzoyl)-1',2',5',6',7',7a'-hexahydrospiro[indoline-3,3'-pyrrolizin]-2-one (**5b**)

White solid. Yield: 93%. M.p. 102-104 °C. FT-IR (KBr, cm^{-1}) ν_{max}: 3196 (NH), 1720 (C=O), 1683 (C=O). ^1H NMR (500 MHz, DMSO-d_6) δ_H: 1.27 (CH_3) (t, 3H, J = 7.0 Hz), 1.67-1.77 (H-6) (m, 2H), 1.83-1.89 (H-7) (m, 2H), 2.33-2.37 (H-8) (m, 1H), 2.54-2.59 (H-8) (m, 1H), 3.79 (O-CH_3) (s, 3H), 3.82 (H-4) (d, 1H, J = 11.0 Hz), 3.94 (O-CH_2 & H-3) (q, 3H, J = 6.8 Hz), 4.82 (H-5) (d, 1H, J = 11.5 Hz), 6.56 (d, 1H, J = 8.0 Hz, Ar-H), 6.86 (d, 1H, J = 8.5 Hz, Ar-H), 6.91-6.97 (m, 2H, Ar-H), 7.05 (d, 1H, J = 1.5 Hz, Ar-H), 7.08-7.13 (m, 3H, Ar-H), 7.23 (d, 1H, J = 7.5 Hz, Ar-H), 7.46-7.48 (m, 2H, Ar-H), 10.22 (NH) (s, 1H). ^{13}C NMR (125 MHz, DMSO-d_6) δ_C: 15.23 (CH_3), 27.17 (C-7), 30.14 (C-6), 47.98 (C-4), 52.40 (C-8), 55.96 (O-CH_3), 63.57 (C-3), 64.19 (O-CH_2), 71.84 (C-5), 73.05 (C-2), 110.05, 112.27, 113.72, 115.79 (d, J_{CF} = 22.5 Hz), 119.97, 121.51, 125.24, 127.77, 129.68, 130.89 (d, J_{CF} = 8.8 Hz), 132.83, 134.05, 142.35, 147.39, 149.46, 164.27, 166.27, 179.86 (C=O), 196.01 (C=O). HRMS (ESI, m/z): $[M+H]^+$ Calcd. for $C_{30}H_{30}FN_2O_4$ 501.2190; Found 501.2183.

2'-(4-chlorobenzoyl)-1'-(4-ethoxy-3-methoxyphenyl)-1',2',5',6',7',7a'-hexahydrospiro[indoline-3,3'-pyrrolizin]-2-one (**5c**)

White solid. Yield: 90%. M.p. 154-156 °C. FT-IR (KBr, cm^{-1}) ν_{max}: 3155 (NH), 1716 (C=O), 1680 (C=O). ^1H NMR (500 MHz, DMSO-d_6) δ_H: 1.28 (CH_3) (t, 3H, J = 7.0 Hz), 1.69-1.77 (H-6) (m, 2H), 1.84-1.89 (H-7) (m, 2H), 2.33-2.37 (H-8) (m, 1H), 2.55-2.57 (H-8) (m, 1H), 3.79 (O-CH_3) (s, 3H), 3.81 (H-4) (d, 1H, J = 11.5 Hz), 3.94 (O-CH_2 & H-3) (q, 3H, J = 7.0 Hz), 4.80 (H-5) (d, 1H, J = 11.5 Hz), 6.54 (d, 1H, J = 7.5 Hz, Ar-H), 6.86 (d, 1H, J = 8.5 Hz, Ar-H), 6.92-6.96 (m, 2H, Ar-H), 7.04 (d, 1H, J = 2.0 Hz, Ar-H), 7.09-7.12 (m, 1H, Ar-H), 7.23 (d, 1H, J = 7.5 Hz, Ar-H), 7.37 (s, 4H, Ar-H), 10.23 (NH) (s, 1H). ^{13}C NMR (125 MHz, DMSO-d_6) δ_C: 15.28 (CH_3), 27.22 (C-7), 30.14 (C-6), 47.99 (C-4), 52.55 (C-8), 55.93 (O-CH_3), 63.54 (C-3), 64.11 (O-CH_2), 71.93 (C-5), 73.02 (C-2), 110.06, 112.13, 113.57, 119.92, 121.55, 125.13, 127.77, 128.92, 129.79, 132.69, 135.95, 138.45, 142.31, 147.33, 149.35, 179.72 (C=O), 196.53 (C=O). HRMS (ESI, m/z): $[M+H]^+$ Calcd. for $C_{30}H_{30}ClN_2O_4$ 517.1894; Found 517.1895.

2'-(4-bromobenzoyl)-1'-(4-ethoxy-3-methoxyphenyl)-1',2',5',6',7',7a'-hexahydrospiro[indoline-3,3'-pyrrolizin]-2-one (**5d**)

White solid. Yield: 88%. M.p. 164-166 °C. FT-IR (KBr, cm^{-1}) ν_{max}: 3153 (NH), 1712 (C=O), 1678 (C=O). ^1H NMR (500 MHz, DMSO-d_6) δ_H: 1.28 (CH3) (t, 3H, J = 7.0 Hz), 1.69-1.76 (H-6) (m, 2H), 1.85-1.89 (H-7) (m, 2H), 2.33-2.37 (H-8) (m, 1H), 2.55 (H-8) (t, 1H, J = 8.3 Hz), 3.79 (O-CH3) (s, 3H), 3.81 (H-4) (d, 1H, J = 11.0 Hz), 3.94 (O-CH2 & H-3) (q, 3H, J = 7.0 Hz), 4.80 (H-3) (d, 1H, J = 11.5 Hz), 6.55 (d, 1H, J = 8.0 Hz, Ar-H), 6.86 (d, 1H, J = 8.0 Hz, Ar-H), 6.91-6.95 (m, 2H, Ar-H), 7.04 (s, 1H, Ar-H), 7.11 (t, 1H, J = 7.8 Hz, Ar-H), 7.23 (d, 1H, J = 7.5 Hz, Ar-H), 7.29 (d, 2H, J = 8.5 Hz, Ar-H), 7.50 (d, 2H, J = 8.5 Hz, Ar-H), 10.22 (NH) (s, 1H). ^{13}C NMR (125 MHz, DMSO-d_6) δ_C: 15.27 (CH_3), 27.20 (C-7), 30.14 (C-6), 47.98 (C-4), 52.28 (C-8), 55.96 (O-CH_3), 63.52 (C-3), 64.16 (O-CH_2), 71.90 (C-5), 73.01 (C-2), 110.08, 112.19, 113.65, 119.94, 121.55, 125.14, 127.67, 127.77, 129.77, 129.87, 131.86, 132.71, 136.28, 142.32, 147.36, 149.40, 179.73 (C=O), 196.71 (C=O). HRMS (ESI, m/z): $[M+H]^+$ Calcd. for $C_{30}H_{30}BrN_2O_4$ 561.1389; Found 561.1385.

1'-(4-ethoxy-3-methoxyphenyl)-2'-(4-nitrobenzoyl)-1',2',5',6',7',7a'-hexahydrospiro[indoline-3,3'-pyrrolizin]-2-one (**5e**)

White solid. Yield: 76%. M.p. 117-119 °C. FT-IR (KBr, cm^{-1}) ν_{max}: 3160 (NH), 1716 (C=O), 1604 (C=O). ^1H NMR (500 MHz, DMSO-d_6) δ_H: 1.29 (CH_3) (t, 3H, J = 7.0 Hz), 1.68-1.78 (H-6) (m, 2H), 1.84-1.89 (H-7) (m, 2H), 2.33-2.37 (H-8) (m, 1H), 2.52-2.55 (H-8) (m, 1H), 3.78 (H-4) (d, 1H, J = 10.0 Hz), 3.81 (O-CH_3) (s, 3H), 3.89-3.92 (H-3) (m, 1H), 3.96 (O-CH_2) (q, 3H, J = 7.0 Hz), 4.90 (H-5) (d, 1H, J = 11.5 Hz), 6.49 (d, 1H, J = 7.5 Hz, Ar-H), 6.88 (d, 1H,

J = 8.5 Hz, Ar-H), 6.96-7.00 (m, 2H, Ar-H), 7.08 (d, 1H, *J* = 2.0 Hz, Ar-H), 7.11-7.14 (m, 1H, Ar-H), 7.25 (d, 1H, *J* = 7.5 Hz, Ar-H), 7.50 (d, 2H, *J* = 9.0 Hz, Ar-H), 8.10 (d, 2H, *J* = 9.0 Hz, Ar-H), 10.10 (NH) (s, 1H). ^{13}C NMR (125 MHz, DMSO-d_6) δ_C: 15.27 (CH_3), 27.26 (C-7), 30.19 (C-6), 47.94 (C-4), 52.03 (C-8), 55.99 (O-CH_3), 64.16 (C-3), 64.49 (O-CH_2), 72.13 (C-5), 72.94 (C-2), 110.22, 112.22, 113.63, 120.05, 121.71, 123.76, 124.97, 127.64, 129.29, 129.98, 132.55, 142.10, 142.36, 147.40, 149.42, 150.03, 179.54 (C=O), 197.31 (C=O). HRMS (ESI, m/z): $[M+H]^+$ Calcd. for $C_{30}H_{30}N_3O_6$ 528.2135; Found 528.2133.

1'-(4-ethoxy-3-methoxyphenyl)-2'-(4-methylbenzoyl)-1',2',5',6',7',7a'-hexahydrospiro[indoline-3,3'-pyrrolizin]-2-one (**5f**)

White solid. Yield: 85%. M.p. 146-148 ^{o}C. FT-IR (KBr, cm^{-1}) ν_{max}: 3158 (NH), 1716 (C=O), 1676 (C=O). ^{1}H NMR (500 MHz, DMSO-d_6) δ_H: 1.28 (CH_3) (t, 3H, *J* = 7.0 Hz), 1.68-1.77 (H-6) (m, 2H), 1.85-1.89 (H-7) (m, 2H), 2.26 (CH_3) (s, 3H), 2.32-2.36 (H-8) (m, 1H), 2.54-2.59 (H-8) (m, 1H), 3.77 (O-CH_3) (s, 3H), 3.82 (H-4) (t, 1H, *J* = 10.8 Hz), 3.94 (O-CH_2 & H-3) (q, 3H, *J* = 7.0 Hz), 4.80 (H-5) (d, 1H, *J* = 11.5 Hz), 6.55 (d, 1H, *J* = 7.5 Hz, Ar-H), 6.86 (d, 1H, *J* = 8.5 Hz, Ar-H), 6.90-6.93 (m, 2H, Ar-H), 7.01 (d, 1H, *J* = 1.5 Hz, Ar-H), 7.07-7.12 (m, 3H, Ar-H), 7.24 (d, 1H, *J* = 7.5 Hz, Ar-H), 7.34 (d, 2H, *J* = 8.0 Hz, Ar-H), 10.24 (NH) (s, 1H). ^{13}C NMR (125 MHz, DMSO-d_6) δ_C: 15.28 (CH_3), 21.51 (CH_3), 27.17 (C-7), 30.09 (C-6), 48.02 (C-4), 52.56 (C-8), 55.90 (O-CH_3), 62.96 (C-3), 64.10 (O-CH_2), 71.77 (C-5), 73.06 (C-2), 109.99, 112.09, 113.57, 119.81, 121.44, 125.33, 127.94, 128.12, 129.42, 129.61, 132.86, 134.80, 142.32, 143.97, 147.28, 149.32, 179.87 (C=O), 196.59 (C=O). HRMS (ESI, m/z): $[M+H]^+$ Calcd. for $C_{31}H_{33}N_2O_4$ 497.2440; Found 497.2442.

6'-benzoyl-7'-(4-ethoxy-3-methoxyphenyl)-1',6',7',7a'-tetrahydro-3'H-spiro[indoline-3,5'-pyrrolo[1,2-c]thiazol]-2-one (**6a**)

White solid. Yield: 75%. M.p. 202-204 ^{o}C. FT-IR (KBr, cm^{-1}) ν_{max}: 3311 (NH), 1728 (C=O), 1676 (C=O). ^{1}H NMR (500 MHz, DMSO-d_6) δ_H: 1.28 (CH_3) (t, 3H, *J* = 7.0 Hz), 3.04 (H-6) (d, 2H, *J* =4.5 Hz), 3.34 (H-8) (d, 1H, *J* = 10.0 Hz), 3.72 (H-8) (d, 1H, *J* = 10.0 Hz), 3.81 (O-CH_3) (s, 3H), 3.82-3.87 (H-4) (m, 1H), 3.95 (O-CH_2) (q, 2H, *J* = 7.0 Hz), 4.14-4.18 (H-3) (m, 1H), 4.80 (H-5) (d, 1H, *J* = 11.5 Hz), 6.52 (d, 1H, *J* = 8.0 Hz, Ar-H), 6.89 (d, 1H, *J* = 8.5 Hz, Ar-H), 6.94 (t, 1H, *J* = 7.8 z, Ar-H), 7.02 (dd, 1H, *J* = 2.0 & 8.0 Hz, Ar-H), 7.09 (d, 1H, *J* = 2.0 Hz, Ar-H), 7.10-7.13 (m, 1H, Ar-H), 7.29 (t, 2H, *J* = 8.0 Hz, Ar-H), 7.38 (d, 2H, *J* = 7.5 Hz, Ar-H), 7.43 (d, 1H, *J* = 7.5 Hz, Ar-H), 7.48 (t, 1H, *J* = 7.5 Hz, Ar-H), 10.31 (NH) (s, 1H). ^{13}C NMR (125 MHz, DMSO-d_6) δ_C: 15.25 (CH_3), 36.36 (C-6), 51.20 (C-4), 53.90 (C-8), 56.01 (O-

CH_3), 61.81 (C-3), 64.17 (O-CH_2), 73.80 (C-2), 74.86 (C-5), 109.98, 110.07, 112.38, 113.66, 120.35, 121.43, 123.35, 128.45, 128.90, 129.79, 130.28, 132.00, 135.77, 138.58, 142.47, 147.64, 149.49, 178.70 (C=O), 95.95 (C=O). HRMS (ESI, m/z): $[M+H]^+$ Calcd. for $C_{29}H_{29}N_2O_4S$ 501.1848; Found 501.1849.

7'-(4-ethoxy-3-methoxyphenyl)-6'-(4-fluorobenzoyl)-1',6',7',7a'-tetrahydro-3'H-spiro[indoline-3,5'-pyrrolo[1,2-c]thiazol]-2-one (**6b**)

White solid. Yield: 90%. M.p. 207-209 ^oC. FT-IR (KBr, cm^{-1}) ν_{max}: 3321 (NH), 1722 (C=O), 1678 (C=O). ^1H NMR (500MHz, DMSO-d_6) δ_H: 1.29 (CH_3) (t, 3H, J = 7.0 Hz), 3.03 (H-6) (d, 2H, J = 4.5 Hz), 3.34 (H-8) (d, 1H, J = 10.0 Hz), 3.72 (H-8) (d, 1H, J = 10.0 Hz), 3.80 (H-4) (d, 1H, J = 2.0 Hz), 3.81 (O-CH_3) (s, 3H), 3.96 (O-CH_2) (q, 2H, J = 6.8 Hz), 4.11-4.15 (H-3) (m, 1H), 4.76 (H-5) (d, 1H, J = 11.5 Hz), 6.52 (d, 1H, J = 7.5 Hz, Ar-H), 6.89 (d, 1H, J = 8.5 Hz, Ar-H), 6.94 (t, 1H, J = 7.8 Hz, Ar-H), 7.01 (dd, 1H, J = 2.0 & 8.0 Hz, Ar-H), 7.08 (d, 1H, J = 7.08 Hz, Ar-H), 7.11-7.14 (m, 3H, Ar-H), 7.41-7.44 (m, 3H, Ar-H), 10.30 (NH) (s, 1H). ^{13}C NMR (125 MHz, DMSO-d_6) δ_C: 15.26 (CH_3), 36.35 (C-6), 51.08 (C-4), 54.01 (C-8), 56.02 (O-CH_3), 61.90 (C-3), 64.17 (O-CH_2), 73.88 (C-2), 74.89 (C-5), 109.95, 112.37, 113.66, 115.83 (d, J_{CF} = 22.5 Hz), 120.34, 121.40, 123.41, 128.47, 130.23, 130.93 (d, J_{CF} = 10.0 Hz), 132.05, 133.82, 133.84, 142.46, 147.62, 149.48, 164.33, 166.34, 178.79 (C=O), 195.43 (C=O). HRMS (ESI, m/z): $[M+H]^+$ Calcd. for $C_{29}H_{28}FN_2O_4S$ 519.1754; Found 519.1744.

6'-(4-chlorobenzoyl)-7'-(4-ethoxy-3-methoxyphenyl)-1',6',7',7a'-tetrahydro-3'H-spiro[indoline-3,5'-pyrrolo[1,2-c]thiazol]-2-one (**6c**)

White solid. Yield: 89%. M.p. 195-197 ^oC. FT-IR (KBr, cm^{-1}) ν_{max}: 3319 (NH), 1726 (C=O), 1674 (C=O). ^1H NMR (500 MHz, DMSO-d_6) δ_H: 1.29 (CH_3) (t, 3H, J = 7.0 Hz), 3.03 (H-6) (d, 2H, J = 5.0 Hz), 3.32 (H-8) (s, 1H), 3.71 (H-8) (d, 1H, J = 10.0 Hz), 3.80 (H-4) (d, 1H, J = 2.0 Hz), 3.82 (O-CH_3) (s, 3H), 3.96 (O-CH_2) (q, 2H, J = 6.8 & 13.8 Hz), 4.11-4.15 (H-3) (m, 1H), 4.75 (H-5) (d, 1H, J = 11.5 Hz), 6.53 (d, 1H, J = 7.5 Hz, Ar-H), 6.89 (d, 1H, J = 8.0 Hz, Ar-H), 6.92-6.96 (m, 1H, Ar-H), 7.01 (dd, 1H, J = 1.8 & 8.3 Hz, Ar-H), 7.08 (d, 1H, J = 1.5 Hz, Ar-H), 7.12-7.15 (m,1H, Ar-H), 7.33-7.38 (m, 4H, Ar-H), 7.42 (d, 1H, J = 7.5 Hz, Ar-H), 10.31 (NH) (s, 1H). ^{13}C NMR (125 MHz, DMSO-d_6) δ_C: 15.26 (CH3), 36.36 (C-6), 51.02 (C-4), 54.02 (C-8), 56.03 (O-CH3), 61.96 (C-3), 64.17 (O-CH2), 73.84 (C-2), 74.92 (C-5), 109.98, 110.07, 112.38, 113.66, 120.35, 121.43, 123.35, 128.45, 128.90, 129.79, 130.28, 132.00, 135.77, 138.58, 142.47, 147.64, 149.49, 178.70 (C=O), 195.95 (C=O). HRMS (ESI, m/z): $[M+H]^+$ Calcd. for $C_{29}H_{28}ClN_2O_4S$ 535.1458; Found 535.1450.

6'-(4-bromobenzoyl)-7'-(4-ethoxy-3-methoxyphenyl)-1',6',7',7a'-tetrahydro-3'H-spiro[indoline-3,5'-pyrrolo[1,2-c]thiazol]-2-one (**6d**)

White solid. Yield: 83%. M.p. 179-181 °C. FT-IR (KBr, cm^{-1}) ν_{max}: 3317 (NH), 1728 (C=O), 1674 (C=O). ^1H NMR (500 MHz, DMSO-d_6) δ_H: 1.28 (CH_3) (t, 3H, J = 7.0 Hz), 3.03 (H-6) (d, 2H, J = 4.5 Hz), 3.34 (H-8) (d, 1H, J = 10.0 Hz), 3.72 (H-8) (d, 1H, J = 10.5 Hz), 3.80 (H-4) (d, 1H, J = 2.0 Hz), 3.82 (O-CH_3) (s, 3H), 3.95 (O-CH_2) (q, 2H, J = 7.0 & 14.0 Hz), 4.11-4.15 (H-3) (m, 1H), 4.75 (H-5) (d, 1H, J = 12.0 Hz), 6.53 (d, 1H, J = 7.5 Hz, Ar-H), 6.89 (d, 1H, J = 8.5 Hz, Ar-H), 6.94 (t, 1H, J = 7.5 Hz, Ar-H), 7.01 (dd, 1H, J = 2.0 & 8.5 Hz, Ar-H), 7.08 (d, 1H, J = 2.0 Hz, Ar-H), 7.12-7.15 (m, 1H, Ar-H), 7.26 (d, 2H, J = 8.5 Hz, Ar-H), 7.42 (d, 1H, J = 7.5 Hz, Ar-H), 7.51 (d, 2H, J = 8.5 Hz, Ar-H), 10.32 (NH) (s, 1H). ^{13}C NMR (125 MHz, DMSO-d_6) δ_C: 15.27 (CH_3), 36.37 (C-6), 51.03 (C-4), 54.04 (C-8), 56.03 (O-CH_3), 61.92 (C-3), 64.17 (O-CH_2), 73.84 (C-2), 74.92 (C-5), 109.99, 112.37, 113.65, 120.35, 121.43, 123.34, 127.80, 128.47, 129.88, 130.29, 131.85, 131.98, 136.09, 142.48, 147.64, 149.49, 178.69 (C=O), 196.14 (C=O). HRMS (ESI, m/z): $[M+H]^+$ Calcd. for $C_{29}H_{28}BrN_2O_4S$ 579.0953; Found 579.0937.

7'-(4-ethoxy-3-methoxyphenyl)-6'-(4-nitrobenzoyl)-1',6',7',7a'-tetrahydro-3'H-spiro[indoline-3,5'-pyrrolo[1,2-c]thiazol]-2-one **(6e**)

White solid. Yield: 78%. M.p. 119-121 °C. FT-IR (KBr, cm^{-1}) ν_{max}: 3263 (NH), 1724 (C=O), 1606 (C=O). ^1H NMR (500 MHz, DMSO-d_6) δ_H: 1.30 (CH_3) (t, 3H, J = 7.0 Hz), 3.05 (H-6) (d, 2H, J = 5.0 Hz), 3.32 (H-8) (s, 1H), 3.72 (H-8) (d, 1H, J = 10.5 Hz), 3.78 (H-4) (t, 1H, J = 10.5 Hz), 3.84 (O-CH_3) (s, 3H), 3.98 (O-CH_2) (q, 2H, J = 6.8 Hz), 4.10-4.14 (H-3) (m, 1H), 4.84 (H-5) (d, 1H, J = 11.5 Hz), 6.47 (d, 1H, J = 8.0 Hz, Ar-H), 6.91 (d, 1H, J = 8.0 Hz, Ar-H), 6.98 (t, 1H, J = 7.5 Hz, Ar-H), 7.06 (dd, 1H, J = 1.5 & 8.5 Hz, Ar-H), 7.13 (d, 1H, J = 2.0 Hz, Ar-H), 7.16 (t, 1H, J = 7.5 Hz, Ar-H), 7.43 (d, 1H, J = 7.5 Hz, Ar-H), 7.46 (d, 2H, J = 8.5 Hz, Ar-H), 8.11 (d, 2H, J = 8.5 Hz, Ar-H), 10.21 (NH) (s, 1H). ^{13}C NMR (125 MHz, DMSO-d_6) δ_C: 15.28 (CH_3), 36.39 (C-6), 50.87 (C-4), 54.21 (C-8), 56.04 (O-CH_3), 62.75 (C-3), 64.15 (O-CH_2), 73.78 (C-2), 75.06 (C-5), 110.15, 112.37, 113.59, 120.48, 121.58, 123.17, 123.76, 128.34, 129.31, 130.53, 131.82, 141.91, 142.53, 147.66, 149.48, 150.09, 178.50 (C=O), 196.89 (C=O). HRMS (ESI, m/z): $[M+H]^+$ Calcd. for $C_{29}H_{28}N_3O_6S$ 546.1699; Found 546.1696.

7'-(4-ethoxy-3-methoxyphenyl)-6'-(4-methylbenzoyl)-1',6',7',7a'-tetrahydro-3'H-spiro[indoline-3,5'-pyrrolo[1,2-c]thiazol]-2-one (**6f**)

White solid. Yield: 80%. M.p. 200-202 ^{o}C. FT-IR (KBr, cm^{-1}) ν_{max}: 3319 (NH), 1726 (C=O), 1668 (C=O). ^{1}H NMR (500 MHz, DMSO-d_6) δ_H: 1.28 (CH_3) (t, 3H, J = 7.0 Hz), 2.27 (CH_3) (s, 3H), 3.03 (H-6) (d, 2H, J = 4.5 Hz), 3.33 (H-8) (d, 1H, J = 10.5 Hz), 3.72 (H-8) (d, 1H, J = 10.5 Hz), 3.80 (O-CH_3) (s, 3H), 3.84 (H-4) (d, 1H, J = 11.5 Hz), 3.95 (O-CH_2) (q, 2H, J = 7.0 & 14.0 Hz), 4.12-4.15 (H-3) (m, 1H), 4.75 (H-5) (d, 1H, J = 11.5 Hz), 6.53 (d, 1H, J = 8.0 Hz, Ar-H), 6.88 (d, 1H, J = 8.5 Hz, Ar-H), 6.93 (t, 1H, J = 7.5 Hz, Ar-H), 6.98 (dd, 1H, J = 1.5 & 8.5 Hz, Ar-H), 7.06 (d, 1H, J = 1.5 Hz, Ar-H), 7.12 (t, 3H, J = 8.3 Hz, Ar-H), 7.32 (d, 2H, J = 8.5 Hz, Ar-H), 7.43 (d, 1H, J = 7.5 Hz, Ar-H), 10.32 (NH) (s, 1H). ^{13}C NMR (125 MHz, DMSO-d_6) δ_C: 15.26 (CH3), 21.52 (CH3), 36.34 (C-6), 51.26 (C-4), 53.90 (C-8), 56.01 (O-CH3), 61.44 (C-3), 64.16 (O-CH2), 73.89 (C-2), 74.83 (C-5), 109.90, 112.34, 113.67, 120.22, 121.31, 123.54, 128.14, 128.62, 129.41, 130.09, 132.16, 134.62, 142.45, 144.09, 147.60, 149.46, 178.85 (C=O), 195.90 (C=O). HRMS (ESI, m/z): $[M+H]^+$ Calcd. for $C_{30}H_{31}N_2O_4S$ 515.2005; Found 515.1998.

***In silico* studies**

Preparation of ligands, protein targets and molecular docking studies

The structures of BCL2, Caspase 3, and FAS respectively elucidated by X-Ray crystallography (PDB ID: 2W3L, PDB ID: 3GJQ and PDB ID: 3TJM) were obtained from the Protein Data Bank (PDB). The protein targets were prepared according to the previous reports[2,3] using Auto dock Tools 1.5.7. Further, the prediction of the binding site was carried out according to the reported procedure [2]. The docking was site specific, the key amino acids of the 3 targets were obtained from the reports [4-6.] The grid box measuring 40 Å × 40 Å × 40 Å containing the binding pocket and the attributes of the active site was positioned at x = 39.805667 Å, y = 26.935452 Å, and z = -12.414476 Å; x = 40.609477 Å, y = 33.891182 Å and z = 58.019750 Å; x = 1.959955 Å, y = 63.600591 Å and z = 53.006000 Å for BCL2, Caspase 3 and FAS, respectively. During ligand preparation, phytochemical structures, and 5-fluorouracil (standard drug) were sketched using Chem sketch and prepared for the molecular docking studies. Molecular docking studies was carried out using Auto Dock Tools 1.5.7[2]. After minimizing the energy, ligand molecules were stored in the same directory as the protein molecule using the PDBQT format to perform the docking simulation studies. Using a command-line programme called Auto Dock Vina 1.1.2, which disrupts and navigates the ligands into the target site using the Brayden-Fletcher-Goldfarb-Shanno (BGFS) algorithm and evaluates the scoring function of each ligand conformation, the compounds were virtually

screened[7,8]. During the entire docking simulation, ligands remained flexible but proteins were expected to be rigid due to the huge number of torsions permitted during ligand synthesis. Though 10 degrees were permitted for ligand molecules, the first binding poses among ten poses which was created with zero atomic position root-mean-square deviation (RMSD) are the most authentic. Indicating a more efficient binding, it also possesses the highest binding affinity of any location. Biovia Discovery Studio Visualizer 2021, an open-source GUI for visualizing data, was used to complete the visualization of the molecular docking studies. Combining the total number of hydrogen bonds, total number of intermolecular bonds, and binding affinity, the amount of ligand interaction was calculated. The co-crystal ligands (CCLs) of the targets i.e. 2W3L (DRO1166) & 3TJM (7FA500) were removed from their respective protein and redocked with the respective proteins according to the above-mentioned procedure. Whereas 3GJQ (tripeptide Trp-Glu-His-Asp with acetyl group) was docked using Schrodinger Suite. The RMSD of the co-crystal ligand within the complex and the re-docked co-crystal ligands were also determined using Discovery Studio 2021 visualization software which validated the docking procedure with respect to co-crystal ligand.

Molecular dynamics simulation studies and calculation of free energy

Protein targets complexed with the lead ligands & 5-fluorouracil as standard after docking were selected for the molecular dynamics (MD) simulation. The MD simulation studies were performed using GROMACS-2018.1, a biomolecular software package. The CHARMM36 was used as the force field to approximate the ligand structures, and the ligand topology was constructed using Swiss Param server. Conversely, the CHARMM36 forcefield was also used to add protein structure using the pdb2gmx module [9]. The next stage was to use the steepest descent technique to minimize energy in a vacuum over 5000 steps. Each protein complex was spaced 10 Å from the borders of the box. With the appropriate number of Na^+ and Cl^- counterions, the solvent was added to the TIP3P water model to maintain the required 0.15 M salt concentration. Five simulations in all were done at 310 K temperature and 1 bar pressure for 100 ns. The trajectory analysis of the solvent accessible surface area (SASA), ligand hydrogen bond parameters, radius of gyration (Rg), root-mean-square deviation (RMSD), and root-mean-square fluctuation (RMSF) was carried out, and the findings were shown in the graphical manner employing a GUI based software known as XM GRACE for plotting the outcomes of MD simulation studies.

Using the Molecular Mechanics/Poisson-Boltzmann Surface Area (MM-PBSA) approach, binding free energy calculations were performed using protein-ligand complex outcomes along with standard drug 5-fluorouracil obtained from MD simulation studies. The degree of ligand binding to protein can also be assessed using thermodynamics and molecular dynamics simulations. Molecular mechanical energy, polar and apolar solvation energies, and molecular mechanical energy are the three components used in the g_mmpbsa programme with MmPbSaStat.py script was used to calculate the binding free energy for each ligand-protein combination [10,11]. The programme used the GROMACS 2018.1 trajectories as input. Using dt 1000 frames, the computation of ΔG is performed by considering the MD trajectories of the previous 50 ns.

$$\mathbf{\Delta G_{binding} = G_{complex} - (G_{protein} + G_{Ligand})} \quad \mathbf{(1)}$$

$$\mathbf{\Delta G = \Delta E_{MM} + \Delta G_{Solvation} - T\Delta S = \Delta E_{(bonded + non\text{-}bonded)} + \Delta G_{(Polar + non\text{-}polar)} - T\Delta S} \quad \mathbf{(2)}$$

$G_{Binding}$: binding free energy, C_{omplex}: total free energy of the protein-ligand complex, $G_{Protein}$ and G_{Ligand}: total free energies of the isolated protein and ligand in solvent, respectively, ΔG: standard free energy, ΔE_{MM}: average molecular mechanics potential energy in vacuum, $G_{Solvation}$: solvation energy, ΔE: total energy of bonded as well as non-bonded interactions, ΔS: change in entropy of the system upon ligand binding, T: Temperature in Kelvin.

Determination of anti-proliferative potential (cytotoxicity) by SRB assay

The anti-proliferative activity (cytotoxicity) of the compounds (4, 5 and 6 series) were determined according to the previous study[12]. MDA-MB-468 (breast cancer cell line) and HCT 15 (Colorectal cancer cell line) were suspended in 100 µL of DMEM (Dulbecco's Modified Eagle Medium) with 10% FBS (Fetal Bovine Serum) and then seeded into a 96-well plate with a cell density of 1×10^4 cells per well in 100 µL of media. These cells were then incubated at 37°C with 5% CO_2 and 90% relative humidity overnight. To test the effects of compounds on these cells, a stock solution of 100 mM of compound **6f** was prepared using 100% cell culture-grade DMSO (Dimethyl Sulfoxide). A 2x working stock of 1 mM compounds was prepared by diluting the 100 mM compounds stock with DMEM containing 10% FBS. It is important to note that the final concentration of DMSO in the working stock was 0.5%. Various concentrations of compound **6f** were prepared by serial dilution using DMEM. The cells were then treated with increasing concentrations of compounds (62.5, 125, 250, 500 and 1000 µM) with respect to MDA-MB-468 cells, whereas the HCT 15 cells were treated with increasing

concentrations of compounds (62.5, 125, 250, 500, 1000 and 2000 μM) with respect to different durations of 24, 48, and 72 h. Inhibition percentage of cell proliferation was assessed using a Sulforhodamine-B (SRB) assay. The percentage inhibition of cell proliferation was calculated using the following formula:

% inhibition of cell proliferation = (Absorbance of Control – Absorbance of Sample) / (Absorbance of Control) × 100

The experiments were performed in triplicates, and each concentration was tested with at least four replicates to ensure the reliability of the results.

Cell death assay by acridine orange and Ethidium bromide staining

Cell death due to the treatment of compounds was evaluated through a process involving the dual staining of cells with acridine orange (AO) and ethidium bromide (EtBr)[12]. MDA-MB-468 and HCT 15 cells were grown in 6-well plates at a cell density of 0.3×10^6 cells in 2.0 mL of medium per well and allowed to grow for approximately 36 hrs. After this initial growth period, the cells were exposed to varying concentrations of compounds (250, 500 and 1000 μM with respect to MDA-MB-468 cells and 500, 1000 and 2000 μM with respect to HCT 15 cells) and control solution consisting of 0.5% DMSO for a duration of 48 hrs. Subsequently, the cells were treated with trypsin to create a single-cell suspension. The neutralization of trypsin was with the addition of the complete medium. A 20 μL cell suspension was transferred to a separate 1.5 mL microcentrifuge tube, incubated with a mixture of EtBr (100 μM) and acridine orange (100 μM) for 5.0 minutes. The stained cells were mounted on slides and observed using a fluorescence microscope (Olympus U-CMAD3) equipped with fluorescein isothiocyanate (FITC) and tetramethyl-rhodamine isothiocyanate (TRITC) probes. The stained images were created by merging both live and dead cells. Cells with green colour (live cells) and cells with orange colour (dead cells) were analyzed.

Effect of 4,5 and 6 series compounds on cell cycle

The effect of 4,5 and 6 series compounds on cell cycle was conducted according to the study[13]. MDA-MB-468 and HCT 15 cells, at a concentration of 2×10^5 cells per 2 mL per well,

were cultured in a 6-well plate. These cells were then subjected to treatment with compounds at concentrations of 50, 100, and 200 µM. Further, they were treated with DMSO (control) for a duration of 48 hrs. Following the duration of incubation, the culture media were removed, and the cells were washed with PBS (Phosphate-Buffered Saline). Subsequently, the cells were trypsinized, and the resultant cell suspension was subjected to centrifugation at 300× g for 5 minutes at 25 °C. The cells were then fixed by being exposed to 1 mL of cold 70% ethanol for 30 minutes while kept on ice. After centrifugation, the cell pellet was treated with 50 µL of Ribonuclease-A (RNase A) at a concentration of 100 µM for 4 hrs. The treated cell suspension was then mixed with 400 µL of propidium iodide (PI) solution at a stock concentration of 50 µM per 10^6 cells, and this mixture was allowed to incubate for 10 minutes at room temperature. The distribution of the cell cycle was analyzed using flow cytometry equipment (BD FACS Calibur model: 343202-FACSCALIBUR 4 CLR, BD Biosciences, San Jose, CA, USA), equipped with three filters (GFP-515/15, YFP-540/20BP, RFP-610/20BP). Cell analysis was performed using Cell quest pro v.6.0 software.

Assay for Caspase 3 enzyme activity

MDA-MB-468 and HCT 15 cells were cultivated in a 6-well plate at a density of 5 x 10^5 cells/ 2 mL and were then incubated for a whole night at 37°C in a CO_2 incubator. The medium that the cells were using was aspirated, and the cells were treated with the necessary concentrations of experimental compounds (62.5-1000 µM for MDA-MB-468 cells and 62.5-2000 µM for HCT 15 cells) in 2 mL of culture medium. The cells were then incubated for 24 hours at 37°C. After the treatment was completed, the medium was removed from each well and cleaned with PBS. After removing the PBS, a hazardous agent at a concentration of 23µM was added, and the mixture was incubated for 24 hours at 37°C. After the treatment, the medium was aspirated from each well and washed with PBS. 200 µL of trypsin-EDTA solution was added, and the mixture was incubated for 3–4 minutes at 37 °C. Next, 2 mL of culture medium was added, and the cells were harvested directly into 12 x 75 mm polystyrene tubes. The tubes were centrifuged for 5 minutes at 300 x g at 25 °C. The pellet was fixed in 1 mL of cold 70% ethanol, added dropwise to the cell pellet while vertexing to ensure fixation of all cells and reduce clumping. Finally, the mixture was incubated for 30 minutes in a -20°C freezer.

The cells were pelleted at a faster rate than living cells for five minutes, aspirated the supernatant carefully without losing the pellet (Note that ethanol-fixed cells require higher

centrifugal speeds to pellet compared to unfixed cells since they become more buoyant upon fixation). Washed the pellet twice with PBS and 10 µL of Anti–Caspase-3/7 antibody was added. Mixed thoroughly and incubated for 30 minutes in the dark at room temperature (20 to 25°C). 500 µL of D-PBS was added and mixed thoroughly and analyzed the cells by FACS on FL1 channel[14-16].

Cell line	Groups	% Inhibition of cell proliferation		
		24 hrs	48 hrs	72 hrs
	Normal cell	0.25 ± 0.01[a]	0.35 ± 0.08[a]	0.39 ± 0.10[a]

Statistical analysis

All the experiments were performed in triplicates. Results were expressed as the mean ± standard deviation calculated using Graph Pad Prism version 8.1. Duncan's multiple tests were used to calculate "p" value. A "p" value of ≤ 0.05 was considered as significant.

	Control	0.56 ± 0.04[a]	0.58 ± 0.04[a]	0.58 ± 0.04[a]
	VC DMSO	5.31 ± 0.24 [b]	5.37 ± 0.29 [b]	5.40 ± 0.29[b]
	5 fluorouracil (100 µM)	89.27 ± 1.02 [g]	92.25 ± 0.98[g]	94.47 ± 0.85[g]
	Compound **6f** (62.5 µM)	13.45 ± 0.06 [c]	14.12 ± 0.17[c]	17.38 ± 0.25[c]
	Compound **6f** (125 µM)	24.65 ± 0.26 [d]	26.59 ± 0.31[d]	29.54 ± 0.21[d]
	Compound **6f** (250 µM)	46.71 ± 0.50 [e]	48.63 ± 0.27[e]	50.25 ± 0.28[e]
	Compound **6f** (500 µM)	69.83 ± 1.50[f]	71.15 ± 0.45[f]	73.14 ± 1.01[f]
	Compound **6f** (1000 µM)	90.32 ± 0.91[g]	92.54 ± 0.65[g]	94.66 ± 0.79[g]
HCT 15	Normal cell	0.37 ± 0.05[a]	0.40 ± 0.04[a]	0.42 ± 0.06[a]
	Control	0.58 ± 0.01[a]	0.6 ± 0.07[a]	0.61 ± 0.09[a]
	VC DMSO	5.35 ± 0.16[b]	5.45 ± 0.12[b]	5.75 ± 0.15[b]
	5 fluorouracil (100 µM)	89.72 ± 0.53[h]	91.25 ± 0.76[h]	94.45 ± 0.34[h]
	Compound **6f** (62.5 µM)	17.56 ± 0.45[c]	19.25 ± 0.17[c]	22.15 ± 0.24[c]
	Compound **6f** (125 µM)	25.73 ± 0.32[d]	28.64 ± 0.41[d]	31.24 ± 0.55[d]
	Compound **6f** (250 µM)	47.70 ± 0.22[e]	50.24 ± 0.51[e]	54.47 ± 0.27[e]
	Compound **6f** (500 µM)	66.57 ± 0.93[f]	68.75 ± 0.67[f]	71.45 ± 0.55[f]
	Compound **6f** (1000 µM)	72.91 ± 0.26[g]	75.14 ± 0.47[g]	79.14 ± 0.44[g]
	Compound **6f** (2000 µM)	91.87 ± 0.31[i]	94.57 ± 0.51[i]	95.15 ± 0.24[i]

Table S1. Anti-proliferative (Cytotoxicity) of Compound **6f** and other compounds against MDA-MB-468 cell line and HCT 15 cell line.

Values are expressed as mean ± SD. Means in the same column with distinct superscripts are significantly different ($p \leq 0.05$) as separated by the Duncan multiple range test

Cell line	Compounds	Concentration (µM)	% Inhibition of cell proliferation		
			24 hrs	**48 hrs**	**72 hrs**
MDA-MB-468	4a	62.5 µM	3.47 ± 0.06[a]	6.12 ± 0.17[a]	8.38 ± 0.25[a]
		125 µM	9.65 ± 0.26[b]	10.59 ± 0.31[b]	12.54 ± 0.21[b]
		250 µM	14.71 ± 0.5[c]	16.63 ± 0.28[c]	17.25 ± 0.28[c]
		500 µM	18.83 ± 1.50[d]	21.15 ± 0.49[d]	23.14 ± 1.05[d]
		1000 µM	20.32 ± 0.91[e]	22.54 ± 0.65[e]	25.66 ± 0.79[e]
	4b	62.5 µM	4.45 ± 0.30[a]	5.12 ± 0.17[a]	7.38 ± 0.25[a]
		125 µM	10.60 ± 0.26[b]	11.57 ± 0.31[b]	12.60 ± 0.21[b]
		250 µM	14.91 ± 0.50[c]	17.63 ± 0.28[c]	19.48 ± 0.28[c]
		500 µM	20.83 ± 1.50[d]	22.65 ± 0.49[d]	25.44 ± 1.05[d]
		1000 µM	27.32 ± 0.91[e]	32.54 ± 0.65[e]	33.68 ± 0.79[e]
	4c	62.5 µM	8.45 ± 0.30[a]	8.92 ± 0.17[a]	9.38 ± 0.25[a]
		125 µM	11.60 ± 0.2[b]	12.57 ± 0.31[b]	13.90 ± 0.21[b]
		250 µM	15.91 ± 0.50[c]	19.63 ± 0.28[c]	22.48 ± 0.28[c]
		500 µM	23.83 ± 1.50[d]	25.65 ± 0.49[d]	29.44 ± 1.05[d]
		1000 µM	32.32 ± 0.91[e]	35.54 ± 0.65[e]	38.68 ± 0.79[e]
	4d	62.5 µM	10.45 ± 0.30[a]	12.92 ± 0.17[a]	14.38 ± 0.25[a]
		125 µM	15.60 ± 0.26[b]	17.57 ± 0.31[b]	20.90 ± 0.21[b]
		250 µM	22.91 ± 0.50[c]	24.63 ± 0.28[c]	27.48 ± 0.28[c]
		500 µM	30.83 ± 1.50[d]	33.65 ± 0.49[d]	37.44 ± 1.05[d]
		1000 µM	40.32 ± 0.91[e]	42.54 ± 0.65[e]	45.68 ± 0.79[e]
	4e	62.5 µM	12.45 ± 0.30[a]	14.85 ± 0.17[a]	16.83 ± 0.25[a]
		125 µM	18.80 ± 0.26[b]	20.75 ± 0.31[b]	22.68 ± 0.21[b]
		250 µM	24.91 ± 0.50[c]	26.68 ± 0.28[c]	29.84 ± 0.28[c]
		500 µM	32.83 ± 1.50[d]	34.56 ± 0.49[d]	38.50 ± 1.05[d]
		1000 µM	42.42 ± 0.91[e]	44.84 ± 0.65[e]	46.68 ± 0.79[e]
	4f	62.5 µM	12.95 ± 0.30[a]	15.85 ± 0.17[a]	17.93 ± 0.25[a]
		125 µM	19.80 ± 0.26[b]	21.75 ± 0.31[b]	23.98 ± 0.21[b]
		250 µM	25.11 ± 0.50[c]	27.00 ± 0.28[c]	30.84 ± 0.28[c]
		500 µM	33.83 ± 1.50[d]	35.58 ± 0.49[d]	39.50 ± 1.05[d]
		1000 µM	43.72 ± 0.91[e]	45.92 ± 0.65[e]	47.68 ± 0.79[e]
	5a	62.5 µM	15.90 ± 0.30 [a]	19.85 ± 0.17[a]	22.93 ± 0.25[a]
		125 µM	20.80 ± 0.26[b]	23.78 ± 0.31[b]	26.00 ± 0.21[b]
		250 µM	27.15 ± 0.50[c]	28.45 ± 0.28[c]	32.72 ± 0.28[c]
		500 µM	35.83 ± 1.50[d]	37.58 ± 0.49[d]	42.50 ± 1.05[d]
		1000 µM	44.72 ± 0.91[e]	47.92 ± 0.65[e]	49.78 ± 0.79[e]
	5b	62.5 µM	17.90 ± 0.30[a]	20.85 ± 0.17[a]	23.48 ± 0.25[a]
		125 µM	21.92 ± 0.26[b]	24.88 ± 0.31[b]	27.45± 0.21[b]
		250 µM	29.29 ± 0.50[c]	32.45 ± 0.28[c]	34.72 ± 0.28[c]
		500 µM	37.83 ± 1.50[d]	40.58 ± 0.49[d]	43.90 ± 1.05[d]
		1000 µM	46.46 ± 0.91[e]	48.92 ± 0.65[e]	51.78 ± 0.79[e]
	5c	62.5 µM	19.90 ± 0.30[a]	22.85 ± 0.17[a]	25.48 ± 0.25[a]
		125 µM	25.92 ± 0.26[b]	28.88 ± 0.31[b]	30.45± 0.21[b]
		250 µM	35.29 ± 0.50[c]	36.45 ± 0.28[c]	38.72 ± 0.28[c]
		500 µM	42.83 ± 1.50[d]	44.58 ± 0.49[d]	47.90 ± 1.05[d]
		1000 µM	49.57 ± 0.91[e]	52.96 ± 0.65[e]	54.88 ± 0.79[e]
	5d	62.5 µM	20.94 ± 0.30[a]	23.85 ± 0.17[a]	26.68 ± 0.25[a]
		125 µM	27.95 ± 0.26[b]	29.89 ± 0.31[b]	32.45± 0.21[b]

		250 µM	36.73 ± 0.50[c]	38.45 ± 0.28[c]	40.92 ± 0.28[c]
		500 µM	44.83 ± 1.50[d]	46.58 ± 0.49[d]	49.90 ± 1.05[d]
		1000 µM	52.78 ± 0.91[e]	54.76 ± 0.65[e]	56.94 ± 0.79[e]
	5e	62.5 µM	22.48 ± 0.30[a]	24.85 ± 0.17[a]	27.79 ± 0.25[a]
		125 µM	29.95 ± 0.26[b]	30.89 ± 0.31[b]	33.45± 0.21[b]
		250 µM	38.73 ± 0.50[c]	39.45 ± 0.28[c]	42.92 ± 0.28[c]
		500 µM	45.88 ± 1.50[d]	47.58 ± 0.49[d]	52.94 ± 1.05[d]
		1000 µM	53.65 ± 0.91[e]	55.76 ± 0.65[e]	58.94 ± 0.79[e]
	5f	62.5 µM	24.48 ± 0.30[a]	26.85 ± 0.17[a]	29.98 ± 0.25[a]
		125 µM	32.95 ± 0.26[b]	33.90 ± 0.31[b]	36.45± 0.21[b]
		250 µM	39.79 ± 0.50[c]	42.45 ± 0.28[c]	44.95 ± 0.28[c]
		500 µM	46.80 ± 1.50[d]	49.58 ± 0.49[d]	55.94 ± 1.05[d]
		1000 µM	54.69 ± 0.91[e]	56.79 ± 0.65[e]	59.95 ± 0.79[e]
	6a	62.5 µM	11.45 ± 0.06[a]	12.17 ± 0.17[a]	14.45 ± 0.25[a]
		125 µM	20.65 ± 0.26[b]	23.59 ± 0.31[b]	27.60 ± 0.21[b]
		250 µM	38.75 ± 0.50[c]	45.65 ± 0.27[c]	48.89 ± 0.28[c]
		500 µM	60.83 ± 1.5[d]	65.15 ± 0.45[d]	68.17 ± 1.01[d]
		1000 µM	72.32 ± 0.91[e]	76.54 ± 0.65[e]	78.64 ± 0.79[e]
	6b	62.5 µM	9.37 ± 0.06[a]	10.17 ± 0.17[a]	12.33 ± 0.25[a]
		125 µM	18.55 ± 0.26[b]	20.54 ± 0.31[b]	23.67 ± 0.21[b]
		250 µM	35.26 ± 0.50[c]	42.63 ± 0.27[c]	45.80 ± 0.28[c]
		500 µM	58.80 ± 1.50[d]	62.32 ± 0.45[d]	67.21 ± 1.01[d]
		1000 µM	70.12 ± 0.91[e]	73.47 ± 0.65[e]	75.33 ± 0.79[e]
	6c	62.5 µM	7.38 ± 0.06[a]	9.19 ± 0.17[a]	10.20 ± 0.25[a]
		125 µM	16.55 ± 0.26[b]	18.32 ± 0.31[b]	20.47 ± 0.21[b]
		250 µM	32.46 ± 0.50[c]	40.60 ± 0.27[c]	42.84 ± 0.28[c]
		500 µM	54.80 ± 1.50[d]	60.32 ± 0.45[d]	64.21 ± 1.01[d]
		1000 µM	68.20 ± 0.91[e]	70.40 ± 0.65[e]	72.42 ± 0.79[e]
	6d	62.5 µM	10.48 ± 0.06[a]	12.19 ± 0.17[a]	14.38 ± 0.25[a]
		125 µM	22.65 ± 0.27[b]	25.59 ± 0.31[b]	27.44 ± 0.21[b]
		250 µM	43.71 ± 0.50[c]	46.63 ± 0.27[c]	50.28 ± 0.28[c]
		500 µM	68.83 ± 1.50[d]	72.45 ± 0.45[d]	74.17 ± 1.01[d]
		1000 µM	85.32 ± 0.91[e]	88.47 ± 0.65[e]	90.42 ± 0.79[e]
	6e	62.5 µM	12.40 ± 0.06[a]	13.17 ± 0.17[a]	18.78 ± 0.25[a]
		125 µM	25.63 ± 0.26[b]	26.59 ± 0.31[b]	29.54 ± 0.21[b]
		250 µM	44.78 ± 0.50[c]	47.75 ± 0.27[c]	51.27 ± 0.28[c]
		500 µM	66.83 ± 1.50[d]	69.57 ± 0.45[d]	70.38 ± 1.01[d]
		1000 µM	82.42 ± 0.91[e]	84.54 ± 0.65[e]	86.69 ± 0.79[e]
	4a	62.5 µM	7.56 ± 0.40[a]	9.25 ± 0.12[a]	12.15 ± 0.20[a]
		125 µM	15.73 ± 0.32[b]	18.64 ± 0.41[b]	21.24 ± 0.55[b]
		250 µM	27.70 ± 0.22[c]	30.24 ± 0.51[c]	34.75 ± 0.27[c]
		500 µM	36.55 ± 0.93[d]	38.75 ± 0.67[d]	41.45 ± 0.55[d]
		1000 µM	42.91 ± 0.26[e]	45.14 ± 0.47[e]	49.14 ± 0.44[e]
		2000 µM	51.87 ± 0.31[f]	54.50 ± 0.51[f]	56.17 ± 0.24[f]
	4b	62.5 µM	8.45 ± 0.40[a]	10.71 ± 0.12[a]	13.19 ± 0.20[a]
		125 µM	17.73 ± 0.32[b]	19.60 ± 0.41[b]	22.27 ± 0.55[b]
		250 µM	29.72 ± 0.22[c]	32.24 ± 0.51[c]	35.78 ± 0.27[c]
		500 µM	37.59 ± 0.93[d]	39.80 ± 0.67[d]	42.47 ± 0.55[d]
		1000 µM	43.95 ± 0.26[e]	46.18 ± 0.47[e]	50.19 ± 0.44[e]

		2000 µM	52.64 ± 0.31[f]	54.70 ± 0.51[f]	56.57 ± 0.24[f]
	4c	62.5 µM	10.25 ± 0.40[a]	11.91 ± 0.12[a]	13.45 ± 0.20[a]
		125 µM	19.64 ± 0.32[b]	21.60 ± 0.41[b]	23.47 ± 0.55[b]
		250 µM	30.74 ± 0.22[c]	33.45 ± 0.51[c]	36.89 ± 0.27[c]
		500 µM	38.79 ± 0.93[d]	40.80 ± 0.67[d]	42.50 ± 0.55[d]
		1000 µM	44.96 ± 0.26 [e]	47.19 ± 0.47[e]	51.34 ± 0.44[e]
		2000 µM	53.71 ± 0.31[f]	55.72 ± 0.51[f]	57.59 ± 0.24[f]
	4d	62.5 µM	12.25 ± 0.40[a]	14.92 ± 0.12[a]	15.49 ± 0.20[a]
		125 µM	20.64 ± 0.32[b]	22.60 ± 0.41[b]	24.49 ± 0.55[b]
		250 µM	31.74 ± 0.22[c]	34.49 ± 0.51[c]	37.92 ± 0.27[c]
		500 µM	39.75 ± 0.93[d]	41.82 ± 0.67[d]	43.52 ± 0.55[d]
		1000 µM	45.98 ± 0.26[e]	48.22 ± 0.47[e]	52.37 ± 0.44[e]
		2000 µM	54.78 ± 0.31[f]	56.79 ± 0.51[f]	58.65 ± 0.24[f]
	4e	62.5 µM	12.25 ± 0.40[a]	14.92 ± 0.12[a]	15.49 ± 0.20[a]
		125 µM	20.64 ± 0.32[b]	22.60 ± 0.41[b]	24.49 ± 0.55[b]
		250 µM	31.74 ± 0.22[c]	34.49 ± 0.51[c]	37.92 ± 0.27[c]
		500 µM	39.75 ± 0.93[d]	41.82 ± 0.67[d]	43.52 ± 0.55[d]
		1000 µM	45.98 ± 0.26[e]	48.22 ± 0.47[e]	52.37 ± 0.44[e]
		2000 µM	54.78 ± 0.31[f]	56.79 ± 0.51[f]	58.65 ± 0.24[f]
	4f	62.5 µM	13.25 ± 0.40[a]	15.95 ± 0.12[a]	16.79 ± 0.20[a]
		125 µM	22.64 ± 0.32[b]	24.67 ± 0.41[b]	26.55 ± 0.55[b]
		250 µM	32.74 ± 0.22[c]	35.68 ± 0.51[c]	38.94 ± 0.27[c]
		500 µM	40.75 ± 0.93[d]	42.87 ± 0.67[d]	44.59 ± 0.55[d]
		1000 µM	46.90 ± 0.26[e]	48.42 ± 0.47[e]	53.77 ± 0.44[e]
		2000 µM	55.79 ± 0.31[f]	57.85 ± 0.51[f]	59.69 ± 0.24[f]
	5a	62.5 µM	14.25 ± 0.40[a]	16.97 ± 0.12[a]	17.88 ± 0.20[a]
		125 µM	23.64 ± 0.32[b]	25.77 ± 0.41[b]	27.55 ± 0.55[b]
		250 µM	33.94 ± 0.22[c]	35.88 ± 0.51[c]	39.48 ± 0.27[c]
		500 µM	41.79 ± 0.93[d]	43.00 ± 0.67[d]	45.60 ± 0.55[d]
		1000 µM	47.92 ± 0.26[e]	49.41 ± 0.47[e]	54.79 ± 0.44[e]
		2000 µM	56.79 ± 0.31[f]	58.85 ± 0.51[f]	60.70 ± 0.24[f]
	5b	62.5 µM	15.29 ± 0.40[a]	17.97 ± 0.12[a]	19.95 ± 0.20[a]
		125 µM	24.67 ± 0.32[b]	26.79 ± 0.41[b]	28.59 ± 0.55[b]
		250 µM	34.94 ± 0.22[c]	36.89 ± 0.51[c]	39.55 ± 0.27[c]
		500 µM	42.77 ± 0.93[d]	44.68 ± 0.67[d]	46.65 ± 0.55[d]
		1000 µM	48.94 ± 0.26[e]	50.47 ± 0.47[e]	53.80 ± 0.44[e]
		2000 µM	55.79 ± 0.31[f]	59.89 ± 0.51[f]	61.72 ± 0.24[f]
	5c	62.5 µM	17.45 ± 0.40[a]	19.88 ± 0.12[a]	21.97 ± 0.20[a]
		125 µM	25.87 ± 0.32[b]	27.59 ± 0.41[b]	30.47 ± 0.55[b]
		250 µM	35.98 ± 0.22[c]	37.76 ± 0.51[c]	40.58 ± 0.27[c]
		500 µM	43.79 ± 0.93[d]	45.85 ± 0.67[d]	47.88 ± 0.55[d]
		1000 µM	49.90 ± 0.26[e]	52.49 ± 0.47[e]	54.88 ± 0.44[e]
		2000 µM	56.79 ± 0.31[f]	60.75 ± 0.51[f]	62.78 ± 0.24[f]
	5d	62.5 µM	19.45 ± 0.40[a]	21.56 ± 0.12[a]	23.00 ± 0.20[a]
		125 µM	26.95 ± 0.32[b]	28.89 ± 0.41[b]	31.49 ± 0.55[b]
		250 µM	37.03 ± 0.22[c]	39.42 ± 0.51[c]	41.69 ± 0.27[c]
		500 µM	44.87 ± 0.93[d]	46.89 ± 0.67[d]	48.90 ± 0.55[d]
		1000 µM	50.95 ± 0.26[e]	53.86 ± 0.47[e]	55.90 ± 0.44[e]
		2000 µM	58.79 ± 0.31[f]	61.48 ± 0.51[f]	63.79 ± 0.24[f]

	5e	62.5 µM	21.02 ± 0.40[a]	23.59 ± 0.12[a]	25.07 ± 0.20[a]
		125 µM	27.95 ± 0.32[b]	29.89 ± 0.41[b]	32.97 ± 0.55[b]
		250 µM	38.25 ± 0.22[c]	40.42 ± 0.51[c]	42.92 ± 0.27[c]
		500 µM	45.88 ± 0.93[d]	47.99 ± 0.67[d]	49.95 ± 0.55[d]
		1000 µM	52.96 ± 0.26[e]	54.89 ± 0.47[e]	56.92 ± 0.44[e]
		2000 µM	59.88 ± 0.31[f]	62.48 ± 0.51[f]	64.96 ± 0.24[f]
	6a	62.5 µM	22.32 ± 0.40[a]	24.79 ± 0.12[a]	26.77 ± 0.20[a]
		125 µM	28.99 ± 0.32[b]	31.95 ± 0.41[b]	33.98 ± 0.55[b]
		250 µM	40.25 ± 0.22[c]	43.67 ± 0.51[c]	45.88 ± 0.27[c]
		500 µM	47.90 ± 0.93[d]	51.28 ± 0.67[d]	53.95 ± 0.55[d]
		1000 µM	54.00 ± 0.26[e]	56.77 ± 0.47[e]	58.97 ± 0.44[e]
		2000 µM	60.22 ± 0.31[f]	63.85 ± 0.51[f]	65.97 ± 0.24[f]
	6b	62.5 µM	19.56 ± 0.45[a]	21.05 ± 0.17[a]	23.45 ± 0.24[a]
		125 µM	25.79 ± 0.32[b]	29.65 ± 0.41[b]	32.27 ± 0.55[b]
		250 µM	37.75 ± 0.22[c]	40.44 ± 0.51[c]	44.49 ± 0.27[c]
		500 µM	46.57 ± 0.93[d]	49.78 ± 0.67[d]	51.58 ± 0.55[d]
		1000 µM	62.91 ± 0.26[e]	65.14 ± 0.47[e]	69.14 ± 0.44[e]
		2000 µM	71.87 ± 0.31[f]	74.57 ± 0.51[f]	76.52 ± 0.24[f]
	6c	62.5 µM	20.48 ± 0.45[a]	23.05 ± 0.17[a]	25.45 ± 0.24[a]
		125 µM	35.77 ± 0.32[b]	39.69 ± 0.41[b]	42.78 ± 0.55[b]
		250 µM	47.79 ± 0.22[c]	49.45 ± 0.51[c]	52.48 ± 0.27[c]
		500 µM	56.57 ± 0.93[d]	59.78 ± 0.67[d]	63.59 ± 0.55[d]
		1000 µM	64.91 ± 0.26[e]	66.74 ± 0.47[e]	70.84 ± 0.44[e]
		2000 µM	73.87 ± 0.31[f]	75.67 ± 0.51[f]	78.94 ± 0.24[f]
	6d	62.5 µM	23.48 ± 0.45[a]	25.35 ± 0.17[a]	27.68 ± 0.24[a]
		125 µM	38.77 ± 0.32[b]	43.89 ± 0.41[b]	45.79 ± 0.55[b]
		250 µM	49.81 ± 0.22[c]	52.45 ± 0.51[c]	55.49 ± 0.27[c]
		500 µM	59.67 ± 0.93[d]	60.85 ± 0.67[d]	64.89 ± 0.55[d]
		1000 µM	66.95 ± 0.26[e]	69.78 ± 0.47[e]	73.89 ± 0.44[e]
		2000 µM	75.89 ± 0.31[f]	78.87 ± 0.51[f]	81.52 ± 0.24[f]
	6e	62.5 µM	25.48 ± 0.45[a]	27.35 ± 0.17[a]	29.68 ± 0.24[a]
		125 µM	40.77 ± 0.32[b]	42.89 ± 0.41[b]	45.27 ± 0.55[b]
		250 µM	50.85 ± 0.22[c]	53.45 ± 0.51[c]	57.49 ± 0.27[c]
		500 µM	61.68 ± 0.93[d]	63.89 ± 0.67[d]	65.92 ± 0.55[d]
		1000 µM	67.95 ± 0.26[e]	72.88 ± 0.47[e]	74.92 ± 0.44[e]
		2000 µM	76.41 ± 0.31[f]	79.97 ± 0.51[f]	82.85 ± 0.24[f]

Values are expressed as mean ± SD. Means in the same column with distinct superscripts (a – f) are significantly different ($p \leq 0.05$) as separated by the Duncan multiple range test

Table S2. Caspase 3 assay of MDA-MB-468 and HCT 15 cells.

Name of the cell line	Groups	% Caspase 3 expressing cells
MDA-MB-468	Control	2.0 ± 0.04^{b}
	Vehicle control	0.62 ± 0.38^{a}
	5 fluorouracil (100 µM)	96.35 ± 0.44^{g}
	Compound **6f** (62.5 µM)	8.40 ± 0.23^{c}
	Compound **6f** (125 µM)	17.27 ± 0.70^{d}
	Compound **6f** (250 µM)	36.37 ± 1.41^{e}
	Compound **6f** (500 µM)	70.84 ± 1.86^{f}
	Compound **6f** (1000 µM)	97.54 ± 1.29^{g}
HCT 15	Control	2.0 ± 0.02^{b}
	Vehicle control	0.70 ± 0.38^{a}
	5 fluorouracil (100 µM)	96.03 ± 0.48^{h}
	Compound **6f** (62.5 µM)	7.58 ± 0.35^{c}
	Compound **6f** (125 µM)	16.84 ± 0.41^{d}
	Compound **6f** (250 µM)	35.36 ± 0.74^{e}
	Compound **6f** (500 µM)	62.49 ± 1.28^{f}
	Compound **6f** (1000 µM)	94.63 ± 1.93^{h}
	Compound **6f** (2000 µM)	89.27 ± 0.97^{g}

Values are expressed as mean ± SD. Means in the same column with distinct superscripts (a – h) are significantly different ($p \leq 0.05$) as separated by the Duncan multiple range test.

Table S3. Apoptotic assay of MDA-MB-468 and HCT 15 cells.

Name of the cell line	Groups	% Dead cells
MDA-MB-468	Control	2.00 ± 0.02^{a}
	Vehicle control	2.50 ± 0.38^{a}
	5 fluorouracil (100 µM)	93.03 ± 0.54^{e}
	Compound **6f** (250 µM)	45.75 ± 1.19^{b}
	Compound **6f** (500 µM)	83.31 ± 1.14^{d}
	Compound **6f** (1000 µM)	79.30 ± 0.19^{c}
HCT 15	Control	2.00 ± 0.02^{a}
	Vehicle control	2.70 ± 0.38^{a}
	5 fluorouracil (100 µM)	86.15 ± 0.64^{e}
	Compound **6f** (500 µM)	76.49 ± 1.31^{d}
	Compound **6f** (1000 µM)	73.57 ± 0.08^{c}
	Compound **6f** (2000 µM)	70.27 ± 0.18^{b}

Values are expressed as mean ± SD. Means in the same column with distinct superscripts (a - e) are significantly different ($p \leq 0.05$) as separated by the Duncan multiple range test.

Table S4. Cell cycle analysis of MDA-MB-468 cells after 48 h.

Concentration (µM)	Sub G_o/G_1 (%)	G_o/G_1 (%)	S (%)	G_2/M
Vehicle control	1.78	72.5	13.4	6.87
5 fluorouracil (100 µM)	35.46	51.25	8.6	1.54
Compound **6f** (50 µM)	17.49	67.41	12.05	4.55
Compound **6f** (100 µM)	48.65	38.48	14.5	3.14
Compound **6f** (200 µM)	44.5	41.41	7.75	5.47

Table S5. Cell cycle analysis of HCT 15 cells after 48 h.

Concentration (µM)	Sub G_o/G_1 (%)	G_o/G_1 (%)	S (%)	G_2/M
Vehicle control	4.12	72.41	6.92	19.25
5 fluorouracil (100 µM)	1.15	54.88	5.25	40.56
Compound **6f** (50 µM)	3.37	62.5	14	23.12
Compound **6f** (100 µM)	1.6	44.2	4.25	48.85
Compound **6f** (200 µM)	2.87	46.5	6.2	43.25

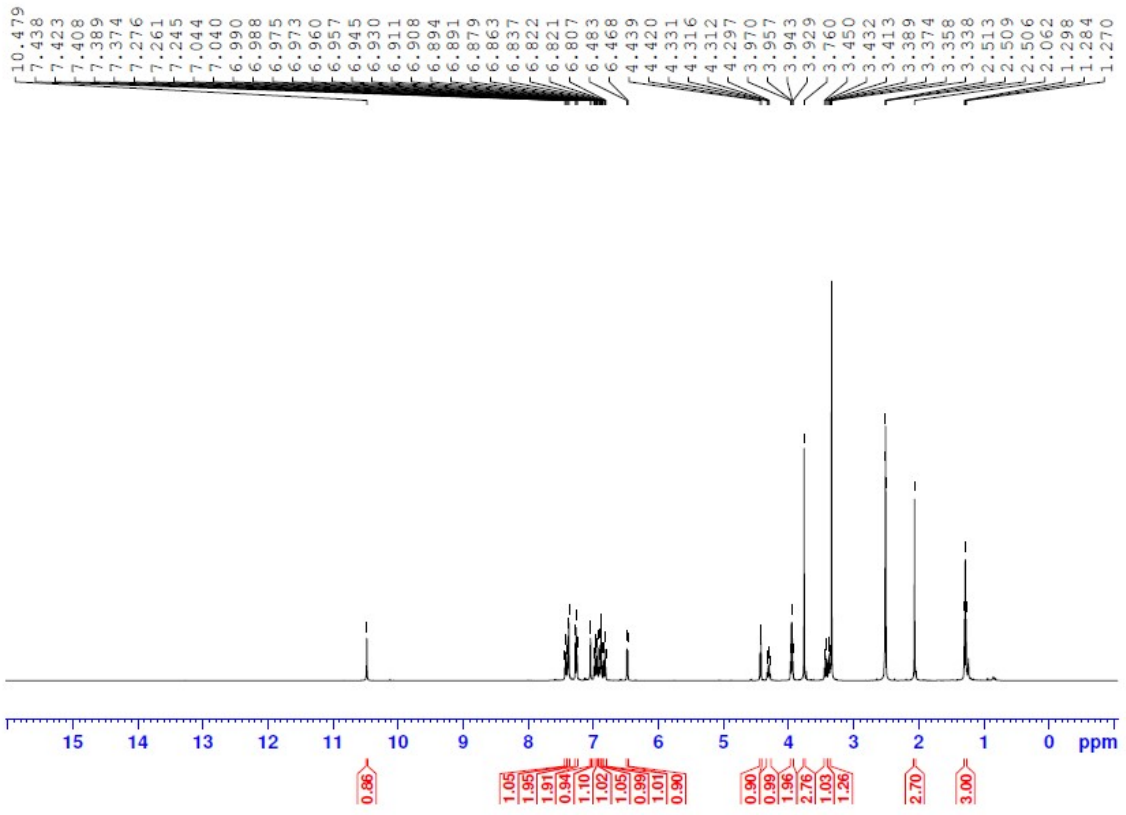

Figure S1. ^{1}H NMR spectrum of compound **4a**.

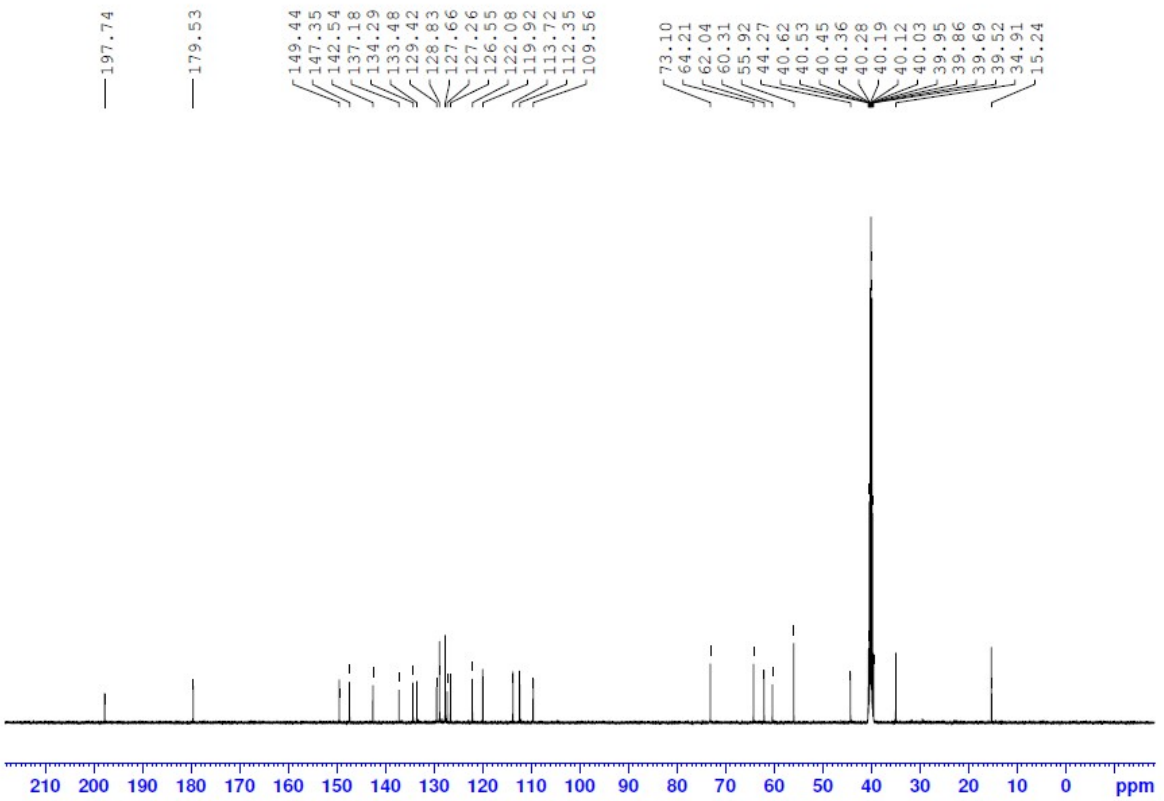

Figure S2. ^{13}C NMR spectrum of compound **4a**.

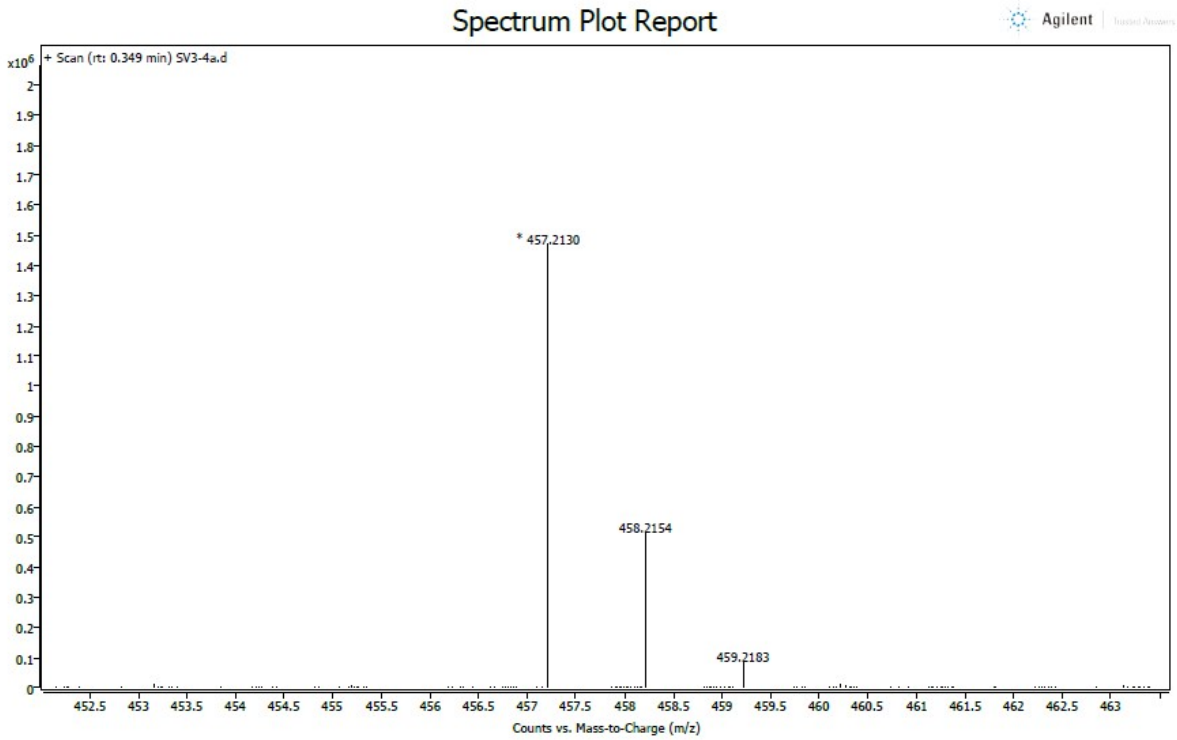

Figure S3. HR-MS spectrum of compound **4a**.

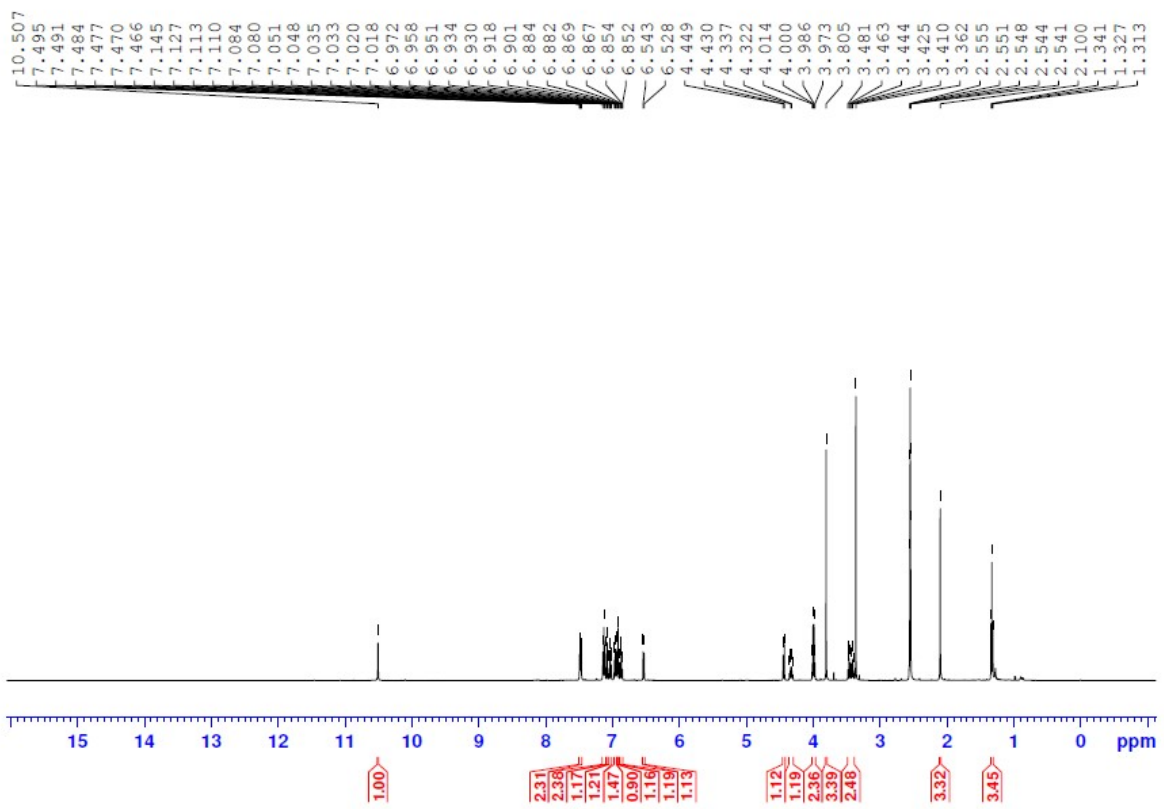

Figure S4. ^{1}H NMR spectrum of compound **4b**.

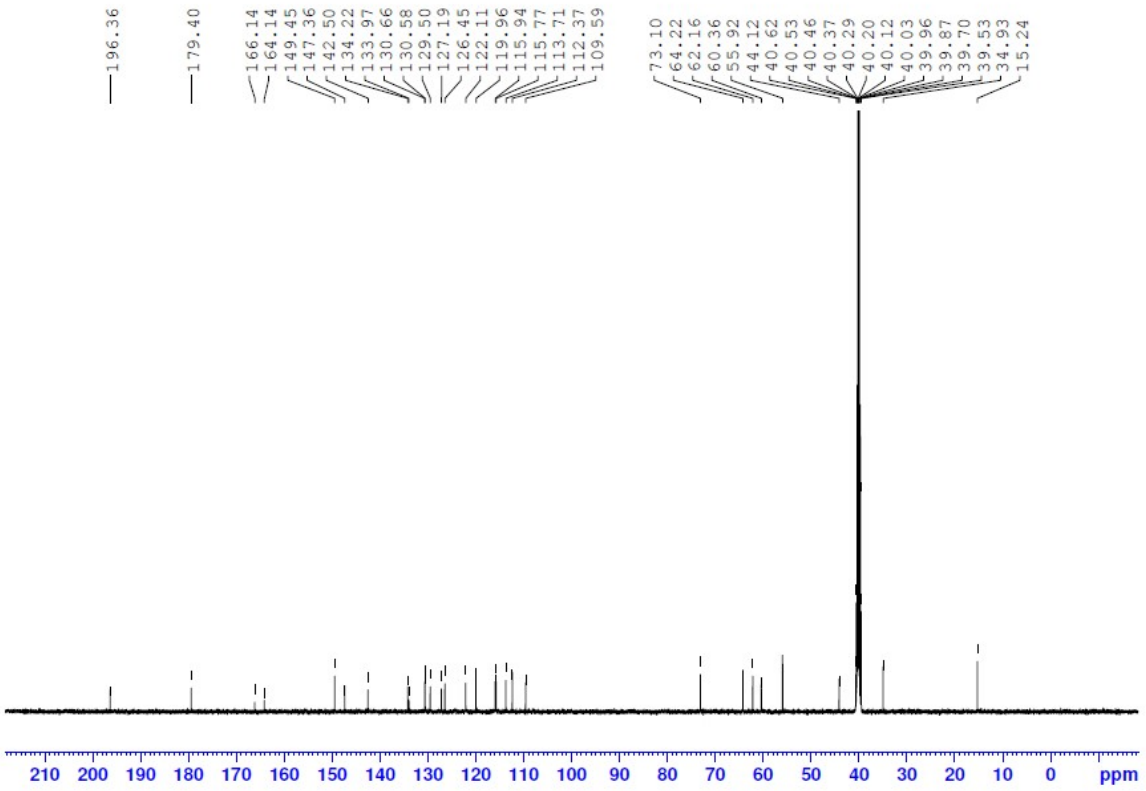

Figure S5. ^{13}C NMR spectrum of compound **4b**.

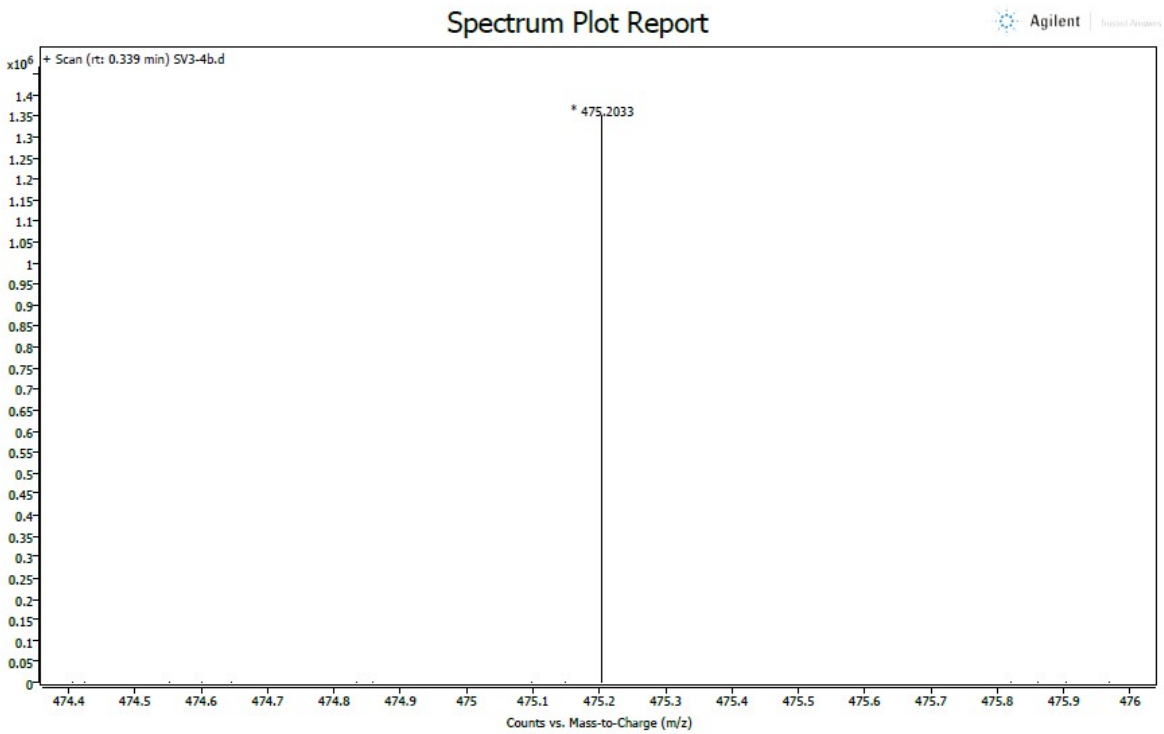

Figure S6. HR-MS spectrum of compound **4b**.

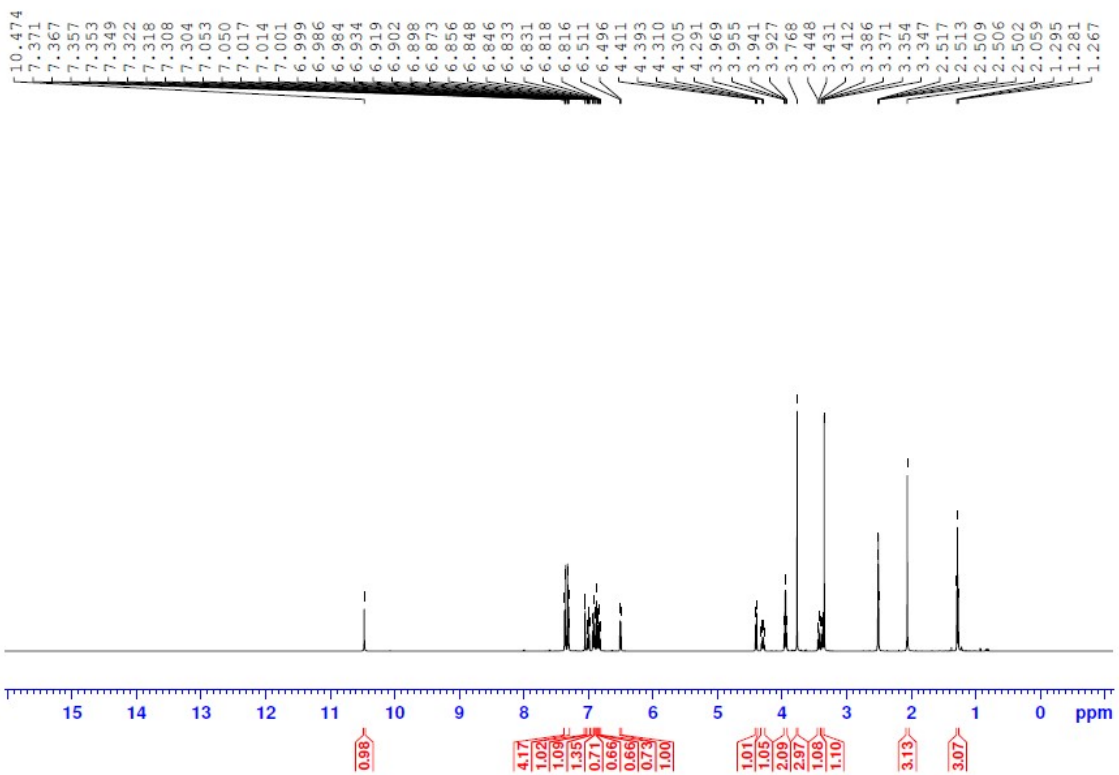

Figure S7. ^{1}H NMR spectrum of compound **4c**.

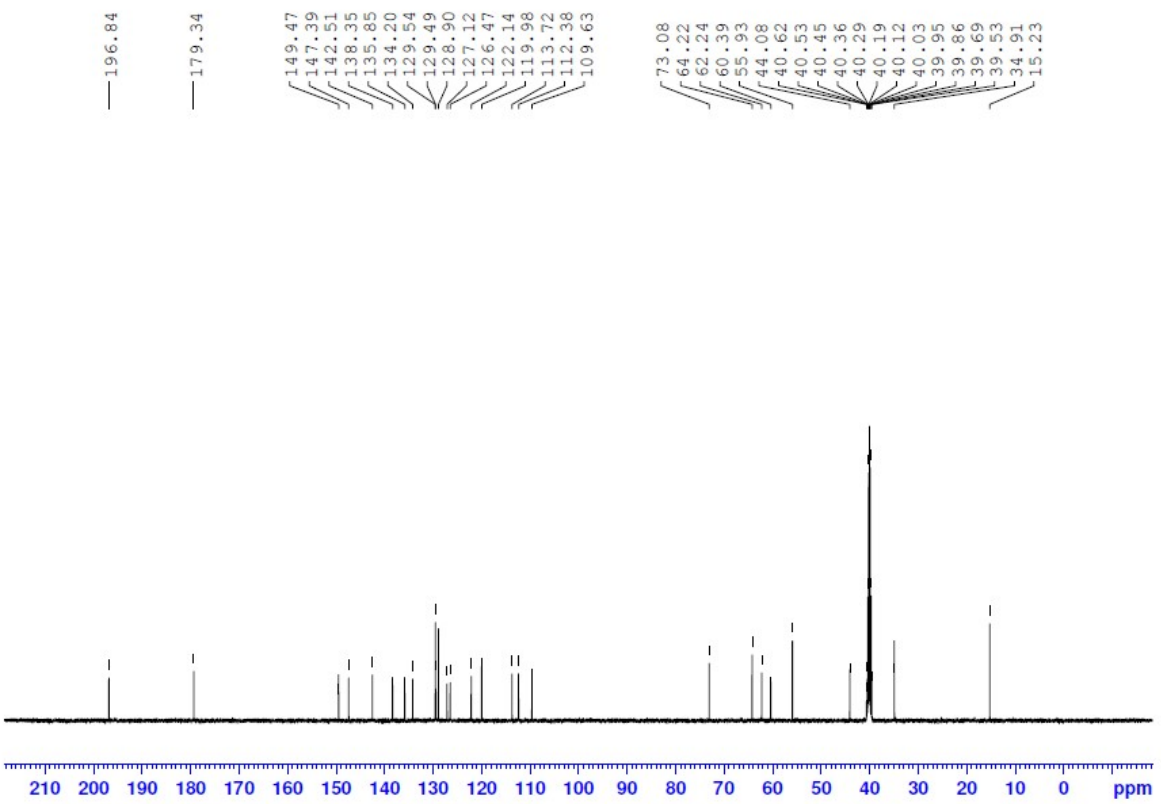

Figure S8. ^{13}C NMR spectrum of compound **4c**.

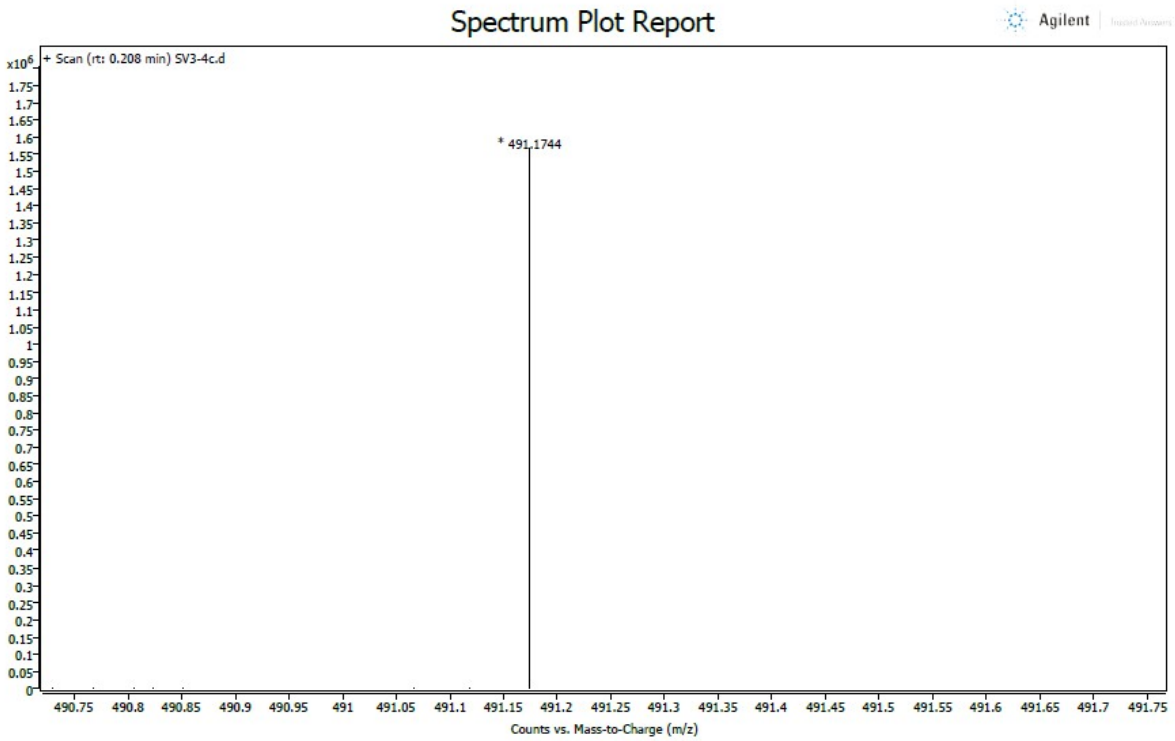

Figure S9. HR-MS spectrum of compound **4c**.

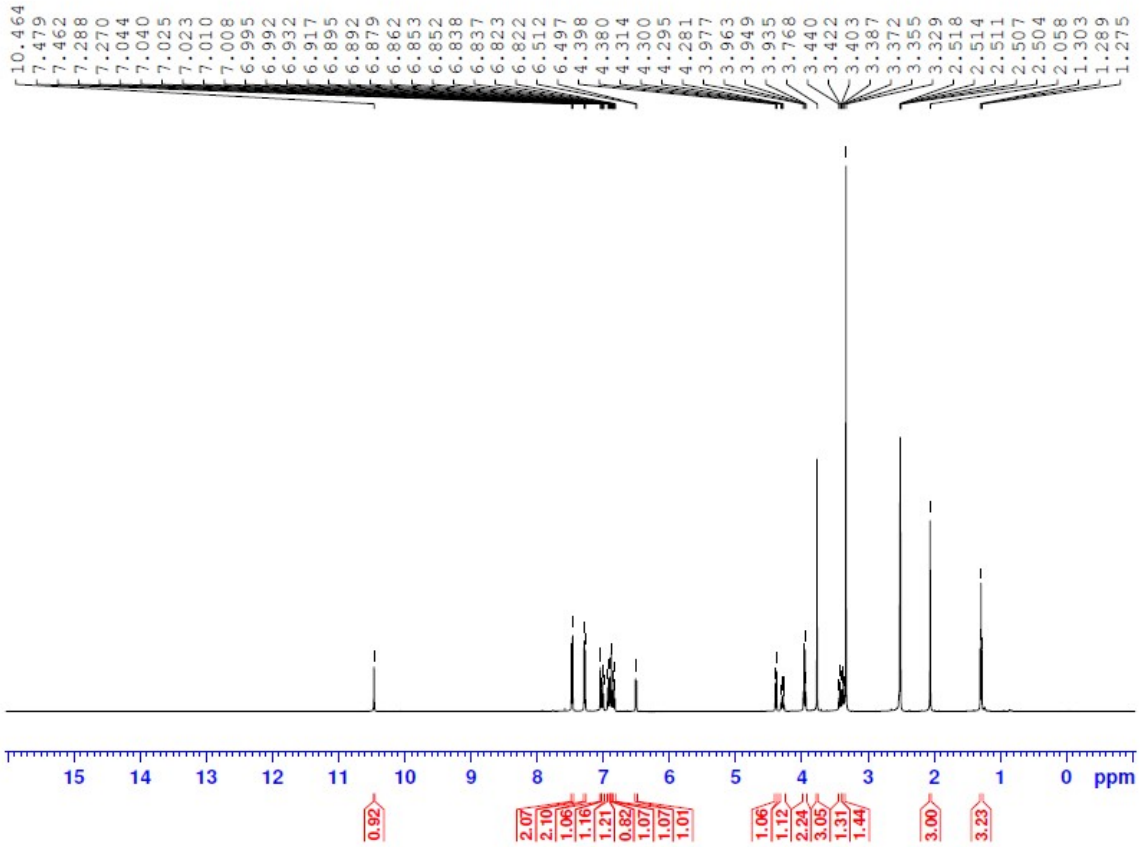

Figure S10. ^{1}H NMR spectrum of compound **4d**.

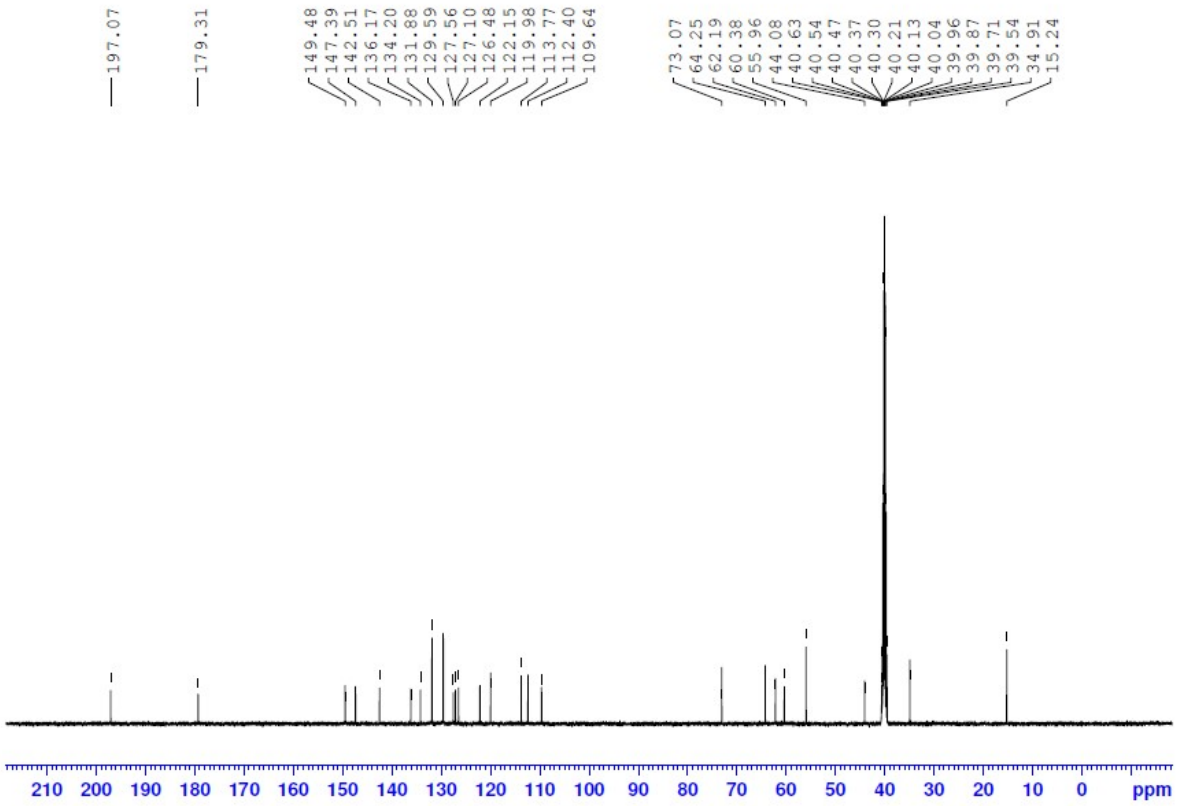

Figure S11. ^{13}C NMR spectrum of compound **4d**.

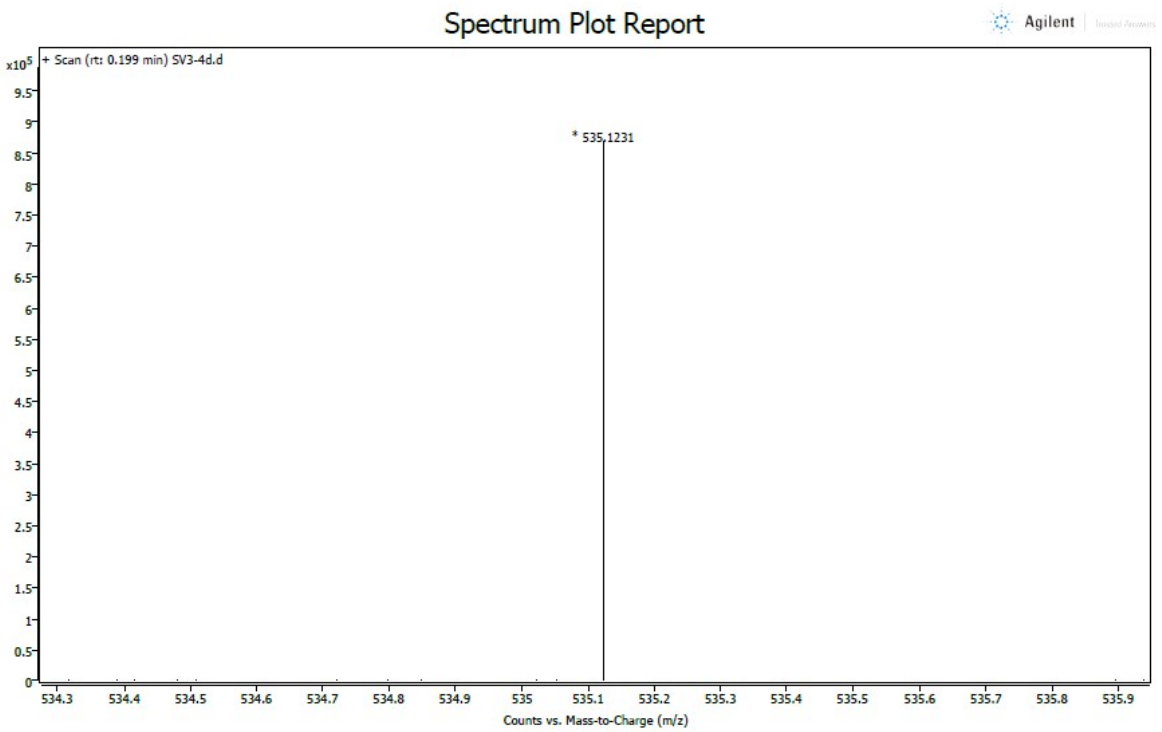

Figure S12. HR-MS spectrum of compound **4d**.

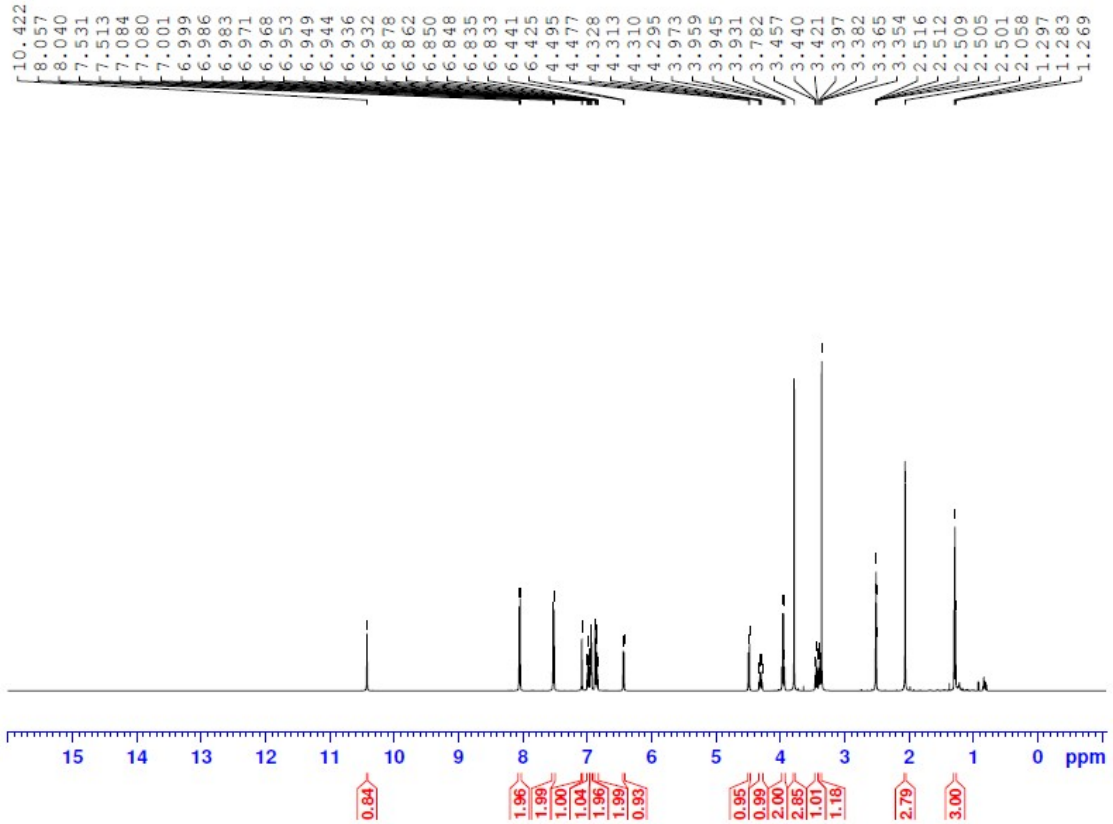

Figure S13. ^{1}H NMR spectrum of compound **4e**.

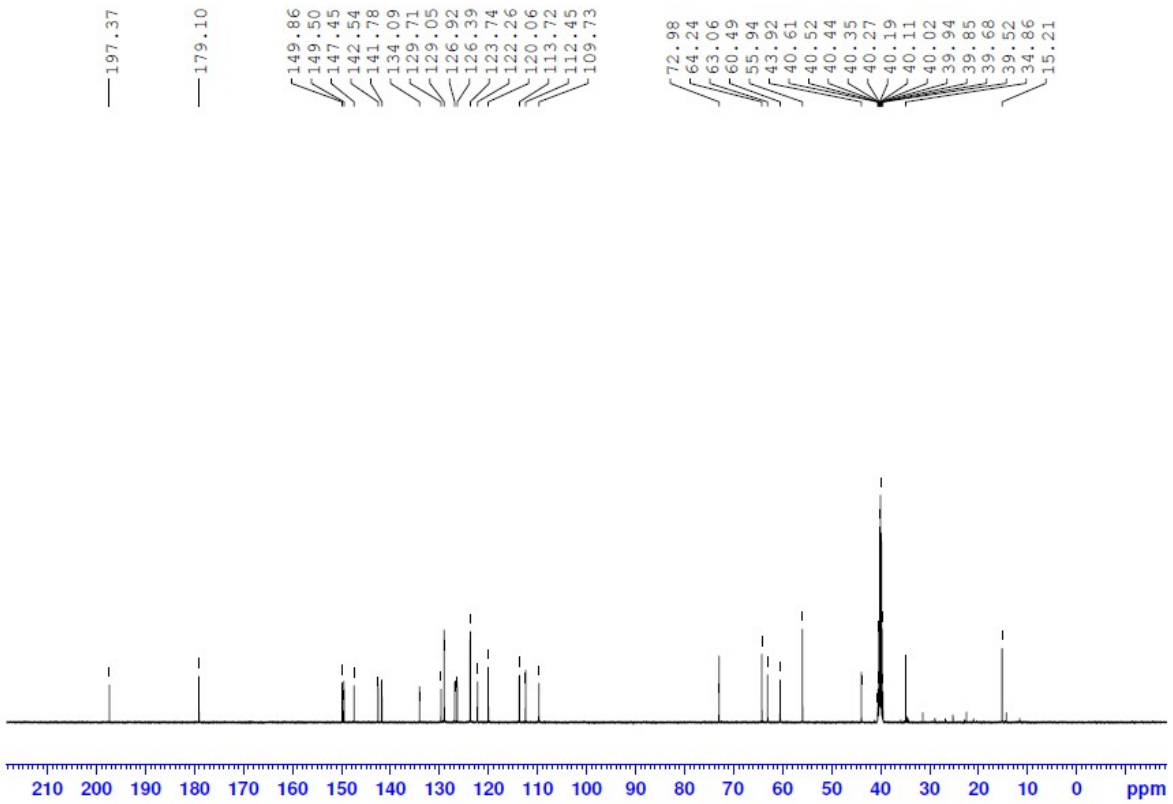

Figure S14. ^{13}C NMR spectrum of compound **4e**.

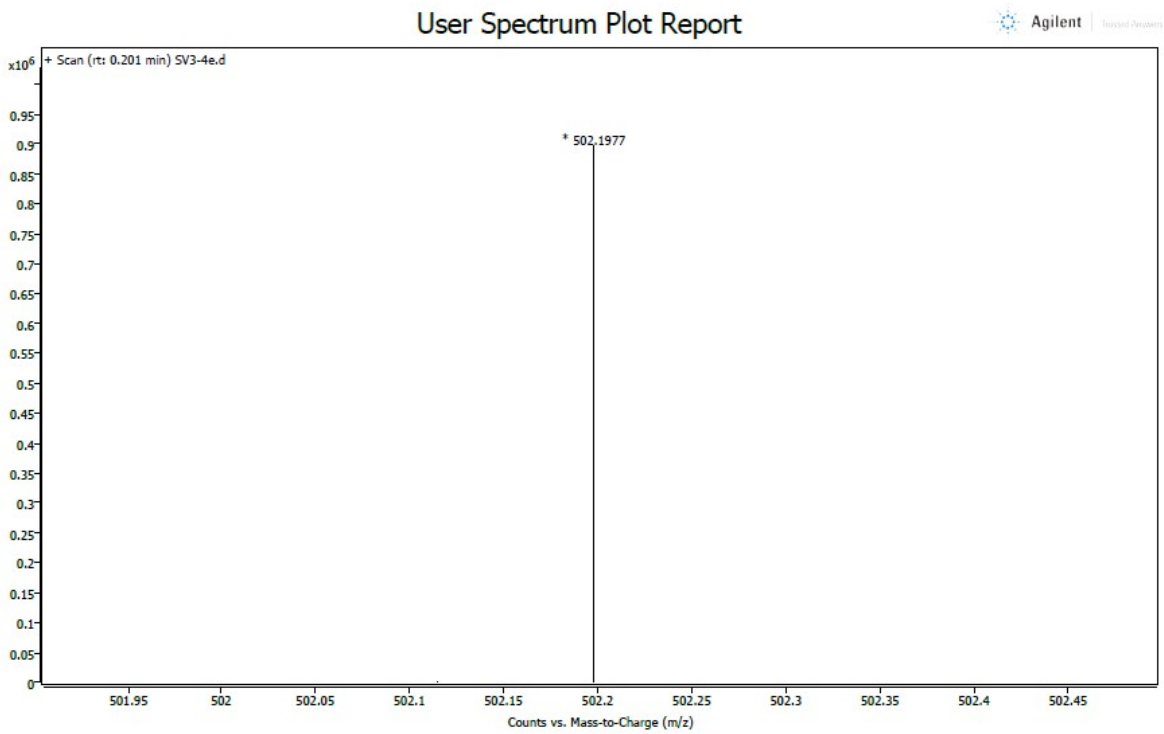

Figure S15. HR-MS spectrum of compound **4e**.

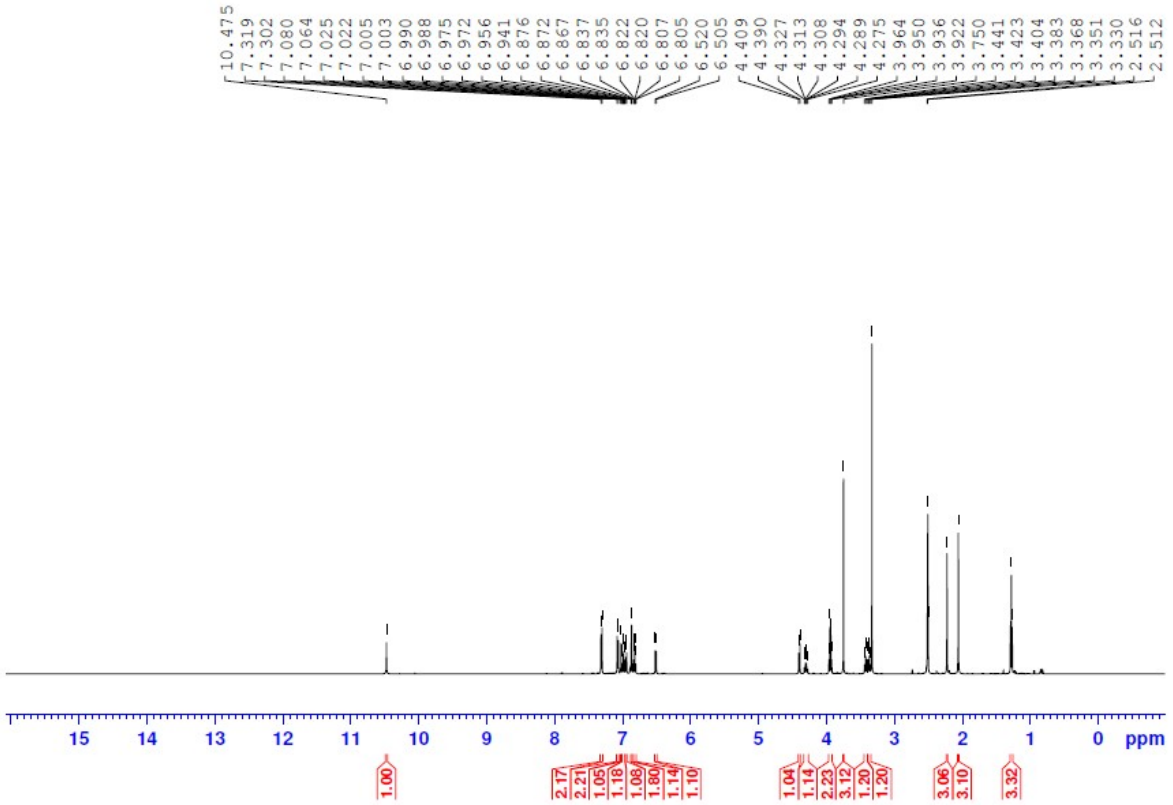

Figure S16. ^{1}H NMR spectrum of compound **4f**.

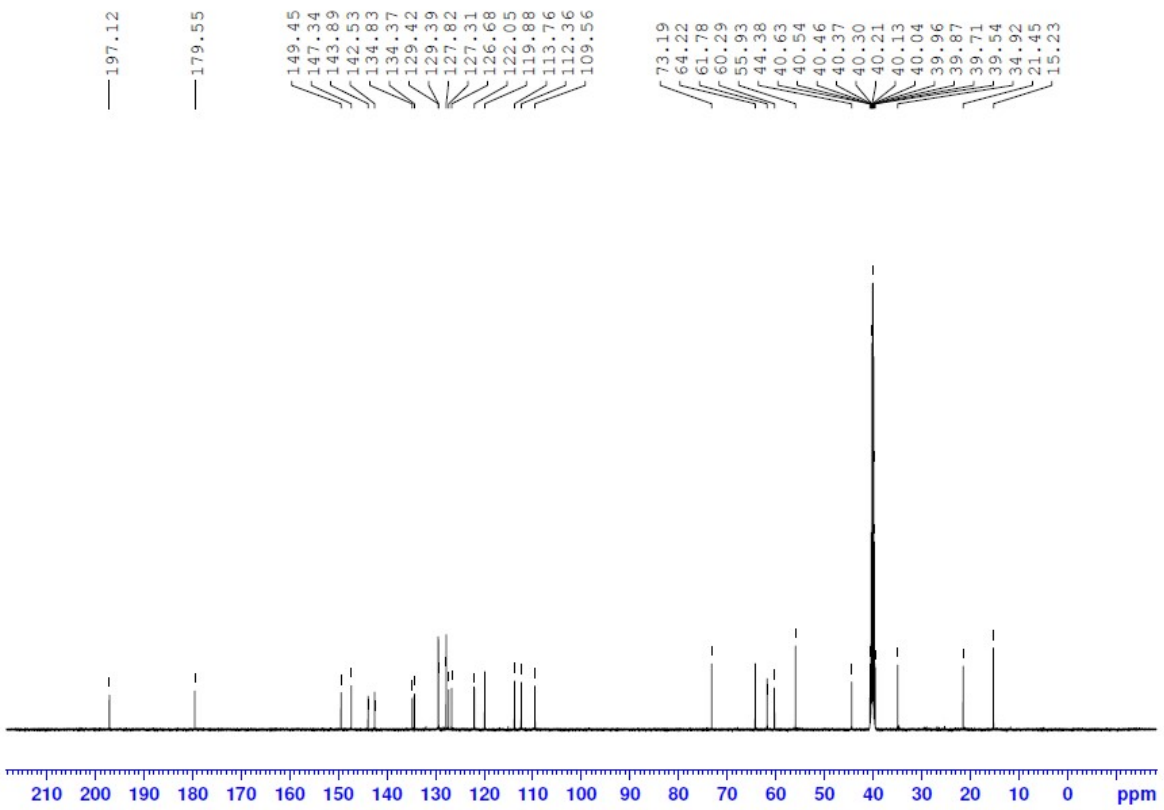

Figure S17. ^{13}C NMR spectrum of compound **4f**.

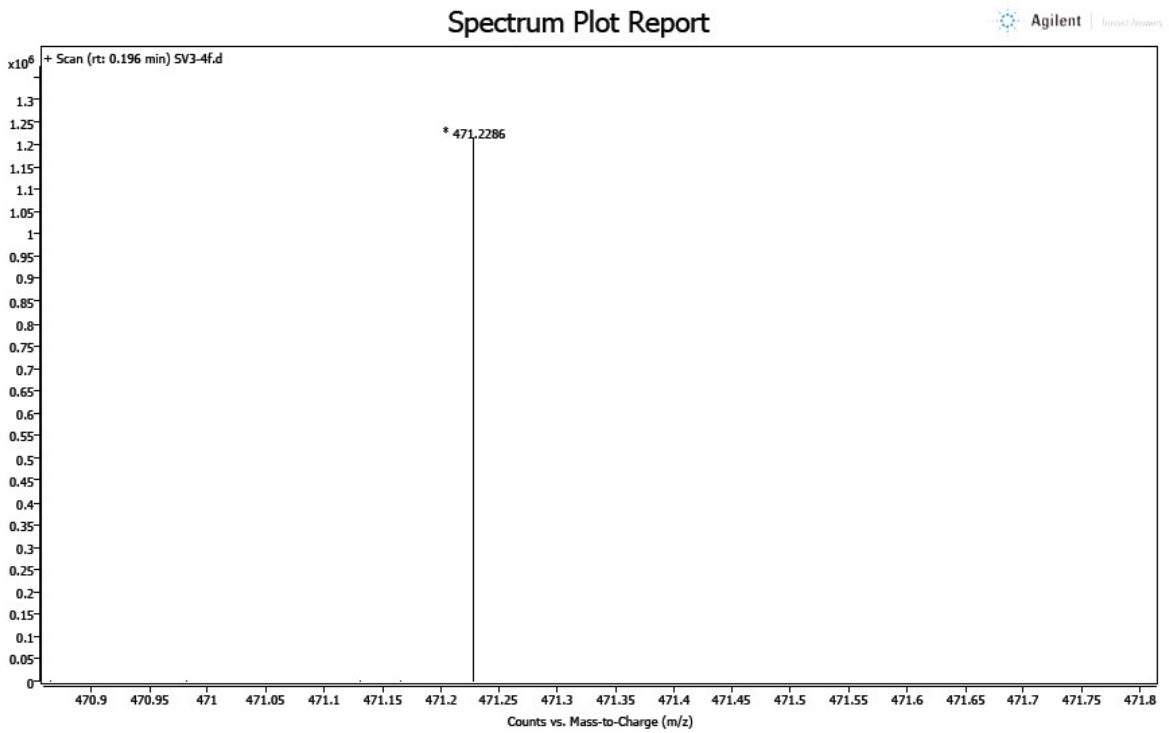

Figure S18. HR-MS spectrum of compound **4f**.

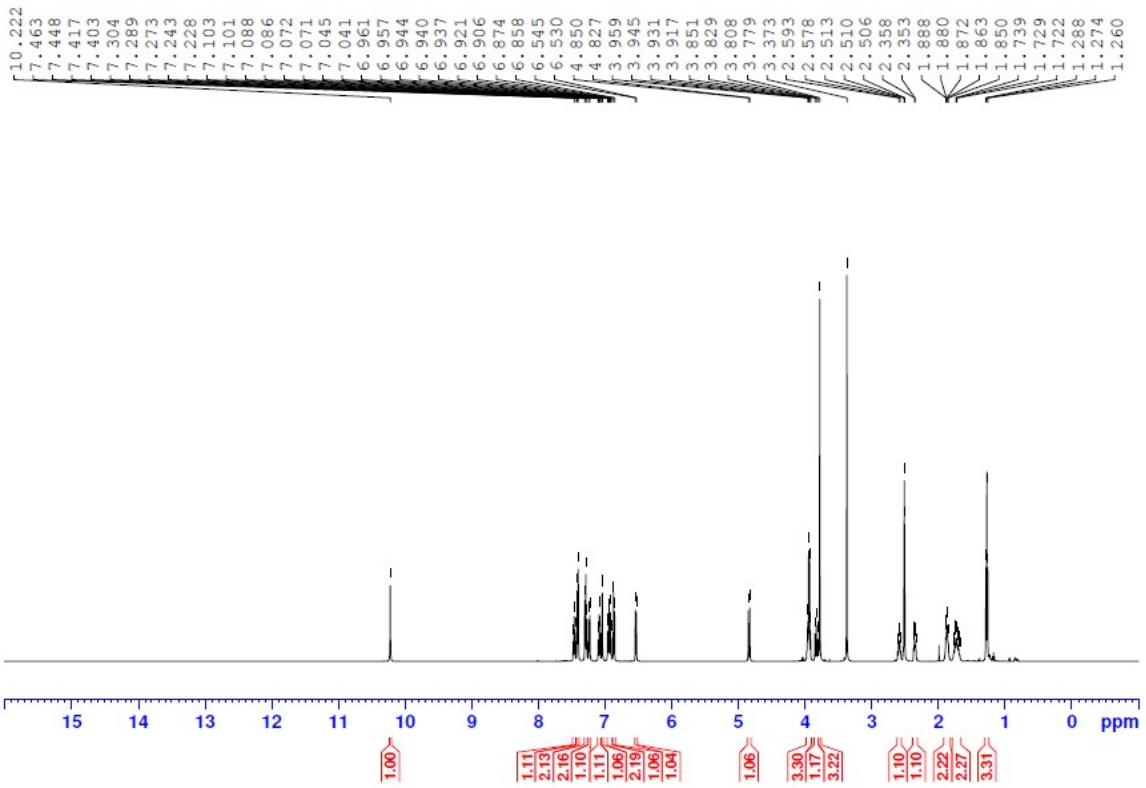

Figure S19. ^{1}H NMR spectrum of compound **5a**.

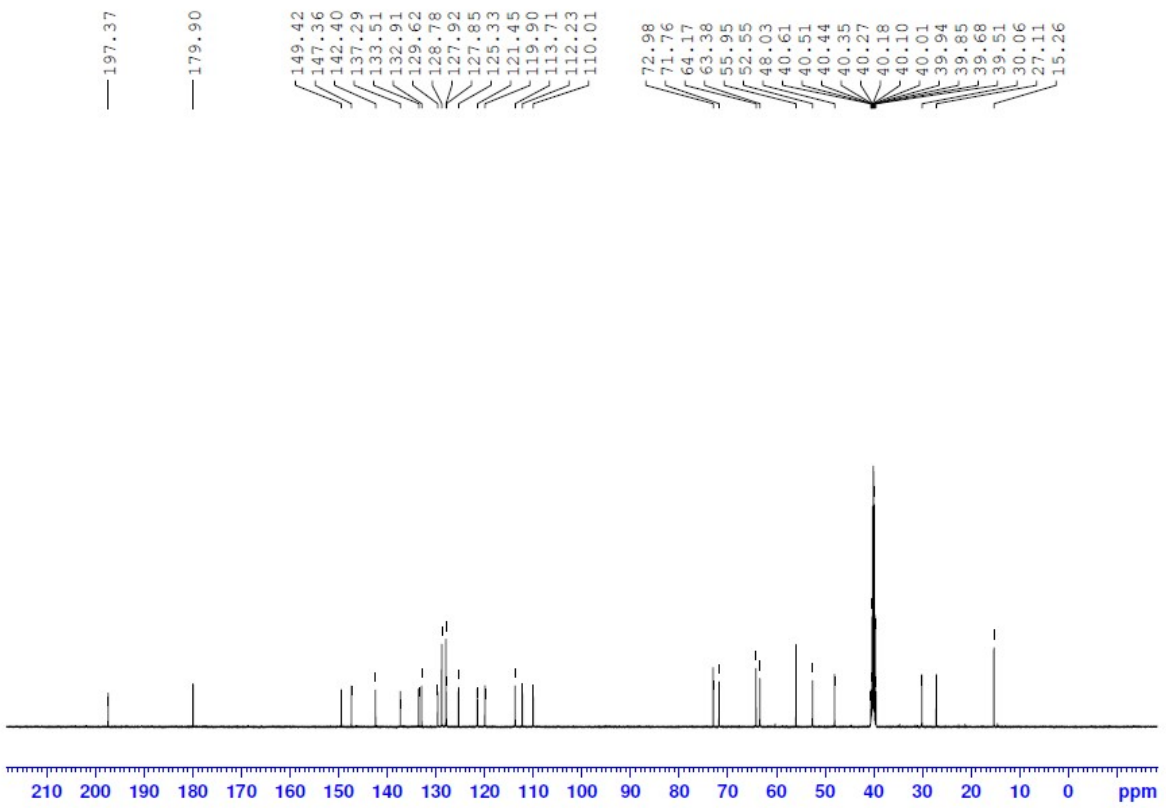

Figure S20. ^{13}C NMR spectrum of compound **5a**.

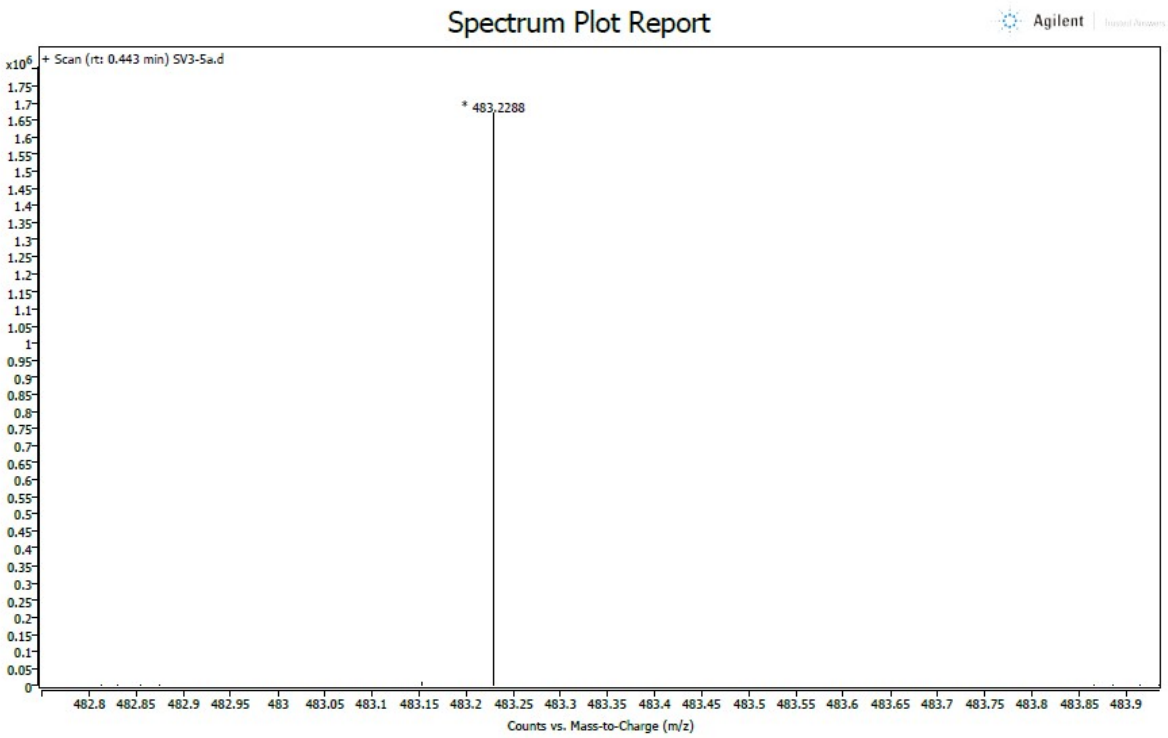

Figure S21. HR-MS spectrum of compound **5a**.

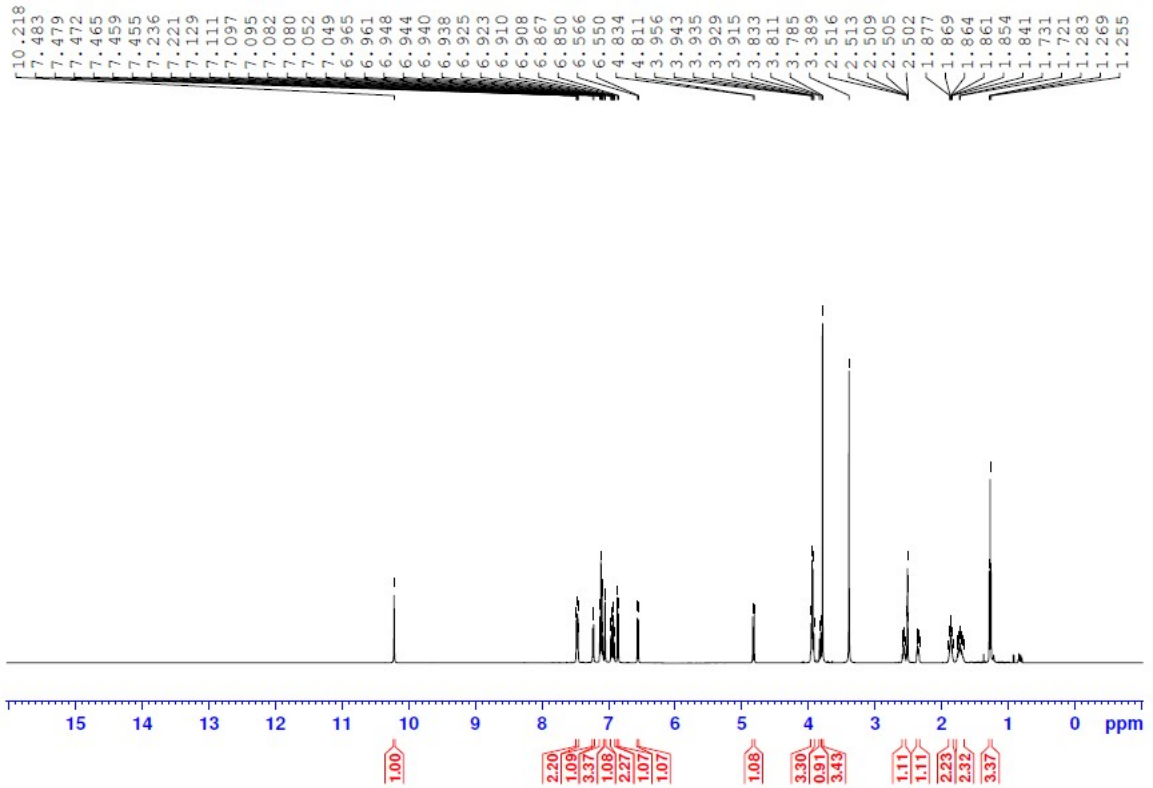

Figure S22. ^{1}H NMR spectrum of compound **5b**.

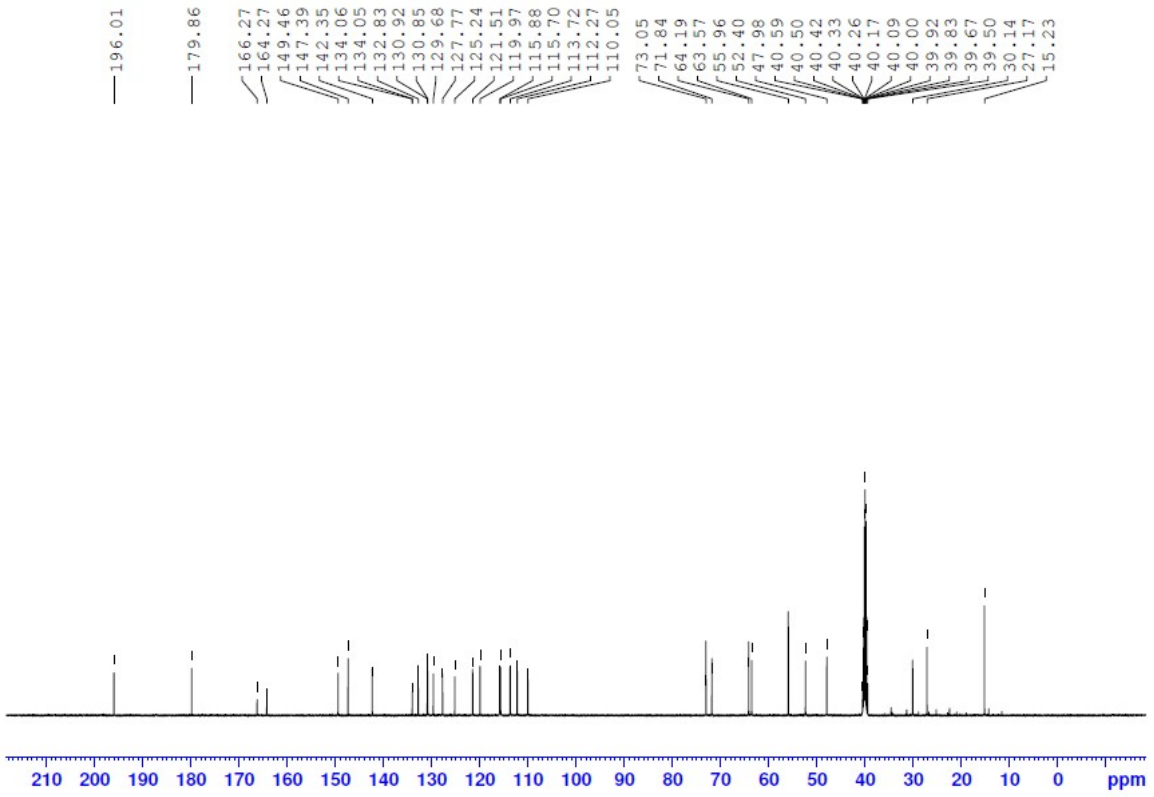

Figure S23. ^{13}C NMR spectrum of compound **5b**.

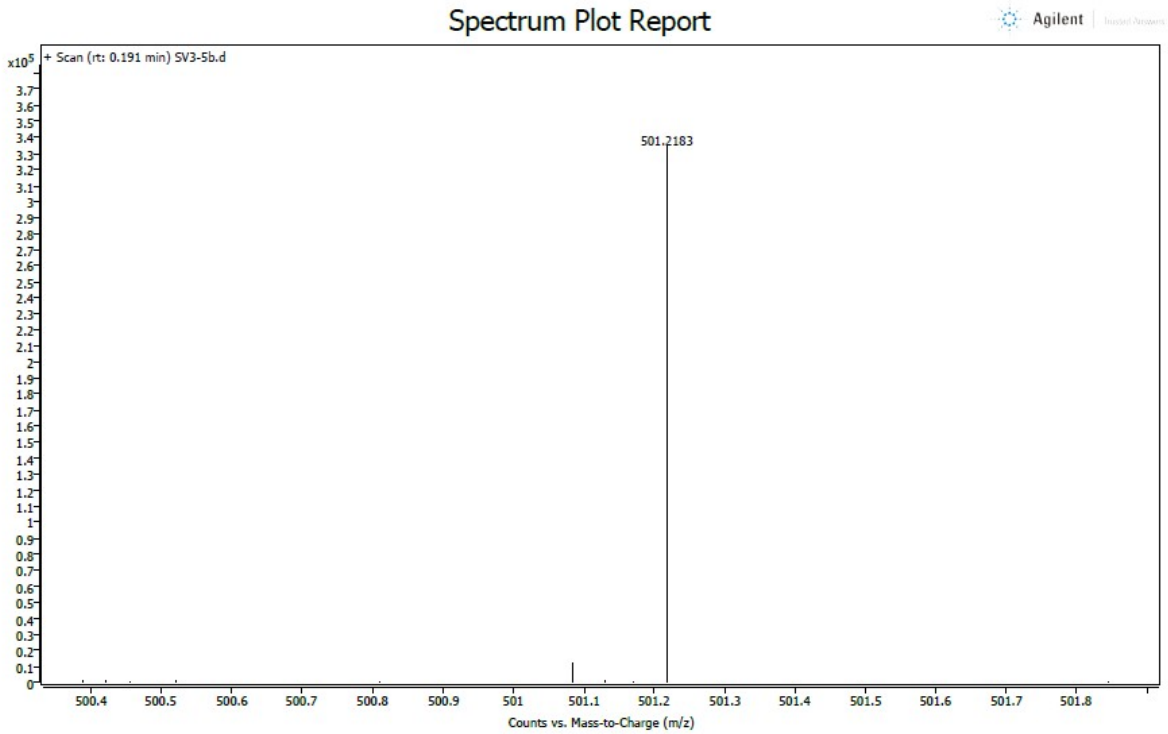

Figure S24. HR-MS spectrum of compound **5b**.

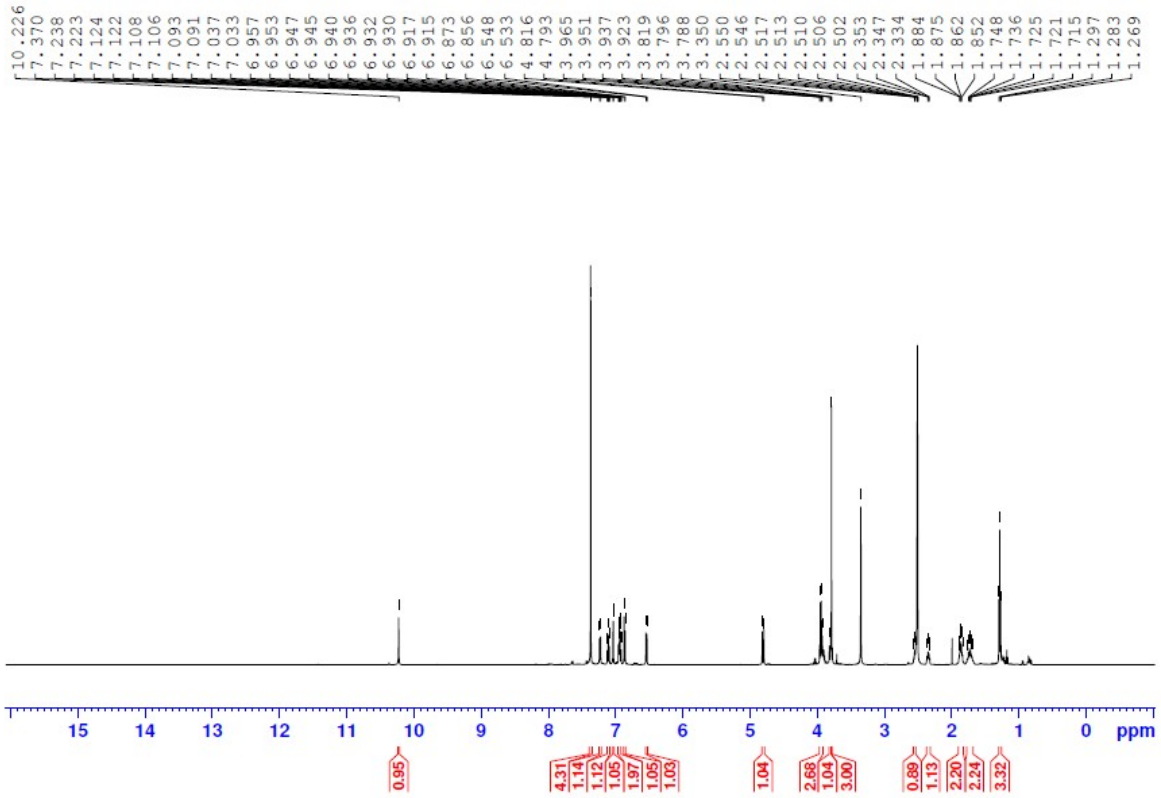

Figure S25. ^{1}H NMR spectrum of compound **5c**.

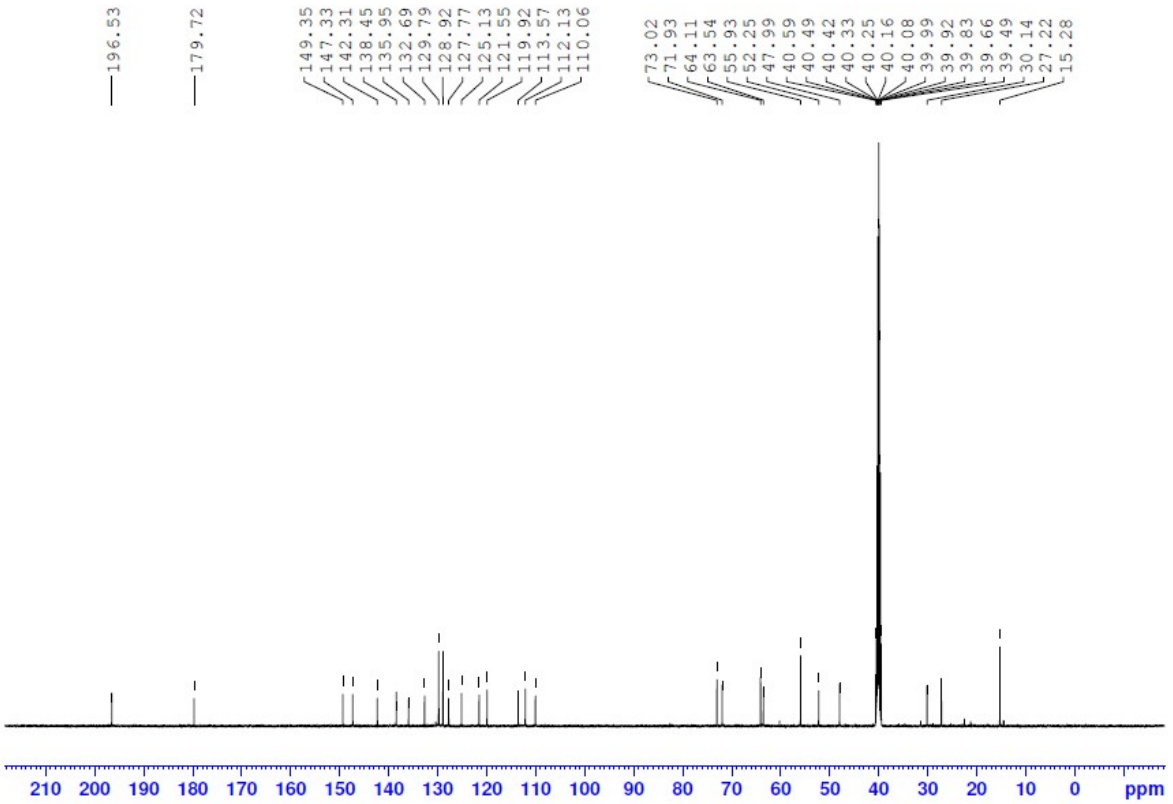

Figure S26. ^{13}C NMR spectrum of compound **5c**.

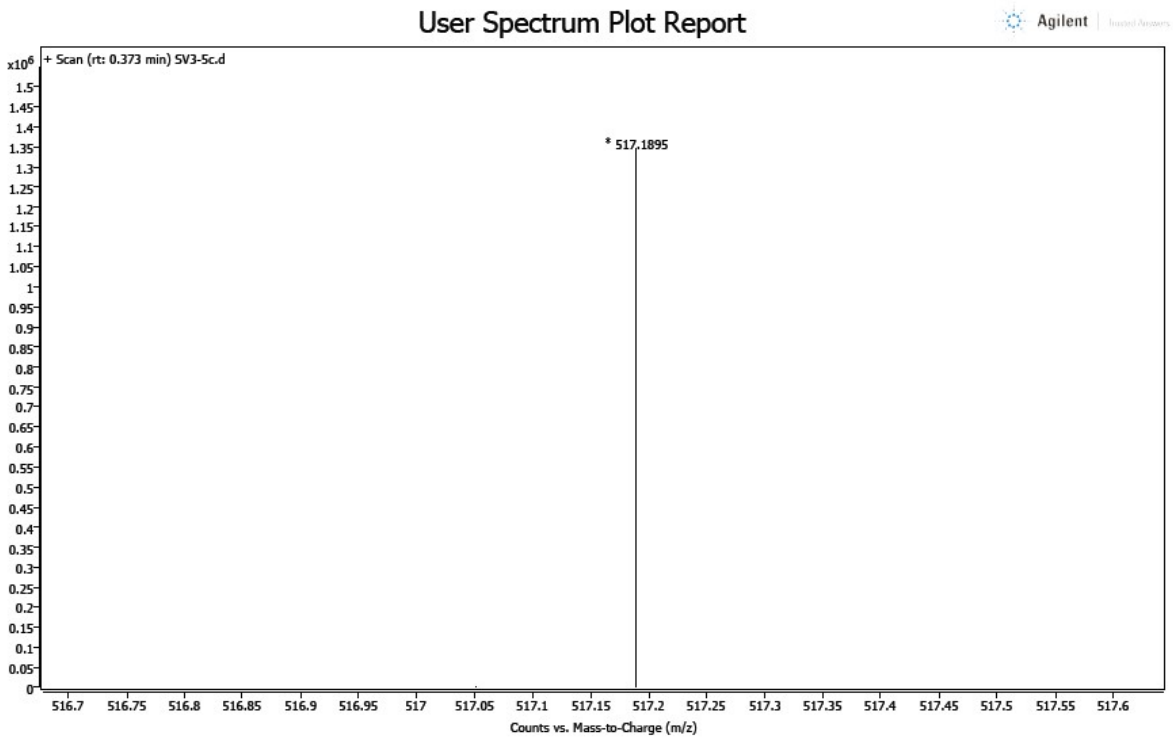

Figure S27. HR-MS spectrum of compound **5c**.

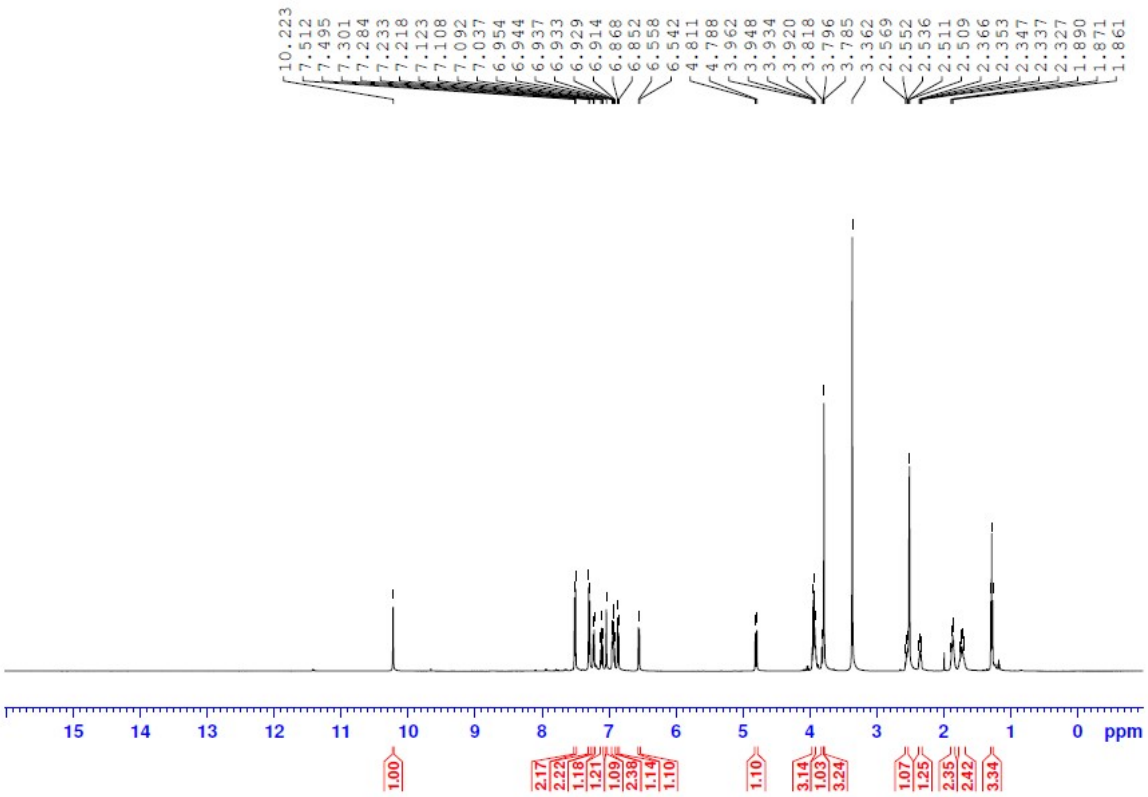

Figure S28. ^{1}H NMR spectrum of compound **5d**.

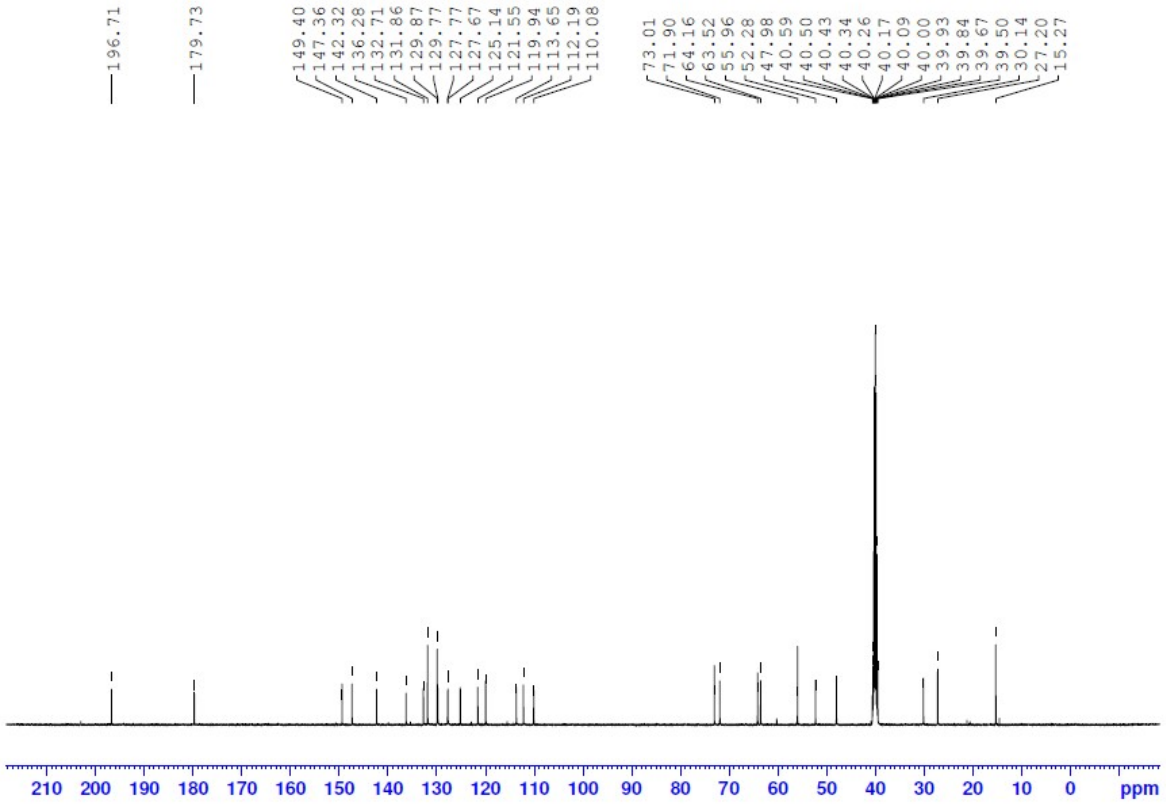

Figure S29. ^{13}C NMR spectrum of compound **5d**.

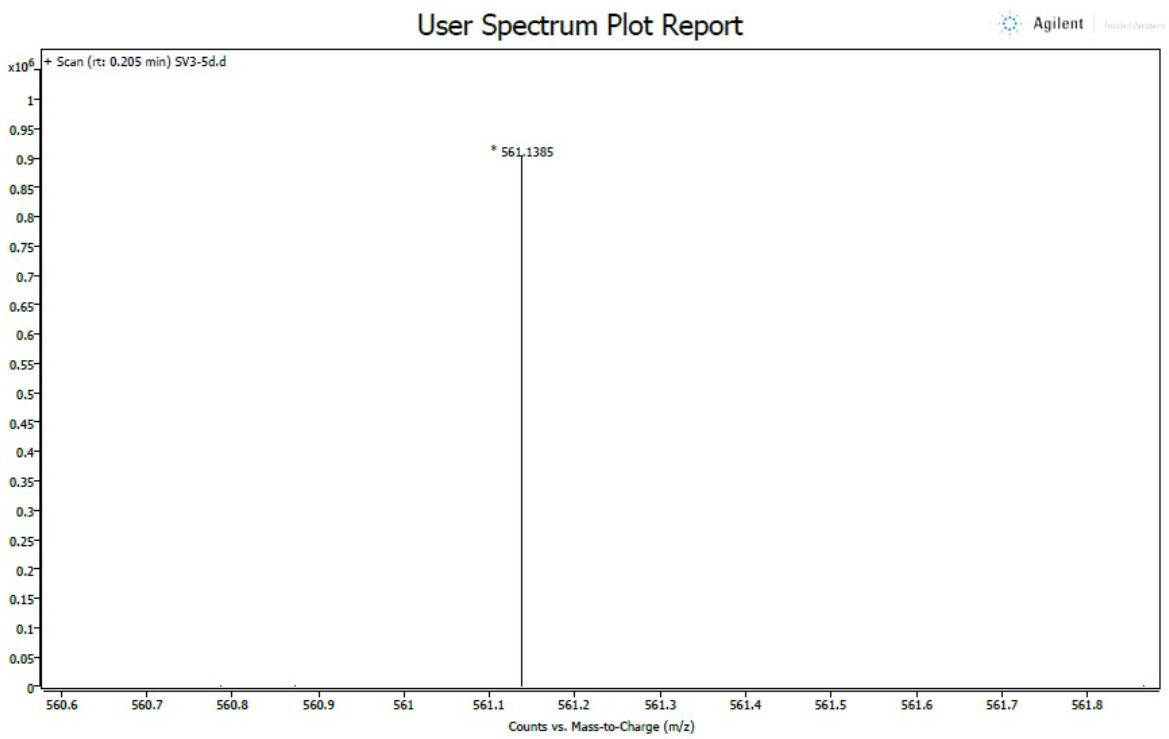

Figure S30. HR-MS spectrum of compound **5d**.

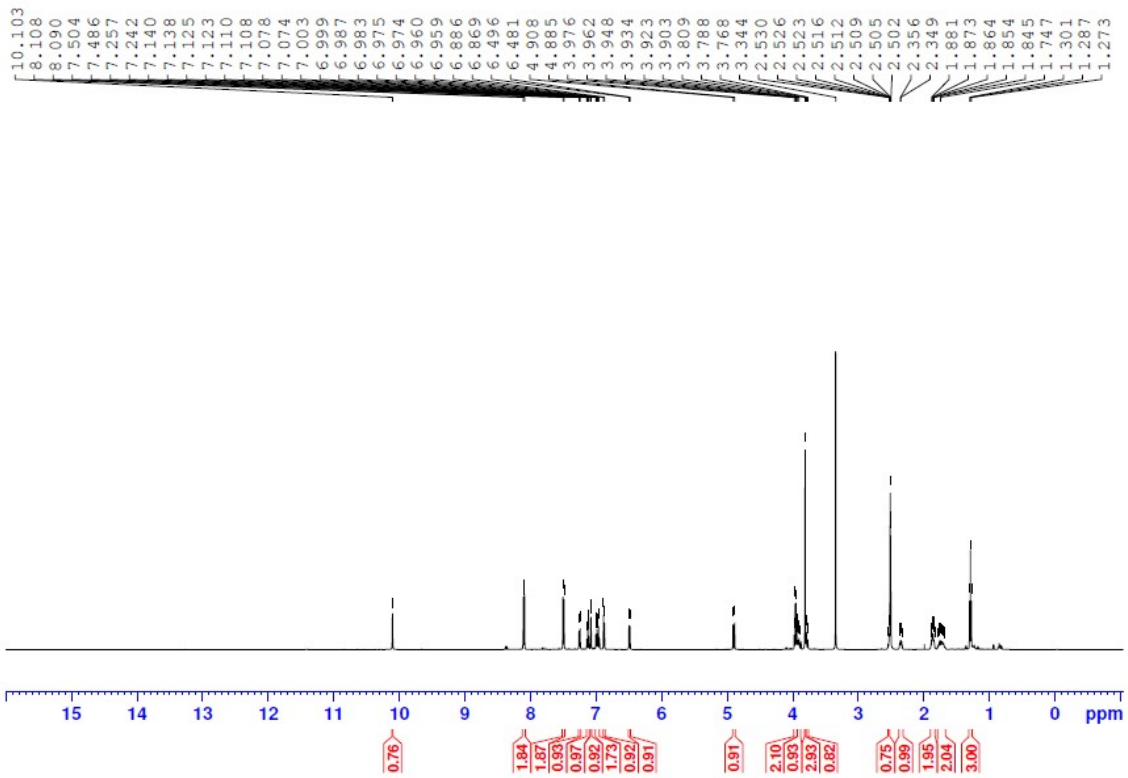

Figure S31. ^{1}H NMR spectrum of compound **5e**.

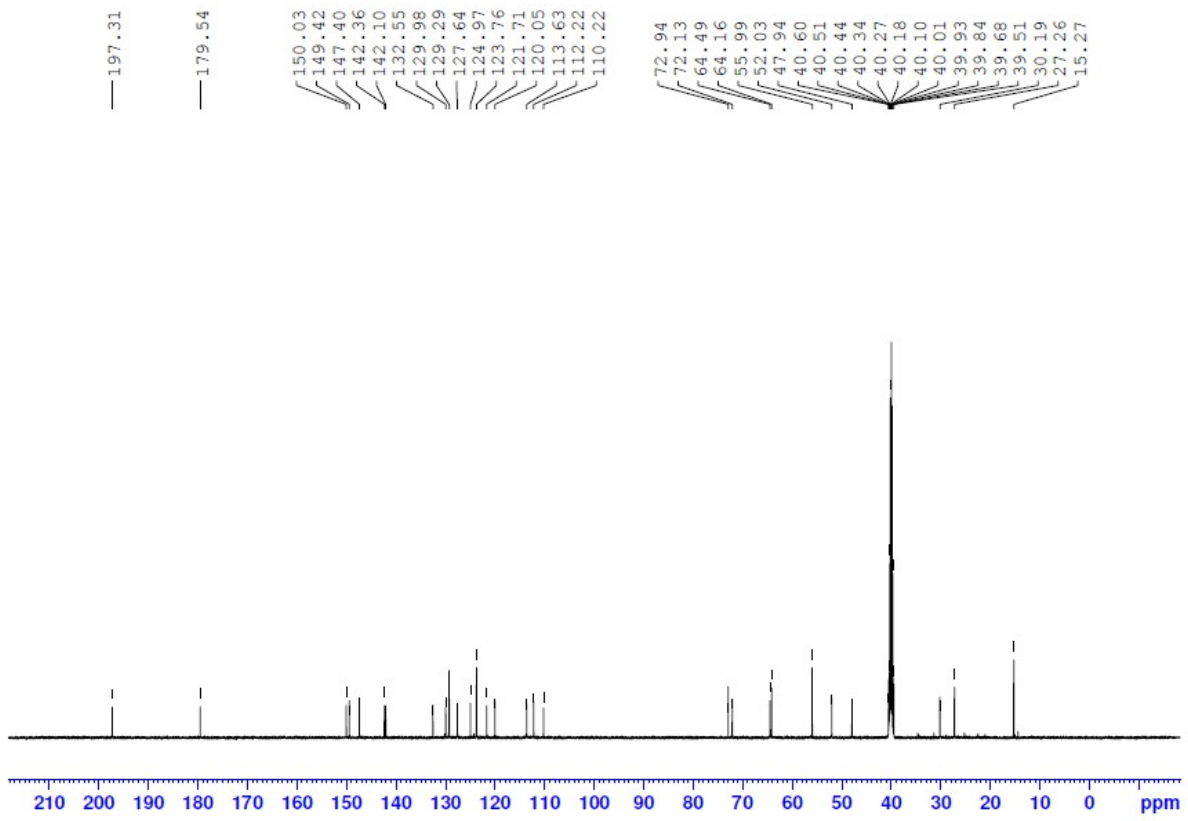

Figure S32. ^{13}C NMR spectrum of compound **5e**.

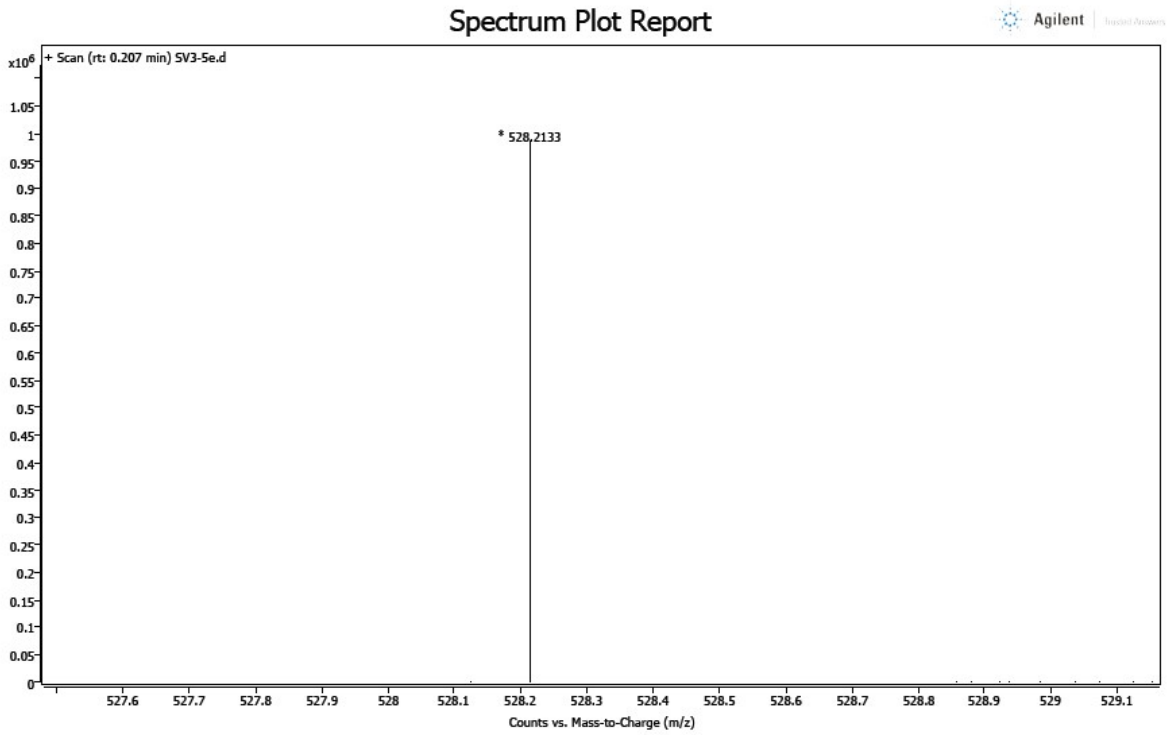

Figure S33. HR-MS spectrum of compound **5e**.

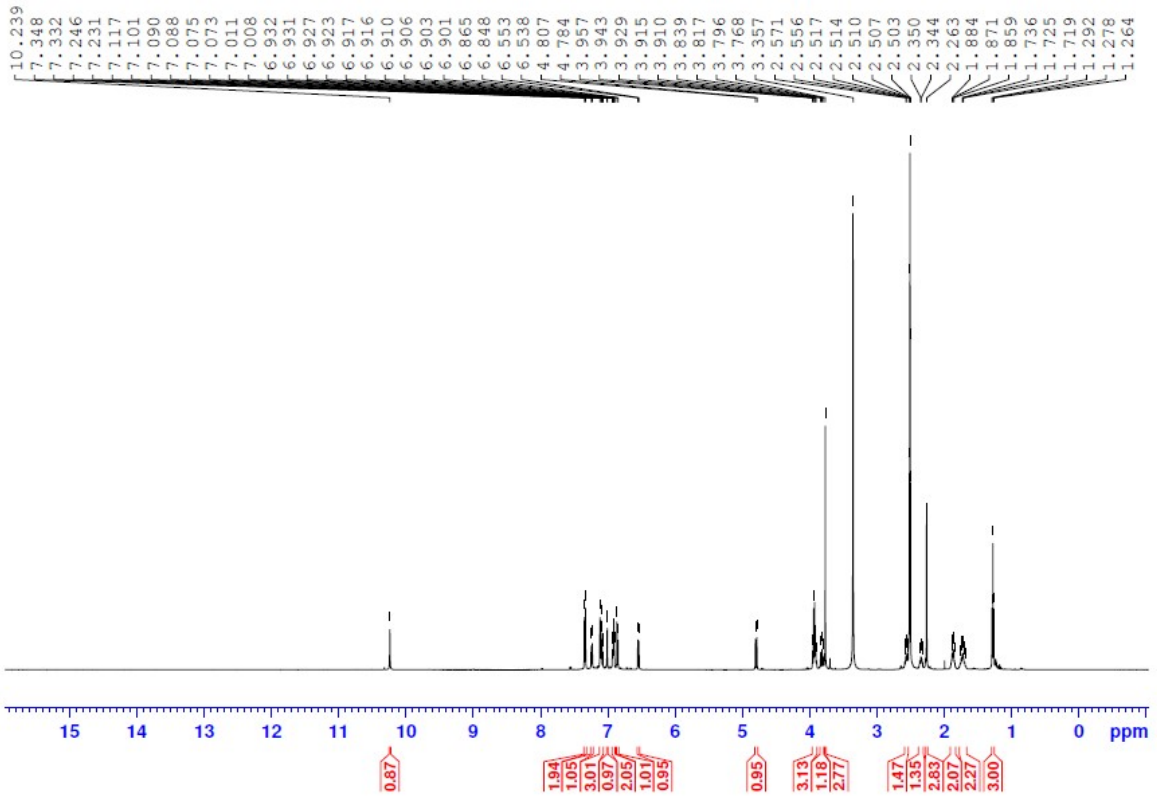

Figure S34. ^{1}H NMR spectrum of compound **5f**.

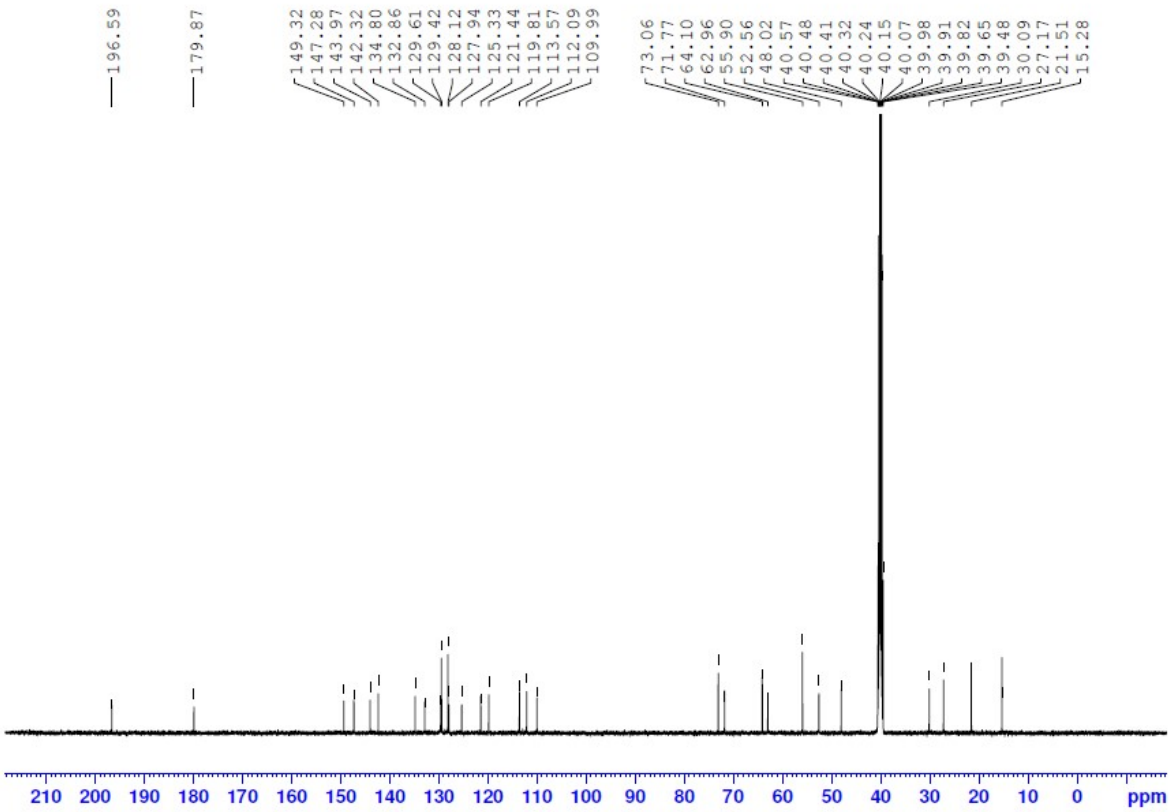

Figure S35. ^{13}C NMR spectrum of compound **5f**.

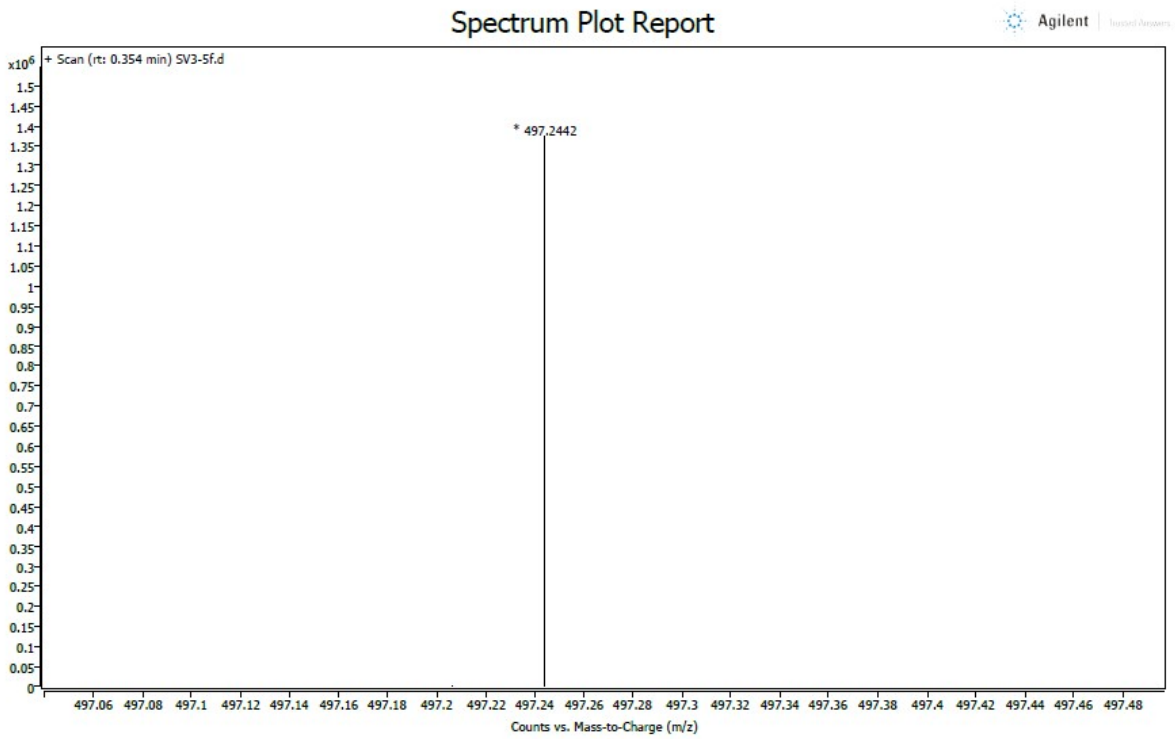

Figure S36. HR-MS spectrum of compound **5f**.

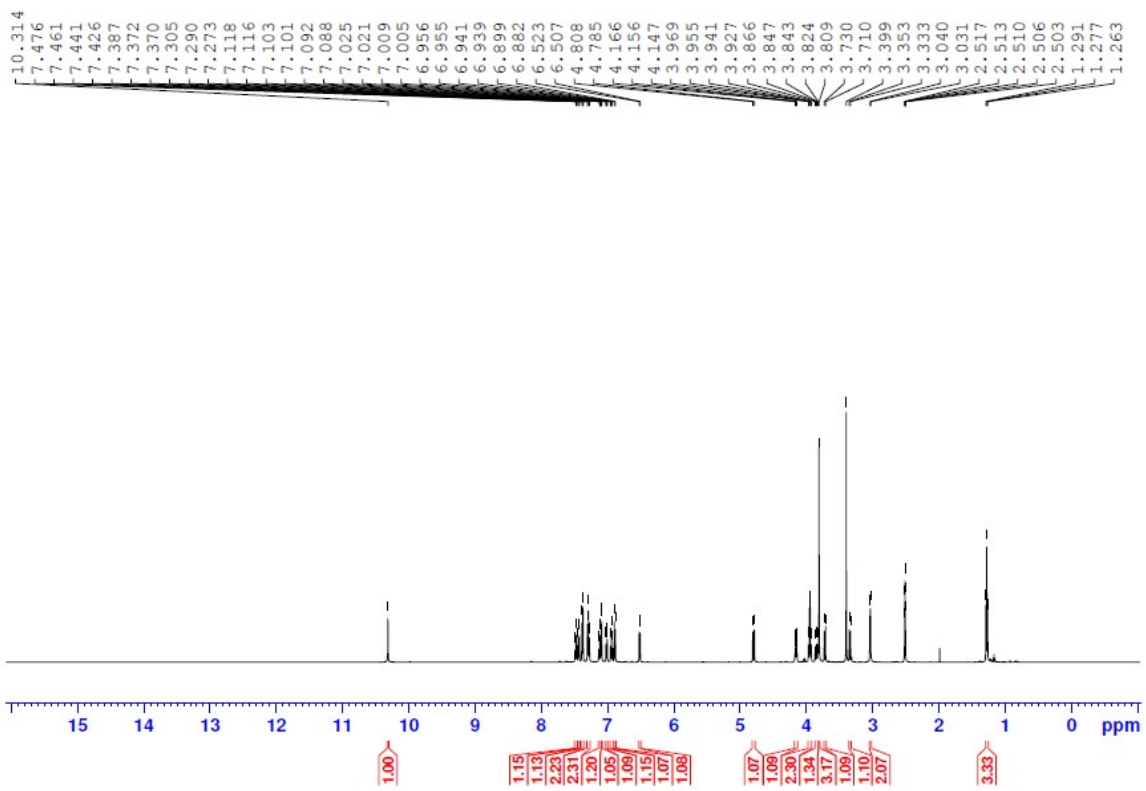

Figure S37. ^{1}H NMR spectrum of compound **6a**.

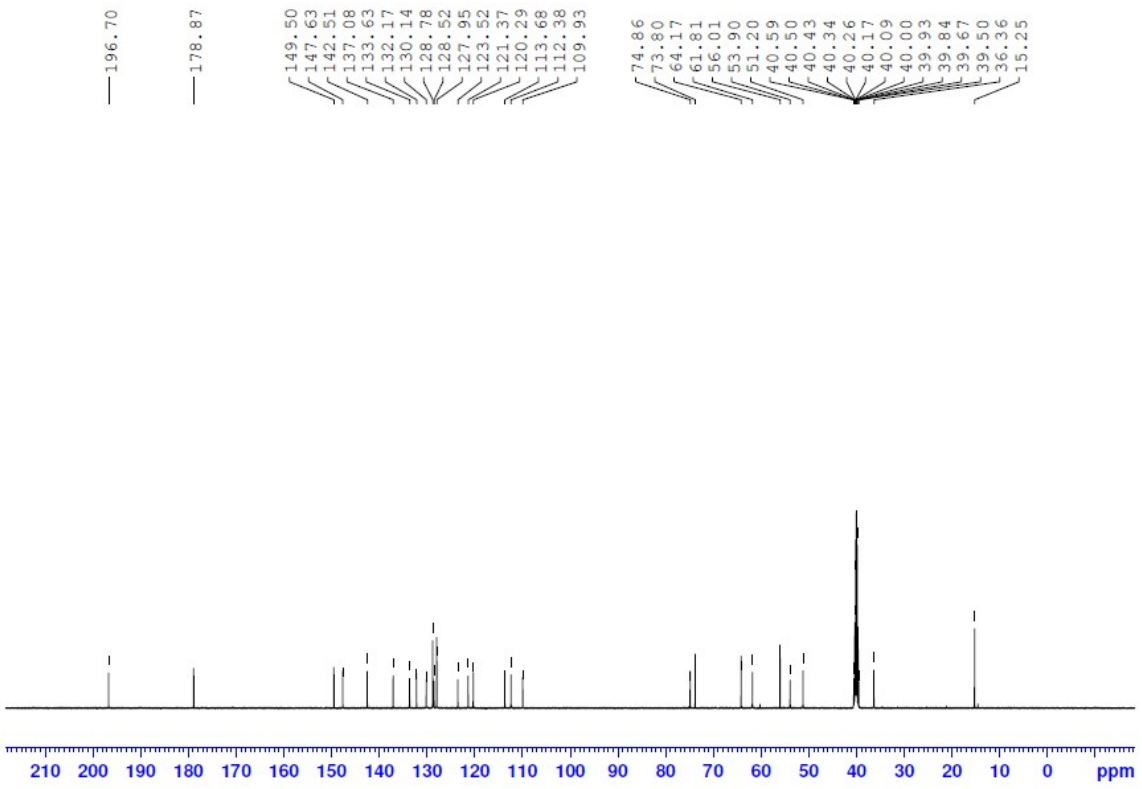

Figure S38. ^{13}C NMR spectrum of compound **6a**.

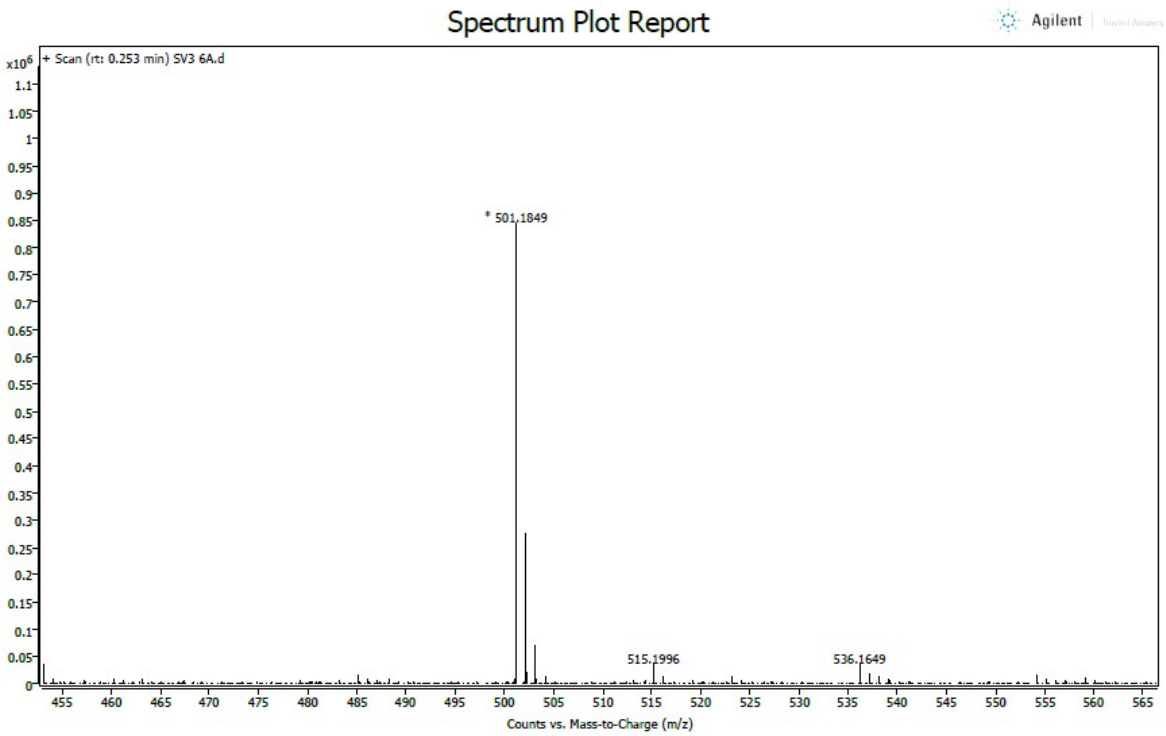

Figure S39. HR-MS spectrum of compound **6a**.

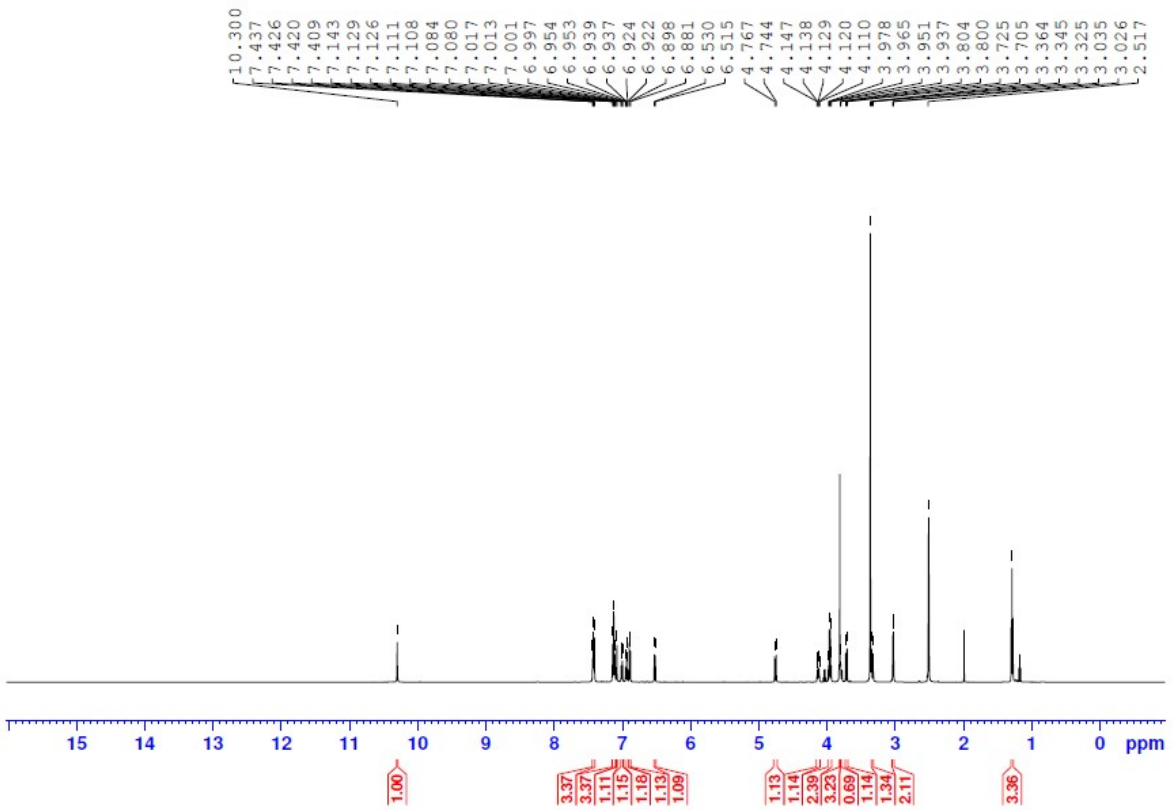

Figure S40. ^{1}H NMR spectrum of compound **6b**.

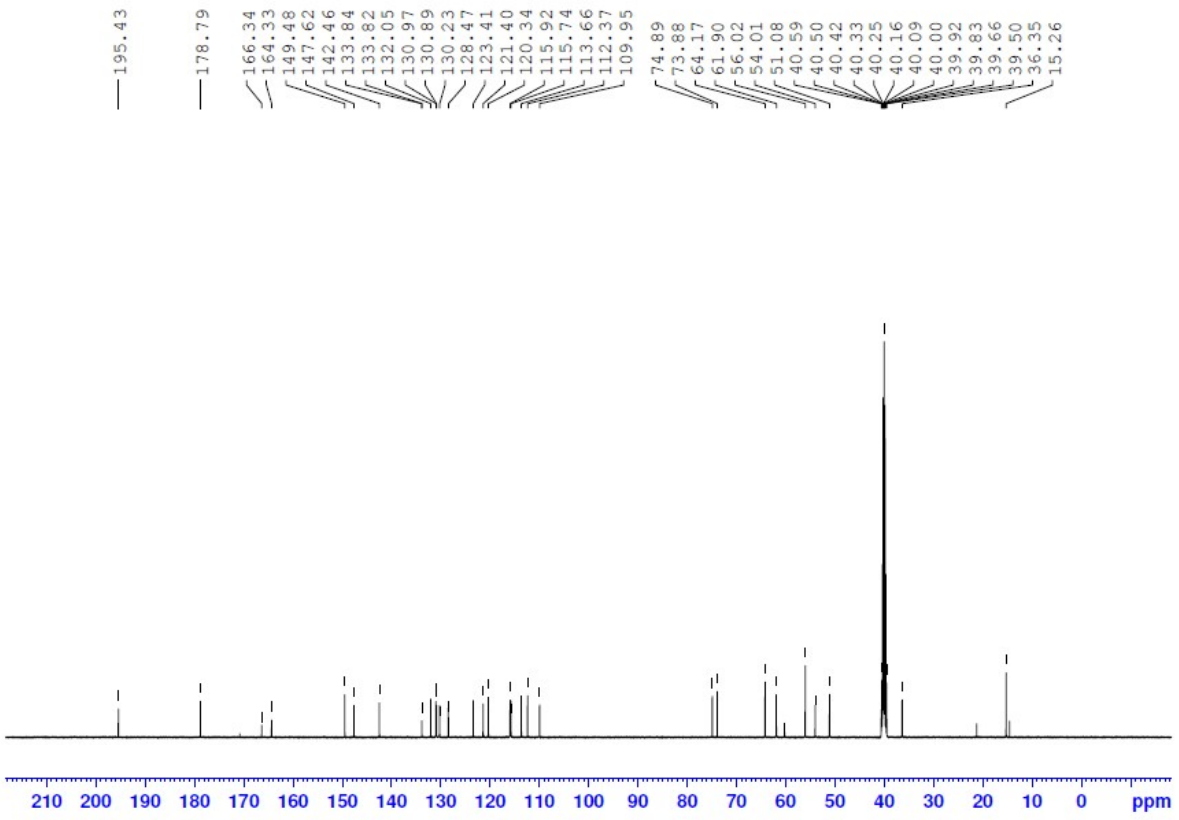

Figure S41. ^{13}C NMR spectrum of compound **6b**.

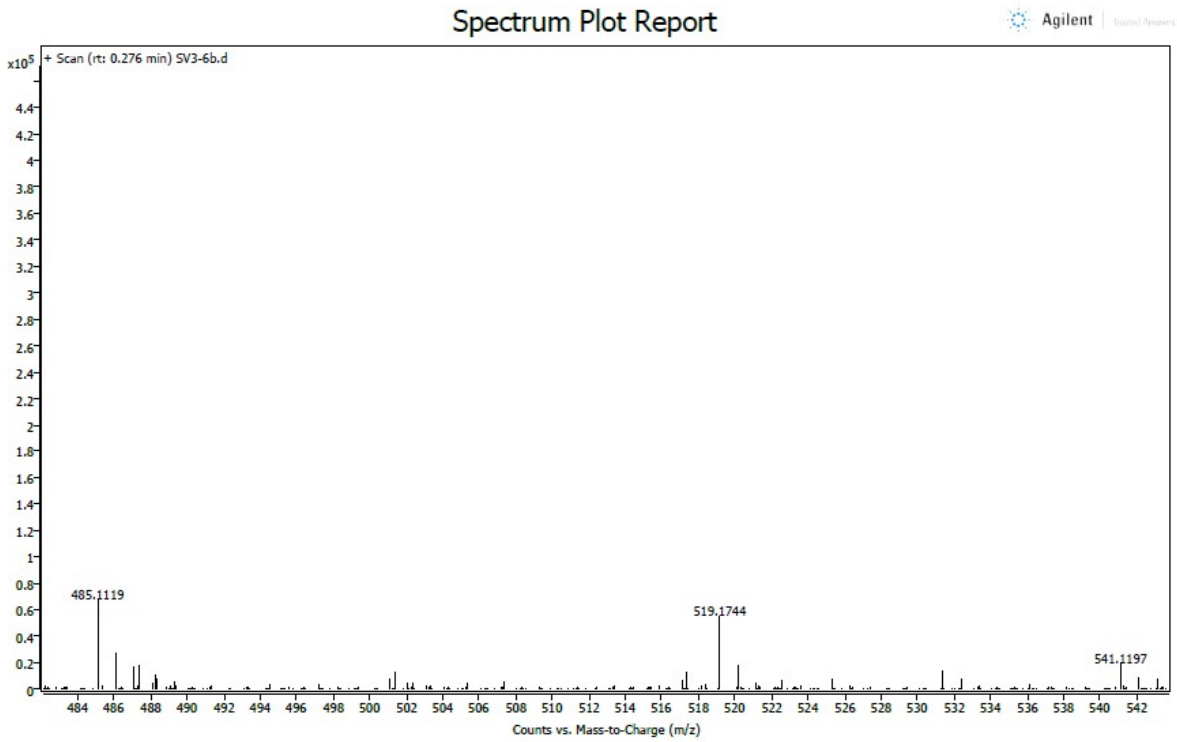

Figure S42. HR-MS spectrum of compound **6b**.

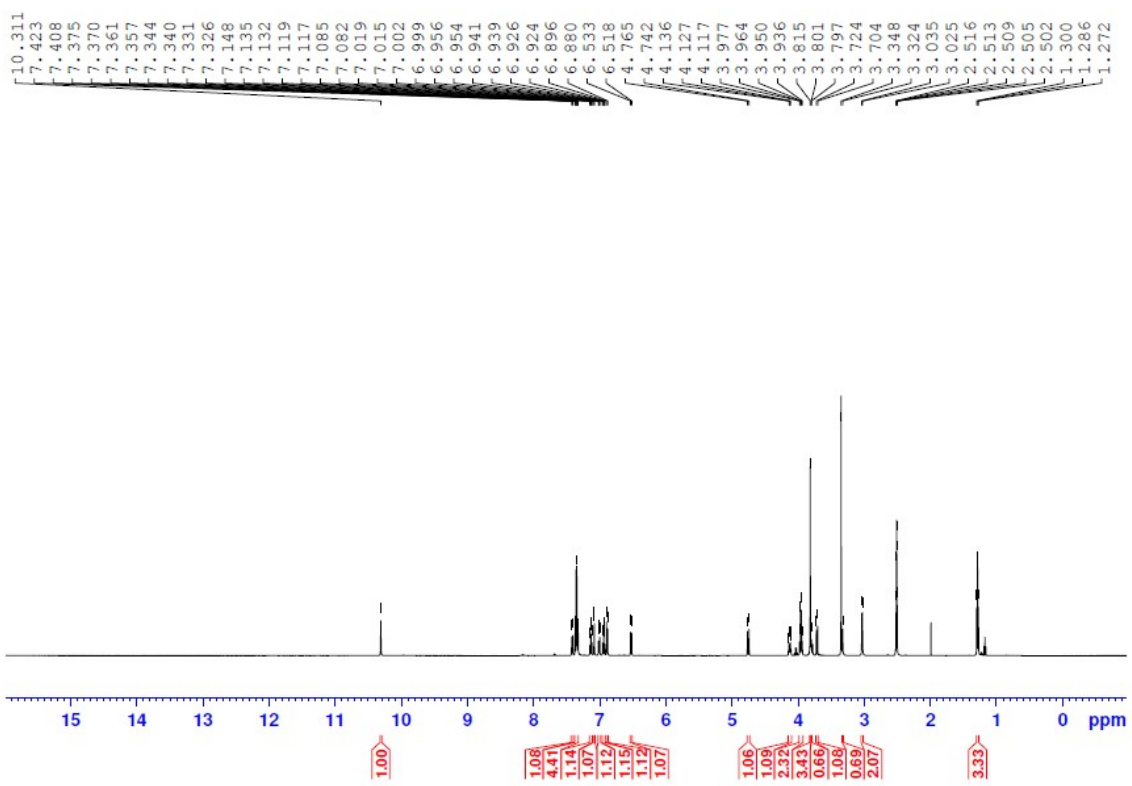

Figure S43. ^{1}H NMR spectrum of compound **6c**.

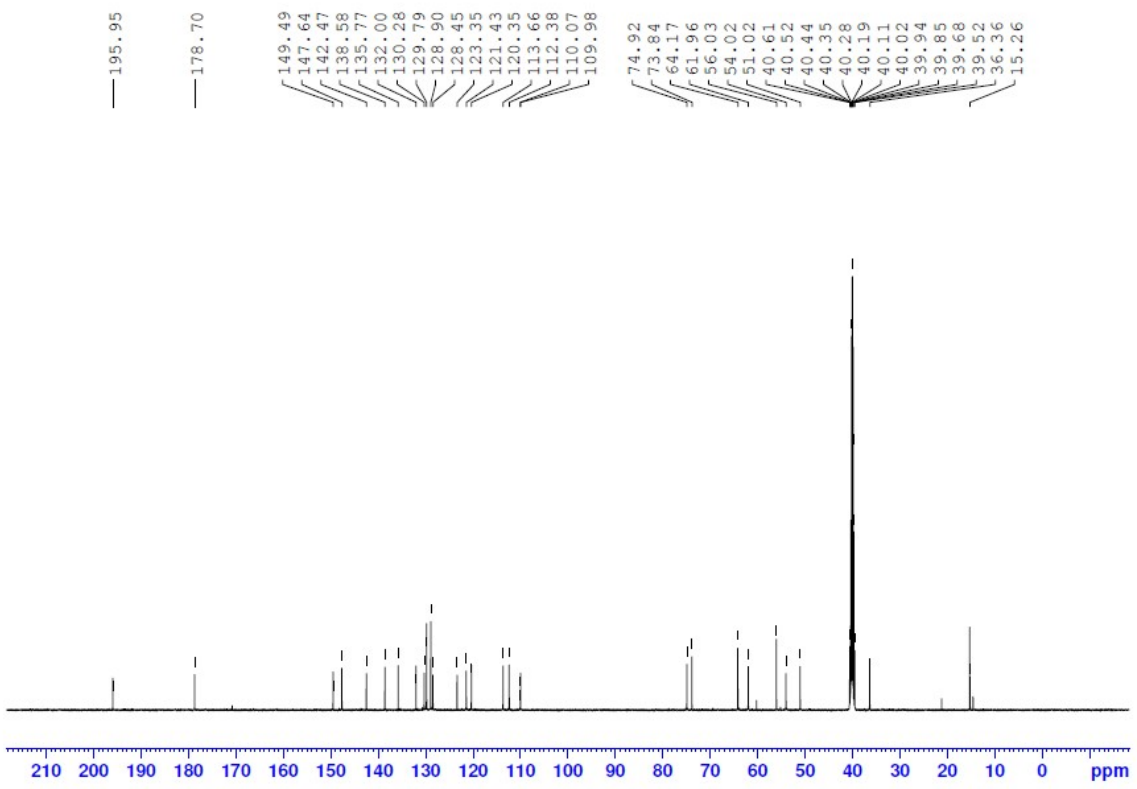

Figure S44. ^{13}C NMR spectrum of compound **6c**.

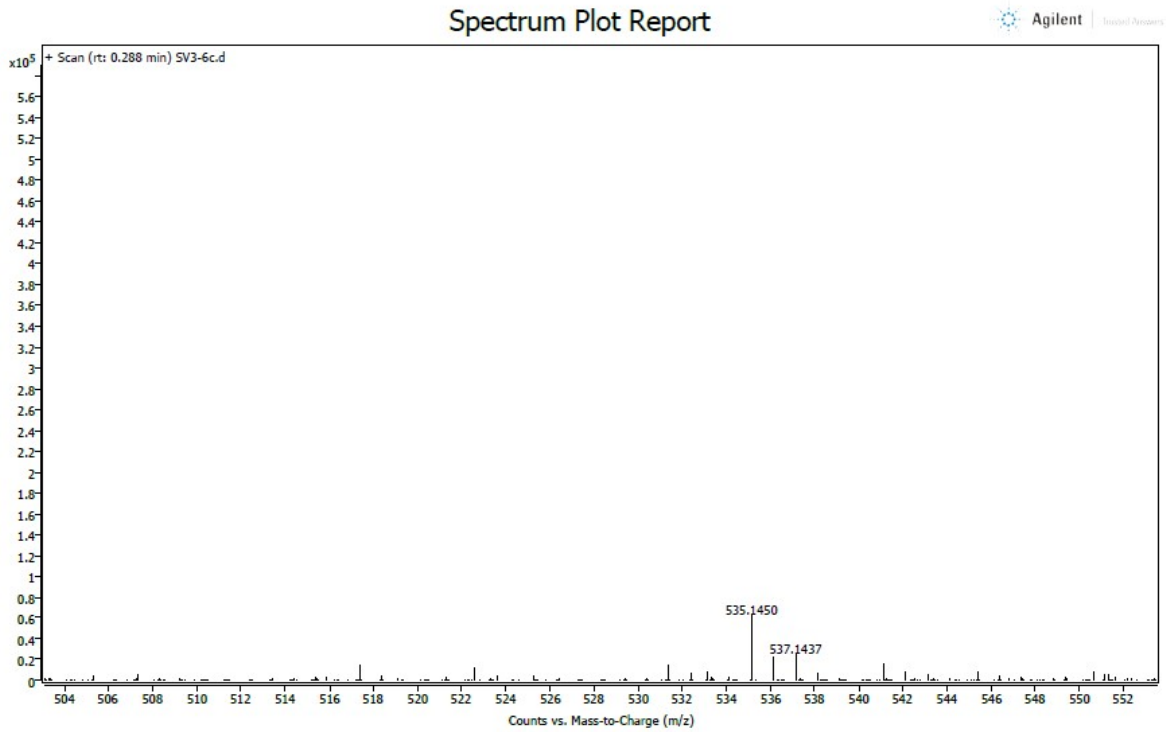

Figure S45. HR-MS spectrum of compound **6c**.

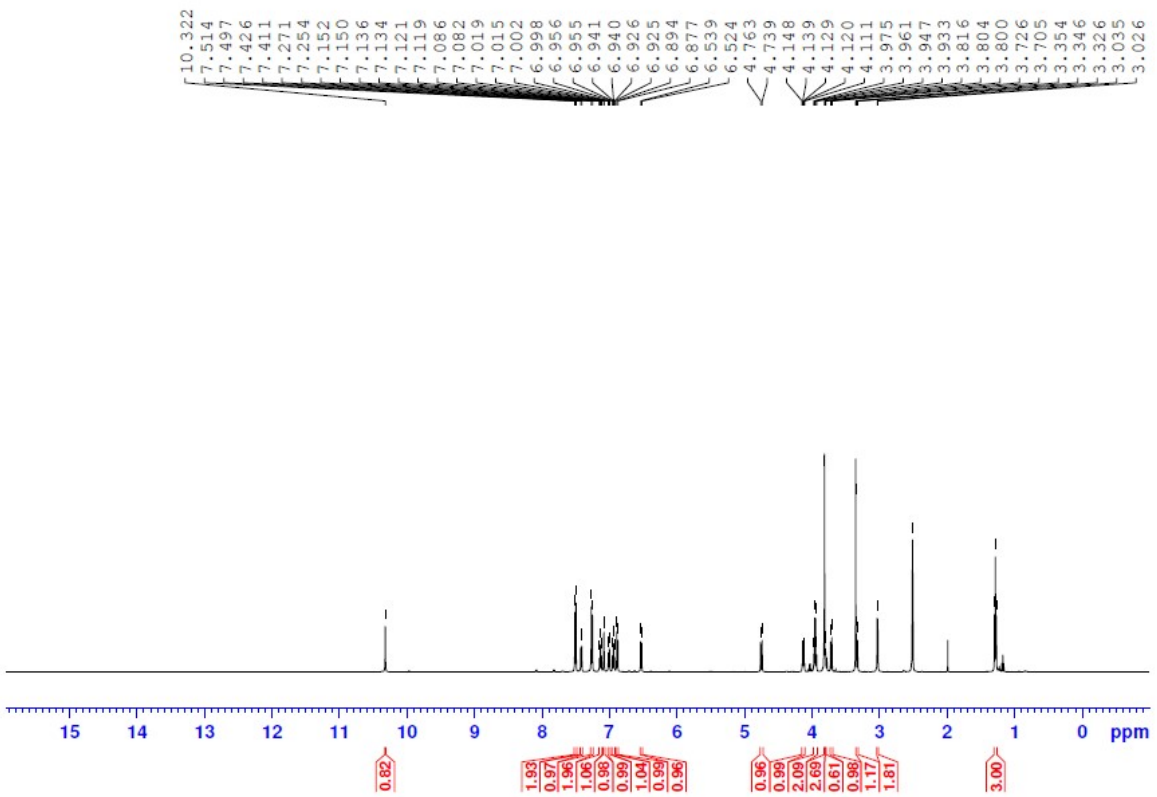

Figure S46. ^{1}H NMR spectrum of compound **6d**.

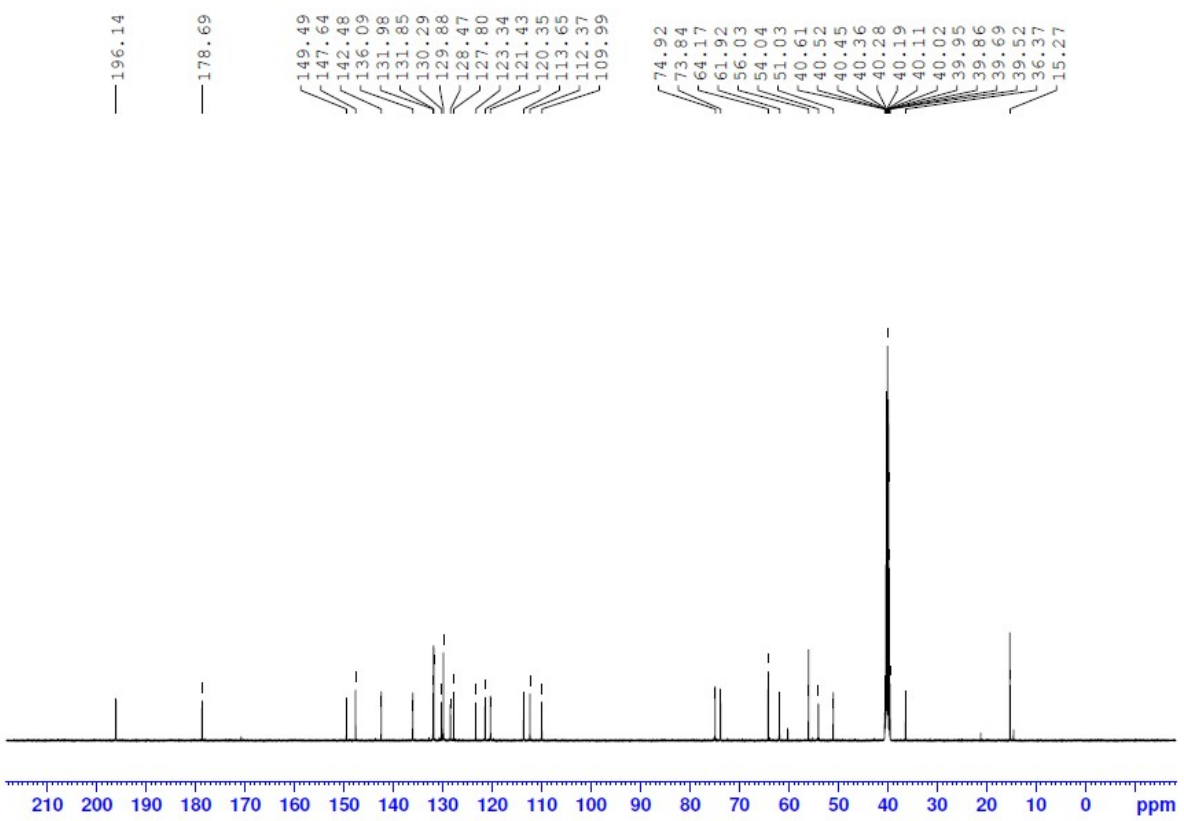

Figure S47. ^{13}C NMR spectrum of compound **6d**.

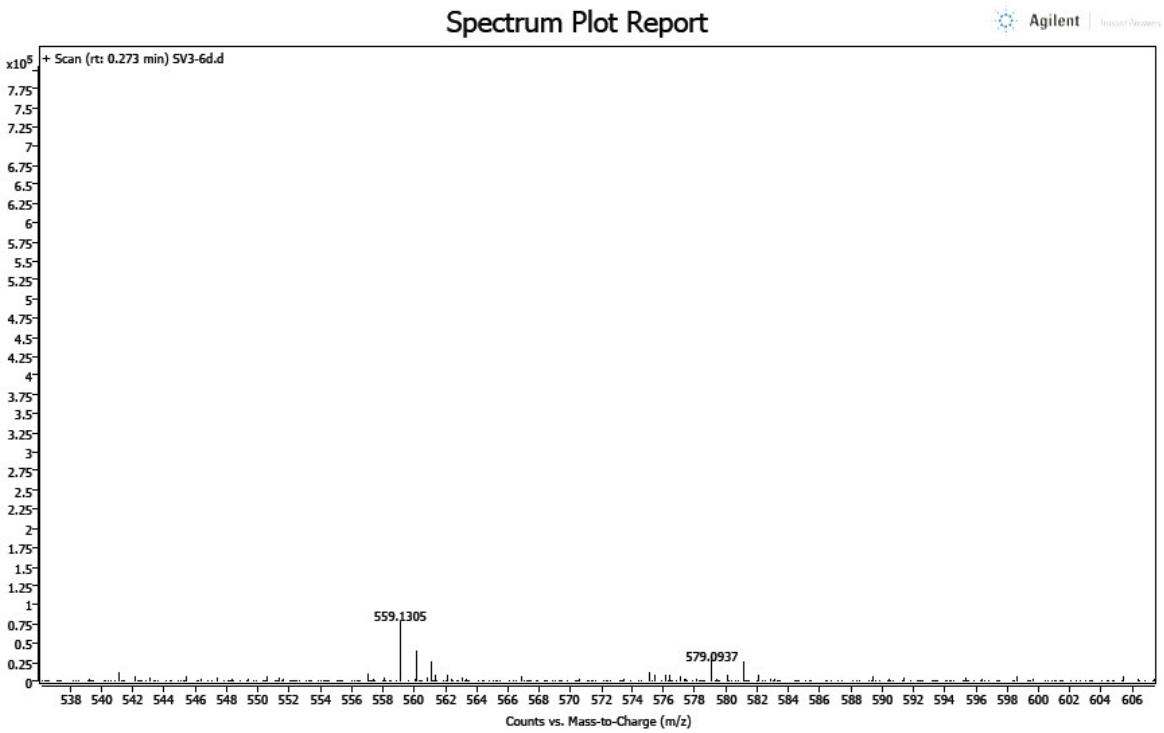

Figure S48. HR-MS spectrum of compound **6d**.

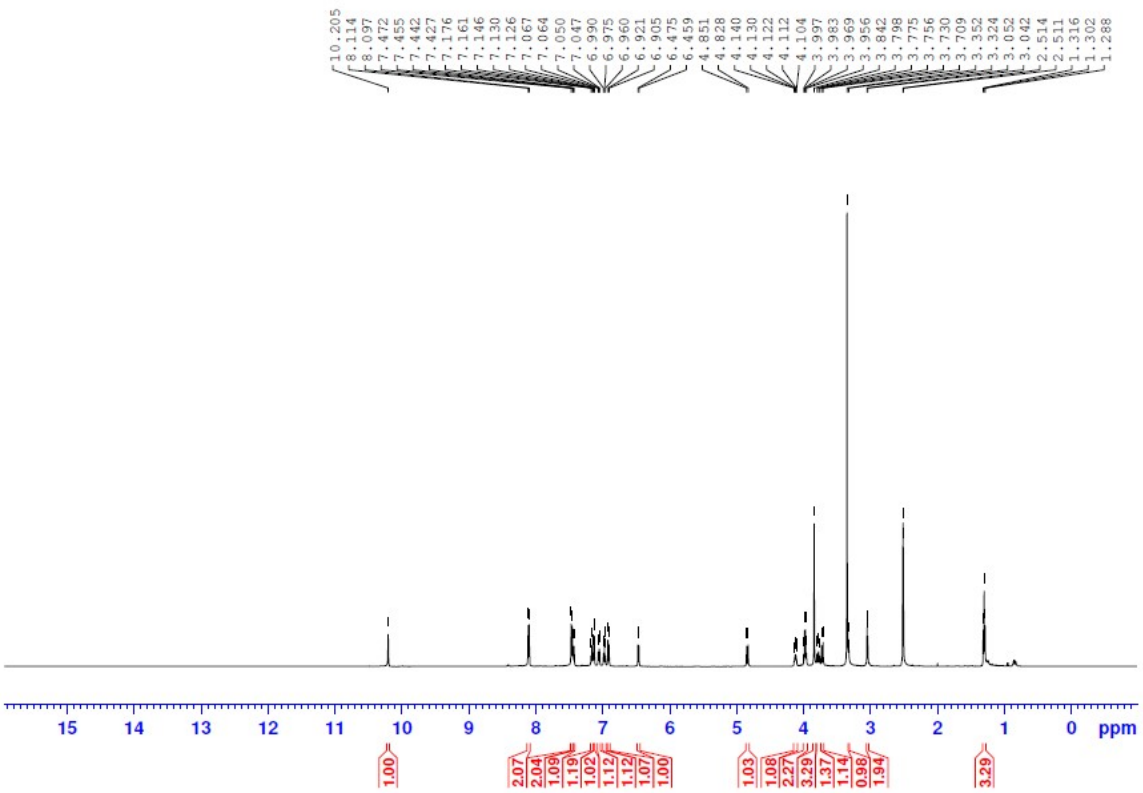

Figure S49. ^{1}H NMR spectrum of compound **6e**.

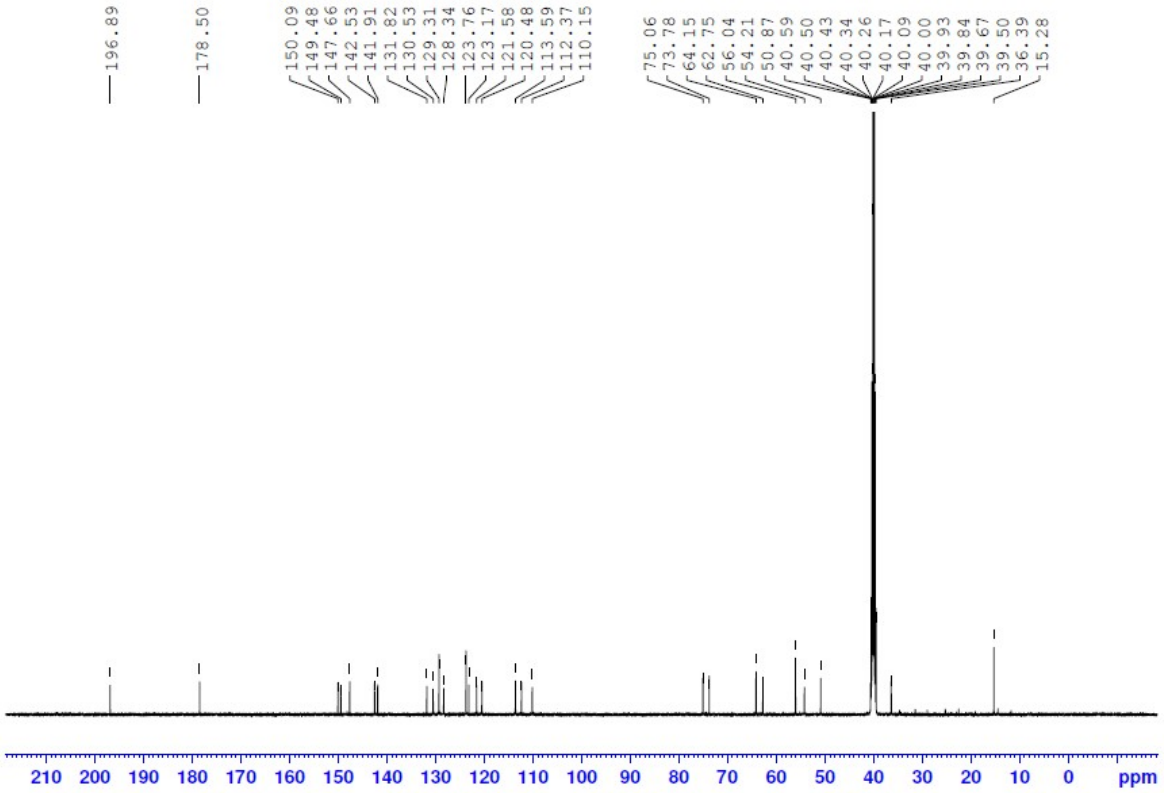

Figure S50. ^{13}C NMR spectrum of compound **6e**.

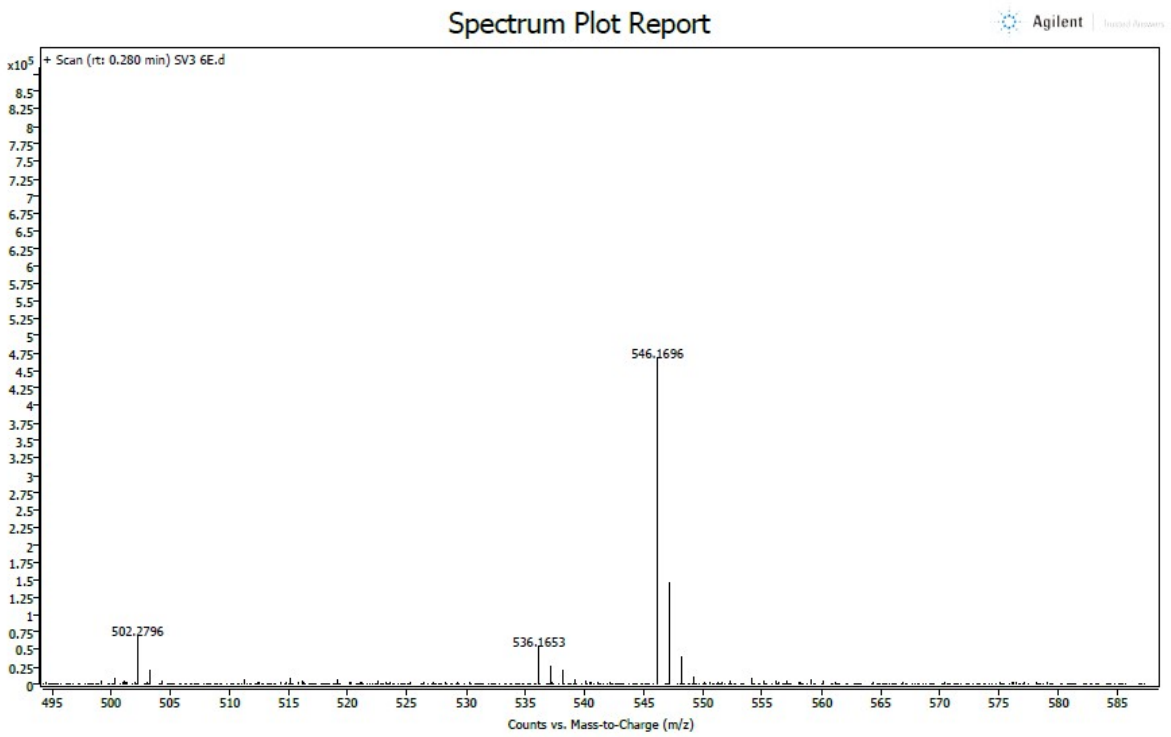

Figure S51. HR-MS spectrum of compound **6e**.

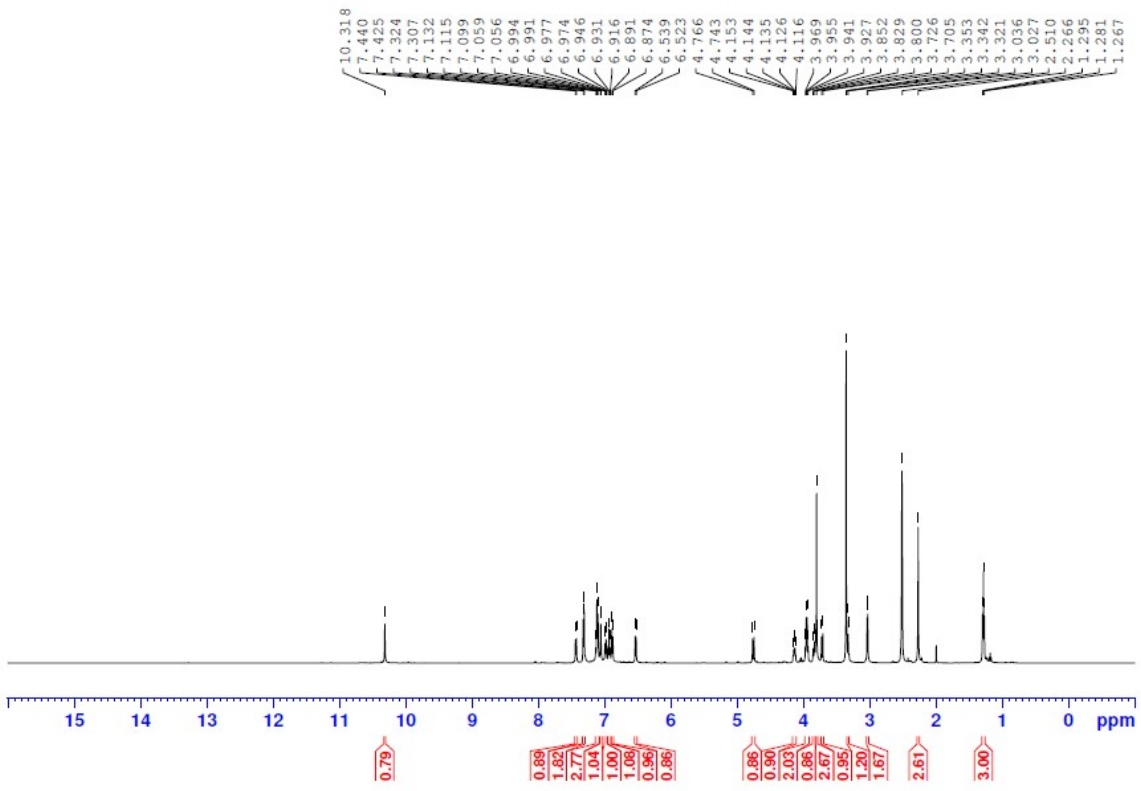

Figure S52. ^{1}H NMR spectrum of compound **6f**.

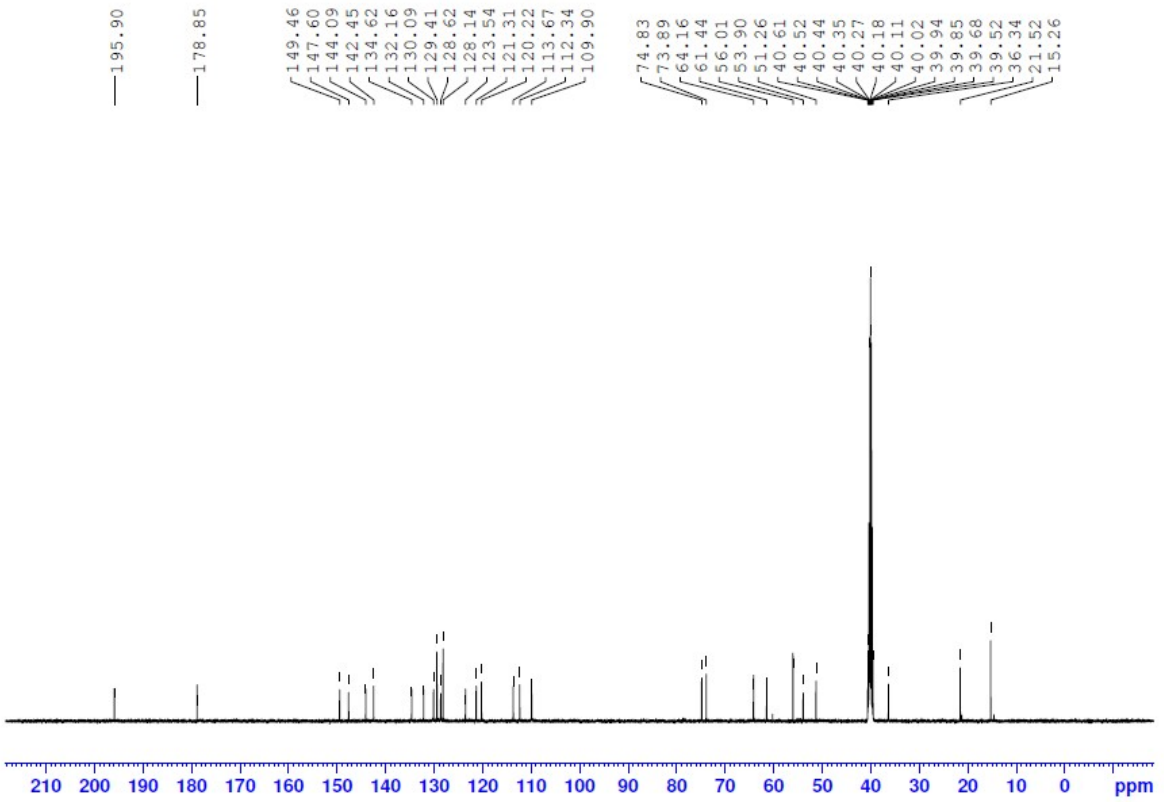

Figure S53. ^{13}C NMR spectrum of compound **6f**.

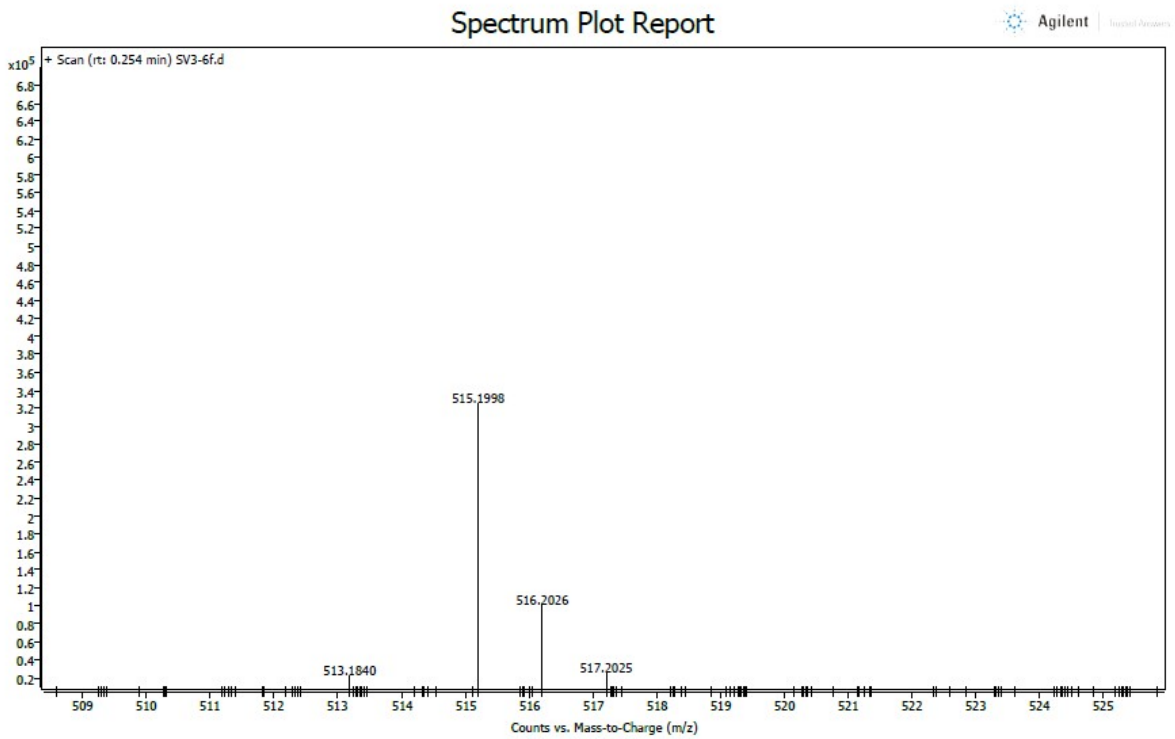

Figure S54. HR-MS spectrum of compound **6f**.

References

1 F. Anam, A. Abbas, K. M. Lo, S. Hameed, P. Ramasami, Y. Umar, A. Ullah and M. M. Naseer, Synthesis, crystal structure, experimenta; and theoretical investigations of 3-(4-ethoxy-3-methoxyphenyl)-1-phenylprop-2-en-1-one, *J. Mol. Struct.* 2017, **1127**, 742-750.

2 S. M. Patil, K. R. Maruthi, S. N. Bajpe, V. M. Vyshali, S. Sushmitha, C. Akhila and R. Ramu, Comparative molecular docking and simulation analysis of molnupiravir and remdesivir with SARS-CoV-2 RNA dependent RNA polymerase (RdRp), *Bioinform*., 2021, **17**, 932-939.

3 R. M. Martiz, S. M. Patil, M. Abdulaziz, A. Babalghith, M. Al-Areefi, M. Al-Ghorbani, J. M. Kumar, A. Prasad, N. P. M. Nagalingaswamy and R. Ramu, Defining the Role of Isoeugenol from Ocimum tenuiflorum against Diabetes Mellitus-Linked Alzheimer's Disease through Network Pharmacology and Computational Methods, *Molecules*, 2022, **27**, 2398.

4 J. Porter, A. Payne, B. de Candole, D. Ford, B. Hutchinson, G. Trevitt, J. Turner, C. Edwards, C. Watkins, I. Whitcombe and J. Davis, Tetrahydroisoquinoline amide substituted phenyl pyrazoles as selective BCL2 inhibitors, *Bioorg. Med. Chem. Lett*., 2009, **19**, 230-233.

5 B. Fang, G. Fu, J. Agniswamy, R. W. Harrison and I. T. Weber, Caspase-3 binds diverse P4 residues in peptides as revealed by crystallography and structural modelling, *Apoptosis*, 2009, **14**, 741-752.

6 W. Zhang, B. Chakravarty, F. Zheng, Z. Gu, H. Wu, J. Mao, S. J. Wakil and F. A. Quiocho, Crystal structure of FAS thioesterase domain with polyunsaturated fatty acyl adduct and inhibition by dihomo-γ-linolenic acid, *Proc. Natl. Acad. Sci*., 2011, **108**, 15757-15762.

7 R. M. Martiz, S. M. Patil, D. T. Hombegowda, A. M. Shbeer, T. Alqadi, M. Al-Ghorbani, R. Ramu and A. Prasad, Phyto-Computational Intervention of Diabetes Mellitus at Multiple Stages Using Isoeugenol from Ocimum tenuiflorum: A Combination of Pharmacokinetics and Molecular Modelling Approaches, *Molecules*, 2022, **27**, 6222.

8 S. M. Patil, R. M. Martiz, R. Ramu, P. S. Shirahatti, A. Prakash, S. J. Chandra and V. L. Ranganatha, In silico identification of novel benzophenone–coumarin derivatives as

SARS-CoV-2 RNA-dependent RNA polymerase (RdRp) inhibitors, *J. Biomol. Struct. Dyn*., 2022, **40**, 13032–13048.

9 N. Nivetha, S. M. Patil, R. Ramu and S. Velmathi, Stereoselective synthesis of highly functionalized aminobenzothiazole-fused spirooxindole derivatives: in silico and in vitro anti-diabetic studies, *Synthesis*, 2023, **55**, 4145-4162.

10 S. M. Patil, K. A. Al-Mutairi, N. Firdose, R. Ramu and R. M. Martiz, Pharmacoinformatics based screening discovers swertianolin from Lavandula angustifolia as a novel neuromodulator targeting epilepsy, depression, and anxiety, *S. Afr. J. Bot*., 2022, **149**, 712–730.

11 H. Sajal, S. M. Patil, R. Raj, A. M. Shbeer, M. Ageel and R. Ramu, Computer-Aided Screening of Phytoconstituents from Ocimum tenuiflorum against Diabetes Mellitus Targeting DPP4 Inhibition: A Combination of Molecular Docking, Molecular Dynamics, and Pharmacokinetics Approaches, *Molecules*, 2022, **27**, 5133.

12 P. G. Anantharaju, D. B. Reddy, M. A. Padukudru, C. M. Chitturi, M. G. Vimalambike and S. V. Madhunapantula, Induction of colon and cervical cancer cell death by cinnamic acid derivatives is mediated through the inhibition of Histone Deacetylases (HDAC), *PLoS One*, 2017, **12**, e0186208.

13 P. K. Veeresh, C. G. Basavaraju, S. Dallavalasa, P. G. Anantharaju, S. M. Natraj, O. A. Sukocheva and S. V. Madhunapantula, Vitamin D3 Inhibits the Viability of Breast Cancer Cells In Vitro and Ehrlich Ascites Carcinomas in Mice by Promoting Apoptosis and Cell Cycle Arrest and by Impeding Tumor Angiogenesis, *Cancers*, 2023, **15**, 4833.

14 A. Breu, K. Rosenmeier, R. Kujat, P. Angele and W. Zink, The cytotoxicity of bupivacaine, ropivacaine, and mepivacaine on human chondrocytes and cartilage, *Anesth. Analg*., 2013, **117**, 514–522.

15 J. Dewangan, S. Srivastava, S. Mishra, A. Divakar, S. Kumar and S. K. Rath, Salinomycin inhibits breast cancer progression via targeting HIF-1α/VEGF mediated tumor angiogenesis in vitro and in vivo, *Biochem. Pharmacol*., 2019, **164**, 326–335.

16 J. Dewangan, D. Tandon, S. Srivastava, A. K. Verma, A. Yapuri and S. K. Rath, Novel combination of salinomycin and resveratrol synergistically enhances the anti-proliferative and pro-apoptotic effects on human breast cancer cells, *Apoptosis*, 2017, **22**, 1246–1259.